ERRATA

p.3; line 5. After 'gauze' add ','.

p.9; line 12. For '0.1-1' read '0.1-1μ'.

p.10; first equation, first term: read $C_2(X^3\Pi_u)$.

p.14; line 12. For figures 6.4 and 6.5, read 6.6 and 6.7 respectively.

p.20; line 13. For 'adsorbed', read 'absorbed'.

p.21; line 4. For 'electron concentration and conductivity' read 'total negative species density'.

p.23;first equation. (I^2/V_p) is all to the power 2/3.

p.34; line 21. For 'Kaff' read 'Kalff'.

p.86; equation 5.21. Close square brackets after term $\frac{\mu_- n_-}{\mu_e}$ instead of at end of right hand side.

p.87; equation 5.23. Close square bracket after term $\left(1 + \frac{\mu_+}{\mu_e}\right)$ instead of at end of right hand side.

The term $\left(\frac{1}{\mu_+} + \frac{1}{\mu_e}\right)$ multiplies the term $\left(u\frac{dn_+}{dx} - D_+\frac{d^2n_+}{dx^2}\right)$.

Equation 5.24. Delete third term on right hand side.

p.93; line 9. Delete reference to Hayhurst and Sugden.

p.96; line 23. For figure 7.1 read figure 6.3.

p.106;Flame A, temperature column. For 2025 read 2023.

p.113;equation 6.1a. In the term raised to the power 3/2, for k^2 read h^2.

p.181;equation A.9. Right hand side should read $35.9\left(\frac{M+m}{mM\alpha^*}\right)^{\frac{1}{2}}$

p.184;line 4. For 'Margenan' read 'Margenau'.

line 9. Read $\alpha = \frac{M}{12m}\left(\frac{eE\lambda}{kT}\right)^{\frac{1}{2}}$

p.185;line 6. $\left(\frac{m}{2\pi kT}\right)$ is all raised to the power 3/2.

THE IONIZATION OF ALKALI METALS IN HYDROCARBON FLAMES

A thesis submitted for the
degree of Doctor of Philosophy
in the Faculty of Science,
University of London

by

Derek Boothman, B. Sc., A.R.C.S.

Department of Chemical Engineering
and Chemical Technology,
Imperial College of Science and Technology,
London, S.W.7.

July 1974.

ACKNOWLEDGEMENTS

This work was supported financially by the S.R.C.

The author wishes to thank primarily Dr. J. Lawton for his helpful comments on and supervision exercised (albeit by remote control) over this work. He is also grateful for the encouragement and help given by Prof. F.J. Weinberg and Dr. A.R. Jones.

For help with the construction of part of the apparatus, he would like to thank Mr. E.F. Barnes, and for preparation of the figures, Mr. M. Bouali.

Finally, his sincerest thanks go to Ms. M. Donovan for her efficient work in producing this excellent typescript.

ABSTRACT

Primarily, the work presented here deals with the ionization and electrical recombination processes of alkali metals in the hot gases produced by hydrocarbon/oxygen/nitrogen flames. The gas convective flow is intercepted normally by a metal gauze between the burner and which a potential is applied. The resultant current-voltage-electrode height characteristics are, using the theoretical developments outlined, interpreted so as to yield positive ion density values. The analysis is so different from other previous attempts to interpret these characteristics as to warrant its description as a new measurement technique, complementary to those already extant.

The range of the saturation current measurement technique is extended to yield quantitative measurements of alkali ionization above the reaction zone.

Combination of the two techniques gives both the ionization cross-sections for sodium and potassium and the three-body recombination coefficient for each of the ions with electrons over a range of temperatures.

In the fuel-lean flames burned, alkali hydroxides are observed to be formed by three-body reactions, rather than the conventional two-body ones encountered in fuel-rich hydrogen flames. This is shown to be feasible on the basis of kinetic theory and the concentrations of the various species involved. Contrary to the hypothesis of other research workers, alkali oxides are not found to be formed in any significant quantities.

Results are discussed critically in the light of other theoretical or experimental investigations, and, wherever relevant, the implications of the present findings for other work are drawn out.

Suggestions are made as to the course of future work carried out along lines similar to those here.

CONTENTS

FIGURES

Figures appear at the end of the chapter to whose text they are most relevant.

CHAPTER 1 INTRODUCTION

1.1 The study of flames

Flames, broadly speaking, may be studied for two reasons. One is in order to control them better so that, for example, furnaces of a more efficient design may be constructed. Such an advance is dependent on a detailed knowledge of the kinetics and fluid dynamics of combustion systems, how to control and alter them, and how to predict these parameters and the properties dependent on them in any given system. Although this side of the research seems at a somewhat primitive level, nevertheless it is developing and potential dividends should not be disregarded.

The second reason concerns flames as high temperature baths for the study both of radicals and ions, the mechanisms by which they are produced, often in super-equilibrium concentrations, and, when so produced, their decay, sometimes catalysed, (Bulewicz and Padley [1,2], Bulewicz, Cotton, Jenkins and Padley [3]) to equilibrium.

Information about these processes may then be used for other systems of interest not necessarily having any connexion with flames; in a recent paper (Boksenberg et al [4]), knowledge of the recombination coefficient for electron-ion collisions is used in conjunction with other parameters to deduce a value of electron density in interstellar space.

Reviews of the mechanism of natural ion formation in hydrocarbon flames are by now almost commonplace, and the reader is referred to Green and Sugden [5], Calcote [6], Peeters, Vinckier and van Tiggelen [7], Peeters and van Tiggelen [8] and, most recently, Miller [9] for information on this. Research into flame radicals

may prove to have received a boost recently with the current interest in atmospheric pollution, and the necessity to try to eliminate noxious flame products such as oxides of nitrogen or carbon monoxide. A review of this may be found in Starkman [10].

1.2 Nature of the present work

The present work is biassed towards the electrical properties of flames, especially those seeded with material readily ionizable both within and downstream of the reaction zone which, in practice, means alkali metal salts. This bias is appropriate for both practical and theoretical reasons.

1.2.1 Practical applications of the results

Practically, this type of work is of importance for some of the problems associated with magneto-hydrodynamic (MHD) power generation. Although direct interest in this has flagged in Britain, a pilot MHD plant was opened in 1965 in Moscow, the research work for it having been done by the U.S.S.R. Academy of Sciences Institute of High Temperature Studies. This low power plant, known as the "U-02" plant, was successful enough to warrant further development, so in 1971 the bigger, 25 MW "U-25" open cycle MHD plant was opened as the first semi-commercial MHD power station. The 270 tons hr^{-1} of high pressure steam created from this generator is used for a conventional power station, thereby making the total capacity of the station 80 MW. In theory, a 2000 MW size station would have an efficiency of some 50-60%, compared with a figure of ca. 40% for a purely conventional system. Soviet research workers seem, at present, to be hoping for an overall efficiency of some 35% for the "U-25" plant, though the

use of a pre-ionizer may improve the generator's performance substantially.

In the "U-25" plant, oxygen enriched air is preheated to ca. 1200°C before being fed into a combustion chamber with natural gas; the resultant combustion products are seeded with potassium carbonate. These gases are then accelerated through a nozzle to the MHD generator proper where the plasma has a velocity of some 850 m sec^{-1} and an operating temperature of ca. 2000°C.*

A different, and less well advanced, application of charged gases is outlined by P.J. Musgrove [11]. This is a plan for electrogasdynamic (EGD) refrigeration at cryogenic temperatures. Here, however, instead of having atomic ions, fine particles (0.1 - 1 diameter) are used, being charged up by a corona discharge and then being moved by the gas stream against the prevailing electric field, finally being discharged by means of a self induced corona discharge. The gas, in doing work by moving charges against the field, suffers a drop in pressure and temperature. The reverse process of converting heat into electrical energy is also feasible, at the comparatively high temperature range of 300-900 K (Musgrove [12], Gourdine [13]).

Thus, the behaviour of charged gases merits further research. We are here concerned mainly with the creation and recombination of charge.

1.2.2 Ionization in flames

Observed ion densities, reaching as much as 10^{13} ions cm^{-3}

* This information is collated from separate accounts: an unsigned article in the "New Scientist" of 4/6/70, and an interview with A. Sheindin, Director of the U.S.S.R. Academy of Sciences High Temprature Institute, appearing in the "Morning Star" of 14/12/71.

at atmospheric pressure, in and just downstream of the reaction zones of hydrocarbon flames are far too high to be explained on the basis of equilibrium thermal ionization of the species present.

An explanation is found in the super-equilibrium production of radicals in the reaction zone. Reviews of this "natural" flame ionization, as noted above, may be found in references 5-9.

Although the excited CH radical is now known (Bulewicz, Padley and Smith [14]) to be formed by the long suspected reaction

$$C_2(X^3\Pi_n) + OH(X^2\Pi) \rightarrow CO(X^1\Sigma^+) + CH(A^2\Delta)$$

whose rate constant is, according to the same authors, $(8 \pm 4)10^{-12}$, CH^* takes no part in the ionization process. It is believed, though not fully established, that this process takes place via

$$CH(X^2\Pi) + O(^3P) \rightarrow CHO^+ + e$$

(Fontijn, Miller and Hogan [15], Bulewicz and Padley [16]). The mechanism for the production of this ground state CH radical is, as yet, still somewhat obscure. Browne, Porter, Verlin and Clark [17] suggest

$$\dot{C}_2H + O \rightarrow CO + CH$$

with a rate constant of $8.3 \cdot 10^{-11}$, and

$$CH_3 + O \rightarrow H_2O + CH$$

has also been suggested by Jones, Becker and Heinsohn [18] in their computer studies, but with a rate constant of only $4.6 \cdot 10^{-15}$.

At one time it was thought that this ionization reaction quoted involved quite a high activation energy. In fact, recent work by Matthews and Warneck [19] has shown it to be nearly thermoneutral (2 ± 5 kcal mole^{-1}). The reaction proceeds at a rate in the range 10^{-13} to 10^{-11}. Green and Sugden [5] suggest $8 \cdot 10^{-13}$,

Calcote, Kurzius and Miller [20] $3 \cdot 10^{-13}$ while for their computer model Jones, Becker and Heinsohn [18] use a value of $9.5 \cdot 10^{-14} \exp(-6/RT)$ and Miller [9] suggests from theoretical studies (Kurzius and Boudart [21]) and the iso-electronic process

$$N + O \rightarrow NO^+ + e$$

that the rate is probably towards the upper end of the range.

The most common reaction of the charged formyl radical, CHO^+, is that with water vapour, viz.

$$CHO^+ + H_2O \rightarrow H_3O^+ + CO$$

This proceeds at a rate given by Miller [9] as $(1.5 \pm 1)10^{-8}$, this figure being an average taken from Green and Sugden [5], Miller [22] and Calcote and Jensen [23].

The ground state CH radical also reacts rapidly with O_2. The inference to be drawn from this is that an oxygen rich flame would probably not produce as much ionization as a fuel rich flame because of the competition for CH. In fact work published at the Twelfth Symposium (Melinek and Lawton's work in Boothman, Melinek, Lawton and Weinberg [24] and Peeters and van Tiggelen [8]) confirms this prediction.

Another ionization mechanism, involving hot electrons, via

$$X + e^* \rightarrow X^+ + 2e$$

has been suggested by Cozens and von Engel [25] but since the maximum electron temperature found in hydrocarbon flames has now been established as being at most only about twice the gas temperature (Bradley and Sheppard [26]) this can probably be ignored. In fact if shifts in plasma potential, due to excessive current drainage caused by large probes, are taken into consideration, then it seems likely that the electron temperature is the same as the gas

temperature except in the reaction zone where there may be a difference of a few hundred degrees (Bradley and Ibrahim [27]).

In a hydrocarbon flame not seeded with metal salts, the positive hydronium ion decays by recombination with an electron:

$$H_3O^+ + e \rightarrow H_2O + H$$

Green and Sugden [5] measured the rate of this reaction as $2.3 \cdot 10^{-7}$; measurements by other authors confirm this. Reported values range from $1 \cdot 10^{-7}$ to $4 \cdot 10^{-7}$ with $2 \cdot 10^{-7}$ being the most widely accepted and quoted figure.

A mass spectrometer will sometimes produce peaks of mass number some multiple of 18 above the hydronium ion, indicating the ion's hydrates. These are, of course, due to subsequent attachment reactions either genuinely downstream of the reaction zone or, alternatively, in the cooler areas around the sampling cone. The recombination coefficient for these hydrates is marginally higher than for the simple hydronium ion.

1.2.3 Metal-seeded hydrocarbon flames

When hydrocarbon flames are seeded with metals there is certainly no diminution of ion and electron densities in the reaction zone. However, even when the metal introduced has too high an ionization potential to produce measurable thermal ionization itself (as, for example, with lead) the ion and electron densities downstream of the reaction zone are observed to be higher than in the corresponding non-seeded case.

This may be explained by a charge exchange process, e.g.

$$Pb + H_3O^+ \rightarrow Pb^+ + H_2O + H$$

followed by a slow three body recombination reaction (the third body being written as 'M')

$$Pb^+ + e + M \rightarrow Pb + M,$$

the latter having a rate constant ranging from $6.1 \cdot 10^{-9}$ at 2265 K to $2.1 \cdot 10^{-8}$ at 1680 K (Hayhurst and Sugden [28]).

If a more easily ionizable metal (e.g. an alkali metal) is used as seed, there is a slow rise to thermodynamic (Saha-Boltzmann) equilibrium ionization in the absence of natural flame chemi-ionization as, for example, in hydrogen-oxygen or hydrogen-air flames. Formerly, it was thought that the set of reactions responsible for this was

$$A + OH \rightarrow A^+ + OH^-$$

$$OH^- + H_2 \rightarrow e + H_2O + H$$

$$A + H_2O \rightarrow AOH + H$$

where A represents an alkali metal atom (Page and Sugden [29]). However, as in the case of the Cozens/von Engel mechanism, further work established that the kinetics were first order (Padley and Sugden [30]) so the thermal ionization mechanism for an alkali may be written

$$A + M \rightarrow A^+ + e + M$$

In the same paper, Padley and Sugden note that even only ca. 1% by volume of an added hydrocarbon produces an equilibrium ion concentration, with negligible further effect when, in their case, all the hydrogen of the flame was substituted for by acetylene, the nitrogen proportion being adjusted to keep the flame temperature constant.

This effect may be explained on the basis of a charge exchange similar to that which happens in the case of lead. Rates for this charge exchange reaction are given by van Tiggelen and de Jaegere [31] for lithium, sodium and potassium: $7.5 \cdot 10^{-10}$,

$1.6 \cdot 10^{-8}$ and $4.6 \cdot 10^{-8}$ respectively; all are exothermic reactions, potassium most of all. Miller [9] quotes rates given in Calcote and Jensen [23] for Pb, Mn, Cr and Zn as well as the three alkalis; they vary from $1 \cdot 10^{-10}$ for Zn, a reaction endothermic by ca. 70 kcal $mole^{-1}$ to $1 \cdot 10^{-9}$ for Pb, endothermic by 24 kcal $mole^{-1}$. As may be expected, there is a correlation between the rate of the reaction and its exothermicity, albeit not one that may be expressed in exact, simple terms.

The charge recombination rate coefficient for lead has already been quoted. The equivalent coefficients for the two metals studied in this work are shown, present results included in figures 6.4 (potassium) and 6.5 (sodium). At flame temperatures the coefficient is, like lead (Hayhurst and Sugden [28]), of order 10^{-8}, increasing as temperature decreases.

While the initial impetus to metal ionization is given, as already pointed out, by charge transfer from flame chemi-ions, further ionization takes place by normal thermal ionization. As might be expected from the Saha equilibrium constant and the cited order of magnitude of the recombination coefficient, thermal ionization cross sections are orders of magnitude above the classical kinetic theory cross sections. Typically, they are in excess of 10^{-12} cm^2 (see Table 7.2).

1.2.4 The theoretical implications of the work

This brings us to the theoretically interesting side of the work. There are a number of different mechanisms for recombination, which proceeds at different rates dependent on the mechanism. It was expected that here the dominant mechanism would be a recombination of a positive alkali metal ion with an

electron (or possibly negative ion), a third body taking away the excess energy in order to conserve both momentum and energy in the collision, but otherwise (i.e. chemically) remaining unchanged.

A number of theories have been put forward to explain the magnitude of the recombination coefficient, α, observed. J.J. Thomson [32] formulated one theory that works quite well at pressures up to about one or two atmospheres, although other mechanisms take over at very low pressures. This involves defining a 'sphere of attraction' of radius a_0 between a positive ion and either a negative one or an electron, such that at its surface the potential energy of electrical interaction is equal to the mean kinetic energy:

$$\frac{e^2}{a_0} = \frac{3}{2} kT$$

$$\text{or} \quad a_0 = \frac{2}{3}\frac{e^2}{kT}$$

In order for recombination to occur it is necessary for the electron or negative ion to lose sufficient energy ($\sim kT$) by collision with a third body while within a distance a_0 of the positive ion. The possibility of such events are calculable from simple kinetic theory. The magnitude of the measured ion-electron recombination coefficient is so high that purely elastic collisions, involving a fractional energy loss for the electron of $\frac{2m_e}{M_i}$, are not sufficient. Inelastic collisions in which the electron induces vibrational and rotational transitions in a molecular third body must be included. Of these collisions, the vibrational ones are the more important; in molecules with a large dipole moment rotational transitions may also be important, but their effect is not easily calculable.

For higher pressures, Langevin [33] proposed another model

in which the ion-ion or ion-electron pair drift towards each other under the influence of their mutual attraction, undergoing many collisions en route. This gave a correct order of magnitude at atmospheric pressure, but, in actual fact, the model is valid only for pressures of ca. one hundred atmospheres and above. Harper [34] carried out an analysis for pressures above ca. 1 atmosphere and came to the conclusion that

$$\alpha_H = f_1 \alpha_L$$

where the subscripts H and L refer to the theories of Harper and Langevin respectively, and f_1 is of order unity. A discussion of this may be found in Loeb [35a].

The intermediate regime between those of Thomson and Langevin (or, more strictly speaking, Harper) was, until comparatively recently, described by a number of empirical bridging formulae.

In 1959, however, Natanson [36] provided a theory which unified the Harper and Thomson approaches. He kept the hypothesis of a 'sphere of attraction' but allowed for energy interchanges between one of the ions and its neutral collision partners. This led to a new value for a_0, $(a_0)_N$, of

$$(a_0)_N = \frac{5}{12} \frac{e^2}{kT}$$

More generally, if the two ions are separated by a distance r when one of them makes a collision then, whereas Thomson states that the kinetic energy of relative motion of the two ions must be less than that necessary to separate them by an infinite distance, Natanson imposes the stricter condition that it should be less than that required to separate them by their original distance apart, r; plus another distance of the order of a mean free path (implying that if one of the ions does travel this further distance it can

then pick up further energy in another collision to enable it to overcome the energy of attraction between the two ions and thereby escape from the 'sphere of attraction').

In the low pressure limit this criterion leads to a radius a_o equal to that already quoted for the Natanson theory. At higher pressures it leads to

$$(a_o)_N^2 = \frac{5\ e^2 \beta\lambda}{12\ kT}$$

where λ is the ionic mean free path and β a constant of order unity.

Taking into account ion concentration gradients and ion path curvature, Natanson went on to derive a recombination coefficient, α_N, which is related to the Thomson one by the relationship

$$\alpha_N = \alpha_T \{1 + \frac{e^2}{(a_o)_N\ kT}\} \exp\{-\frac{e^2}{\beta\lambda\ kT}\}$$

In the high pressure limit this reduces to the Harper formula, while at low pressures

$$\alpha_N = \frac{85}{64}\ \alpha_T$$

and at intermediate pressures there is a smooth transition between the two*.

All these theories, however, are in the realm of classical physics and suffer from the limitations consequent on that. Thomson's theory, for example, assumes that as long as an electron loses a certain amount of energy while within the distance a_o of a positive ion, recombination will then be automatic (i.e. the probability of recombination will be unity). Quantum mechanics gives a rather more subtle analysis of this process, while, in the limiting case, agreeing with classical arguments, which are seen as a statistical average.

---

* Actually $\alpha_N^{-1} = \alpha_H^{-1} + \alpha_T^{-1}$

Pitaevskii [37] tried a different approach, albeit again one based on classical notions. The recombination process was viewed as a diffusion of electrons in energy space described by the Fokker-Planck equation. Pitaevskii's work for a monatomic gas was extended to the case where the third body is a molecule by Dalidchik and Sayasov [38,39], and Sayasov [40] presented a theoretical α-T curve for the process

$$A^+ + e + H_2O \rightarrow A + H_2O$$

This was in good agreement with the results of Hayhurst and Sugden [28], for the case where A^+ was the ionized lead atom, over a temperature range $1685 < T < 2270^{\circ}K$. These theories, however, take no account of the nature of the ion.

The most advanced theories up to date appear to be the semi-quantal theories due to Bates and Khare [41], for the case of a monatomic gas, and Bates, Malaviya and Young [42], for the case of a molecular gas. The population of the available energy levels within the recombining ion are considered. Since these levels do not form a continuum, the use of the Fokker-Planck equation is stated to be invalid; although agreement between Pitaevskii [37] and Bates and Khare [41] is found at low temperatures, (i.e. room temperature and below), Pitaevskii's assumed continuum model probably gives values of α that are too high at high densities and temperatures. At sub-atmospheric pressures Bates and Khare agree with Pitaevskii even at the comparatively high temperatures encountered in flames. Pitaevskii's value of α, α_p, is higher than that predicted by Thomson [32] by a constant factor

$$\frac{\alpha_p}{\alpha_T} = \frac{9}{2}\left(\frac{6}{\pi}\right)^{\frac{1}{2}} \simeq 6{\cdot}2$$

Remarks of much the same tenor apply when Bates, Malaviya

and Young's value of α is compared with that of Dalidchik and Sayasov. A drop in α of some 30-40% is to be expected as the ionic mass rises from 2 a.m.u. to infinity, but the authors claim the theoretical results to be no more accurate than a factor of two due to the nature of the approximations made in their treatment.

In consequence, they point out that more experimental work must be done in order to help clear the way for further advances in theory. A similar state of affairs exists with regard to other ionization parameters, notably the ionization cross-sections of alkali metals measured in flame systems. Theoretical attempts to explain their magnitude have only recently begun to appear. They will be discussed in the context of the results found here (Chapter 7).

1.3 Objects of the present work

The present work is an attempt to help in the clarification of the state of affairs described, by a development of new experimental techniques and the presentation of relevant results.

The parameters measured were the ionization cross sections of potassium and sodium in the products of a premixed hydrocarbon (ethylene)-air flame, and the recombination coefficient of the alkali metal ions with electrons or a mixture of electrons and negative ions in the same products.

CHAPTER 2 AVAILABLE MEASUREMENT TECHNIQUES

2.1 Charge Density Measurements

Up to the time of writing, just two methods have been widely used for measuring charged species concentrations in flames; these entail the use either of microwaves or of Langmuir probes of planar, cylindrical or spherical geometries.* Naturally, the development of another, independent, technique would be a useful addition to this armoury in view of the often contradictory results obtained and because of the uncertainties in interpretation. The discussion below goes into some of these difficulties.

2.1.1 Microwave Techniques

Most microwave experiments make use of a change in the Q factor of a resonant cavity when radiation is adsorbed by electrons (Sugden and Thrush [43], Sugden and Wheeler [44], Padley and Sugden [30], Jensen and Padley [45]). An early attempt (Belcher and Sugden [46]) made use of the direct attenuation of the waves, but this led to values of the electron-neutral collision frequency ($8.8 \cdot 10^{10}$ sec^{-1}) which, in the light of subsequent research, must be adjudged on the low side. That this attempt was only partially successful might be put down to the relative insensitivity of measuring attenuation as compared with measurement of changes in the Q factor. However, there is another factor, probably present in Belcher and Sugden's work, which precludes the use of microwaves to measure total charge concentrations in most flame plasmas of temperature less than ca.1800-2000 K. This is the depletion of free electrons due to their attachment

*Mass spectrometry has also been used with some success, especially to identify the ions present, but its use cannot be called widespread.

to relatively massive species, and the consequent inability of these heavy ions to respond to the AC field vectors of the microwaves. Thus both attenuation and resonant frequency measurements lead to an underestimate of electron concentration and conductivity in many, if not most, low temperature plasmas. Another source of error, not allowed for in early work using this technique, is again the underestimation of electron concentration, this time due to a finite value of the ratio electron-neutral collision frequency to microwave frequency, which reduces the sensitivity of the cavity (Shohet and Moskowitz [47]).

In contrast to Belcher and Sugden, Bulewicz [48], again using microwaves, found electron-neutral collision frequencies and cross sections rather higher than those normally accepted; these results are again dependent on attenuation measurements.

Certain papers (e.g. Keen and Fletcher [49]) have shown good agreement between probe work and microwave cavity techniques, based on either cavity resonance or the upper hybrid frequency, the scatter of the results being only $\pm$ 25%. But the general comment that may be made of most, if not all, of these correlations is that they are limited in their range of applicability especially if they rely, as is the case in Keen and Fletcher's paper, on an empirical calibration. The statement in their paper that disparities exist of a factor of 2-3 between Langmuir probe and other methods is rather more generally true than the good correlation they obtain in the ion density range 10^9-10^{11} cm^{-3} at what is probably room temperature, an elevated electron temperature and what for flames must be a low pressure.

2.1.2 Probe Techniques

Turning to probes, much of the early work was based on the original analysis of Langmuir (Langmuir and Mott-Smith [50]), as later modified by Bohm, Burhop and Massey [51]. As Calcote [52] and Porter, Clark, Kaskan and Browne [53] have pointed out, the results are accurate to a factor of about two, with further advances being dependent on developments in probe theory and/or a more exact knowledge of electronic and ionic collision cross-sections. Calcote [54] published values of both positive ion and electron densities for, inter alia, a low pressure propane-air flame of temperature 2100 K, in which the ratio of the two varied from 16 to 2, reaching a maximum just before the peak electron temperature. Such a discrepancy is probably due to an insufficiency in theory as much as the presence of negative ions.

Great steps forward were taken with the publication of the probe theories of Lam [55], and Su and Lam [55]. Whereas Bohm, Burhop and Massey's theory gave an easily calculated result for ion density from the probe measurements, it did not provide a description of the observed dependence of the current drawn upon the applied voltage. Lam's theory rectified this omission, and Su and Lam's theory was applied to flame systems by Bradley and Matthews [57, 58]. For some time, theories based upon one or other of these two basic theories have held sway.*

For example, Soundy and Williams [59] adapted Su and Lam's theory for negative probes in a high pressure plasma, and

*Bradley and Ibrahim [27], developing the Su and Lam approach, have now been able to derive positive ion densities that are not dependent on some assumed value for the ionic diffusion or mobility coefficients; this may have gone a long way towards eliminating the error of a factor of 2-3 in ion density measurements referred to in the above text.

their formulation was taken over by Kelly and Padley [60], who quote the expression for the positive ion density:

$$n_+ = \frac{1}{4\pi kT} \cdot \frac{1}{(4r_p \mu_+^2)^{2/3}} \left(\frac{I^2}{V_p}\right)^{2/3}$$

Here r_p is the radius of the spherical probe, μ_+ the positive ion mobility, and I the current flowing between the burner top and probe at potential V_p. Kelly and Padley attempted to fit this to a situation involving equilibrium ion density (calculated from Saha's equation), and found a relation between ion density and probe current as indicated by the above equation. For full agreement, however, values of μ_+ of ca. 350 $cm^2\ V^{-1}\ sec^{-1}$ for the alkali metals are needed (Kelly and Padley [61]). These are in disagreement with values of ca. 20 $cm^2\ V^{-1}\ s^{-1}$ at flame temperatures based on simple theoretical calculations (Appendix A and reference 27), although values ranging from 1 to 350 have been reported (Table 1, ref. 27) in flame measurements. At room temperature, Mitchell and Ridler [62] measured $\mu_+ \simeq 2.5\ cm^2\ V^{-1}\ s^{-1}$. It will be noted that

$$\frac{(\mu_+)_{2000}}{(\mu_+)_{300}} \simeq 8 \simeq \left\{\frac{2000}{300}\right\}^1$$

or $$\mu_+ \propto T^1$$

This makes $n_+ \propto T^{-2.3}$, whereas Kelly and Padley [59], in stating that

$$n_+ = \frac{1}{4\pi kT} \left(\frac{1}{4r_p \mu_+^2}\right)^{2/3} \propto T^{-1}$$

appear to be maintaining that μ_+ is independent of temperature. Experimentally, the dependence on temperature was observed to be $\sim T^{-2.5 \pm 0.5}$ which is in line with what might be expected on the

basis of the above arguments.

It should be noted that other probe work is being carried out along slightly different lines by Clements and Smy [63], who maintain, approximately, the dependence of n_+ on I and V_p as given by Kelly and Padley but also take into account plasma flow velocities. Their expressions are, for a thin sheath

$$I = \{72\, r_p^{\,8}\, (n_e e\, u_\infty)^3\, V_p^{\,2}\, \mu_e\, \varepsilon_o\, \pi\, a^{-3}\}^{0.25}$$

and, for a thick sheath,

$$I = (V_p\, r_p)^{0.8}\, (n_e e\, u_\infty)^{0.6}\, \pi\, (6\, \varepsilon_o\, \mu_e)^{0.4}$$

Here u_∞ is the plasma convection velocity, a the radius of an annular insulator which surrounds their plane stagnation probe, of radius r_p, and ε_o is the permittivity of free space. The fact that their probe is planar rather than spherical is not of great consequence, especially if the sheath is thick (i.e. comparable in size with the probe radius), even though the latter of their two expressions was derived for a spherical probe. In the limit of low probe voltages and high electron densities (ca. 10^{12} cm^{-3}), their theory tends to that of Maise and Sabadell [64], which is based on that of Lam (op. cit.) in similar conditions of probe voltage and ion density. However, Maise and Sabadell's expression can fail by about two orders of magnitude if either of these restrictions (low probe voltage and high electron density) is violated, whereas Clements and Smy's expressions do seem to give fair agreement with a microwave-calibrated ion density over a wider range than that of Maise and Sabadell. Clements and Smy's expressions may then be regarded, as they claim, as empirical expressions with a reasonably sound physical basis.

It is noted that, in the case of a thin sheath, the same current-voltage dependence appears as in the Soundy and Williams/Kelly and Padley approach, but the rest of the expression is markedly different. This may possibly explain Kelly and Padley's inferred mobility coefficients.

2.1.3 Other techniques

Besides mass spectrometry, already referred to, other techniques of charge concentration that merit discussion as being of possible relevance at the upper and lower concentration limits measured in this work are infra-red interferometry and RF measurements respectively.

Incoherent 300μ far IR radiation was used by Brown, Bekefi and Whitney [65] to measure, by means of the phase change on passing through a plasma, electron densities in a discharge down as far as 10^{12} cm^{-3}. Recently, Hubner, Jones and Bose [66] and Hubner and Jones [67] have used an HCN 337μ laser to measure electron densities down to $3 \cdot 10^{12}$ cm^{-3}. Without any further development of their technique, densities of half this amount, corresponding to one twentieth of a fringe shift can be measured.

At the other end of the scale, Borgers [68] used alkali-seeded flame gases as the dielectric medium in a parallel plate condenser and observed the behaviour of the resonant circuit which included this. Since a condenser was used, spatial resolution had to be sacrificed and density values had to be averaged over the 2 cm height of the plates. Electron densities measured were in the range 10^{8}-10^{10} cm^{-3}.

Densities in the present work range from 10^{10} cm^{-3} to in excess of 10^{11}. Neither of these techniques is therefore

really adequate for present purposes.

A conclusion to be drawn from this is then that other, independent, methods of measuring ion densities would be useful. Such a method is discussed below. It is similar to the microwave resonant cavity method in that it gives an average density over a given cross-sectional area, but is probably capable of better resolution along an axis normal to that area. (Microwave measurements are usually averaged over an axial distance of ca. 3 mm.) Thus the axial resolution is somewhat similar to that of a fine wire probe, and indeed, the method does use somewhat similar current-voltage characteristics.

2.1.4 Ion Densities from Electrode Measurements

The method adopted in the present work for measuring the positive ion density (and hence conductivity) was based upon the application of a small voltage across the seeded hot flame products, see fig. 3.1 for the general arrangement. The current-voltage characteristics were measured at various heights of the electrode above the burner.

Before describing the technique used, a brief summary of previous work using similar techniques will be given.

Like methods have been used in the past with only qualified success. Within this earlier corpus of work, that of H.A. Wilson, carried out mainly in the first three decades of this century, merits special examination; for the purposes of the present investigation, Wilson's [69] 1931 paper is the most important, although, it may be noted, his earlier paper (Smithells, Dawson and Wilson, [70]) uses a similar technique.

Sheet platinum electrodes, 3 cm x 1 cm, were put at

the end of a long, rectangular burner, having a slit 15 cm x 0.2 cm cut in it for a coal gas- or natural gas-air flame seeded with sodium. A voltage was applied across these electrodes, and the voltage at individual points along the axis of the electrodes measured by a fine wire probe connected through a quadrant electrometer to one of the electrodes. These measurements revealed an essentially uniform field (except in the electrode sheath regions) and an essentially undisturbed electron concentration of $2.5 \cdot 10^{9}$ cm^{-3}; this, combined with an ion production rate of ca. $5 \cdot 10^{12}$ $cm^{-3} \cdot sec^{-1}$, about which there is more than a little doubt, leads to a recombination coefficient of $8.5 \cdot 10^{-7}$ cm^{3} sec^{-1}. If one uses a more realistic value for electron mobility than those of Kean and Wilson (Wilson, op. cit.), Wilson,[71] and Bennett [72] which, although probably depressed by the presence of negative ions, were still being quoted quite uncritically forty and more years later (King [73]; Poncelet, Berendsen and van Tiggelen [74]; Kydd [75]; Fristrom and Westenberg [76]; Feugier [77]) then the recombination coefficient comes out even higher at ca. $5 \cdot 10^{-6}$. A possible cause of Wilson's error seems to lie in his conversion of the observed "nearly uniform potential gradient" into a "uniform" one for the purposes of his analysis. This leads to the neglect of field derivatives and hence electron diffusion velocities in a direction opposed to the field-induced electron velocity in his equation. As a consequence, the electron density he derives is probably an underestimate of the real value.

Poncelet, Berendsen and van Tiggelen (op. cit.) tried, some twenty-five years after Wilson's [69] paper, to measure the ion density in the reaction zones of acetylene-oxygen and

acetylene-nitrous oxide flames. At best, their work could, however, only give order of magnitude results, arising from their model of the reaction zone: in effect, a zone of uniform ion density having a constant 'average' temperature. Their reaction zone thickness is based on a global model of the reaction zone and is related to a specially and somewhat arbitrarily defined "average" temperature, and must be regarded as an arbitrary rather than physically significant quantity.

Their values of ion concentration (corrected downward by a factor of ca. 2.5 to allow for the mistake over mobility referred to above) are still somewhat on the low side, being comparable with, or possibly an order of magnitude or so less than, values obtained by fine probes (corrected to one atmosphere) at much lower temperatures than those used here. (Wortberg [78]; Calcote [52]; Porter [79]; Porter, Clark, Kaskan and Browne [53]; Calcote [54].)

Finally, in this review of attempts to deduce ion concentration from current-voltage characteristics, it is necessary to consider the work emanating from the General Electric Research Laboratories in the early 1960's (Kydd [75]; Lapp and Rich [80]; Harris [81,82]).

In Kydd's paper, a 1 cm^2 molybdenum disc anode is placed parallel to a heated graphite cathode, the axes of both being horizontal. Seeded hot gas from a burner below the pair of electrodes passes up through the inter-electrode space, and a graph is plotted of resistance of the plasma versus inter-electrode distance. Kydd was aware of the difficulty of determining the resistivity of the plasma within the test region and

relating it to the change in overall resistance which results in part from plasma outside this region. He obtained a correction factor by immersing the electrode pair in Na_2CO_3 solutions of standard strengths and conductivities, then comparing the resistance-distance graphs obtained in this way with those obtained when the intervening fluid is a gas plasma. Equivalent graphs are indications of equivalent volume resistivities, according to Kydd's arguments.

However, for a temperature of 2513 K, Kydd's plasma resistivity is $1,25 \cdot 10^3$ ohm cm, which corresponds to a number density of ca. $8 \cdot 10^{11}$ ions cm^{-3}, if a value of $6 \cdot 10^3$ cm^2 V^{-1} s^{-1} is adopted for electron mobility in this C_2H_2/air/K plasma, rather than his assumed value of 2,500. This ion density compares with the $4 \cdot 10^{13}$ cm^{-3} predicted from Saha's equation, or a factor of 50 greater than the one observed by Kydd, who attempts to explain the discrepancy by assuming an error in temperature measurement, or, perhaps, a non-uniform temperature profile; the temperature required for the observed ionization level is stated to be 1950 K.

It would seem that there are more fundamental reasons for the discrepancy than just this temperature error, which Kydd admits would have to be ca. 550 K. Empirical calibration methods are always open to question unless further justification for them is published. It is also not certain whether Kydd's analysis has allowed sufficiently for the relatively cold regions next to his electrodes.

Passing on to the work of Harris, we note a difference in the experimental set-up. A caesium- or potassium-seeded inert gas is passed through an axially located hole into a cylindrical

test section heated to the same temperature as the gases. A voltage is applied across the cylinder ends and the resultant linear part (from 30 mV to 10 V) of the current voltage characteristic is used for substitution in the equation

$$\sigma = \frac{I}{V} \cdot \frac{l}{A}$$

where l and A are the length and cross sectional area of the test section. Beyond the linear region $\partial I/\partial V$ may either increase, due to secondary ionization, or decrease, due to saturation effects; in fact, the current used was much lower than the saturation current. Nevertheless, the method is open to objection since implicit in the method is the assumption that the I/V characteristic actually describes conditions prevailing in the plasma. The fundamental objection to this interpretation is that the electrode sheath regions are ignored, in spite of their possibly dominant contributions.

These criticisms may cast rather more doubt on Harris's conclusions than is warranted, since the values he obtains for electron-neutral collision cross-sections compare favourably with those obtained by more satisfactory methods and rigorous analysis. Harris needed to introduce an empirical correction factor by normalization of his results at that seeding pressure corresponding to maximum conductivity (i.e. when the electron-ion collision frequency is the same as that for electron-neutral collisions). This factor brings his conductivity up to that predicted by Saha. This still leaves unexplained discrepancies between theory and corrected experimental values at other seeding pressures, as Harris points out.

This method, based, as it is, on an empirical

correction factor, which was applied to situations other than that for which it had been obtained, is clearly unsatisfactory. In the case of a reactive flame gas system, where non-equilibrium species concentrations are likely to occur, it is certainly not applicable.

Perhaps the most interesting of these conductivity experiments of the early 60's is that performed by Lapp and Rich. Two tungsten rods are used as electrodes, one above the other, such that their axes are normal to the gas flow from a potassium seeded C_2H_2/air flame. Fine wire probes, connected through a high resistance voltmeter, measure the field at points between the electrodes. A large anode voltage drop is noted, especially if the burner, rather than one of the tungsten rods, is used as the anode, together with a smaller cathode one, and a relatively small field in between.

With a temperature of 2470 K and temperature gradient of only ca. 15 K cm^{-1}, the "conductivity" appears to be constant until secondary ionization sets in. Again, as in Harris's work, this conductivity is given by

$$\sigma = \frac{J}{E}$$

$$= \frac{\partial J}{\partial E}$$

since the current density-field graph is linear until the onset of seconday ionization.

However, this approach gives ion and electron densities in excess of the maximum predicted by Saha's equation, it being assumed that hydroxide formation and electron attachment are negligible. Measurements of electron density using the Hall effect in crossed electric and magnetic fields give good agreement

with Saha, to within a factor of two, which represents the limit of accuracy of that experiment anyway. The apparent excess density of charged species is difficult to explain since, by drawing a current, there is a depletion of the ions, and were the method totally sound, results would tend to be on the low side of the theoretically expected values.

Despite these failures, it was thought, at the start of this work, that, properly treated, a current-voltage characteristic would yield correct values of the undisturbed ion density. The system chosen, described in chapter 3, is somewhat akin to Lapp and Rich's, rather than Kydd's or Wilson's, in that the electrodes are normal to the direction of flow of the plasma, and, as will be shown in chapter 5, this flow figures prominently in the analysis of the readings. The electrodes chosen were somewhat akin to Harris's, being planar, although permeable over their whole surface, in effect, rather than having axial holes as in Harris's case.

Similarities in the current-voltage characteristic between this present work and that of the users of Langmuir probes will be noted, and, from these characteristics, the ion density will be calculated.

The shortcomings of the previous studies using a conduction based technique may be overcome, as will be demonstrated shortly. However, a powerful additional reason for the adoption of a method using an electrode system to measure ion density (and hence conductivity) is the ease with which it can easily be extended to the measurement of absolute rates of ion production, as is discussed below after a brief review of past attempts to measure ion production rates.

2.2 Ion Production Rates

2.2.1 "Rate of growth" of ion density methods

Thermal equilibrium ionization may be approached from either side. We have, above, already noted the mass spectrometric work of Hayhurst and Sugden [28], who observed the decay towards equilibrium of lead ions produced in super-equilibrium concentrations by charge transfer with hydronium ions, thermal ionization being negligible at flame temperatures for lead (ionization potential 7.4 eV).

Equally well, one can observe the growth towards equilibrium of metal ions. Such measurements are made in flames that produce negligible natural ionization, viz. carbon monoxide- or hydrogen-burning in oxygen-nitrogen mixtures, so there can be no possibility of charge transfer reactions or interference from natural chemi-ions.

Even for the low ionization potential alkali metals, the ionization rate is slow enough to restrict these "rate of growth" techniques to temperatures in excess of 2000 K. Hydroxide formation may also cause problems: partly because hydroxide concentrations, which come into the relevant equations for ion growth, have often had to be calculated on the basis of thermodynamic data that are now outdated, and partly because the hydroxide concentration itself may alter due to the decay of radicals towards equilibrium in hydrogen flames burning at less than ca. 2300 K, thereby possibly introducing spurious gradients into the graphs of ion growth.

For low ionization levels charge concentrations are usually measured by either probes or microwaves, as discussed

above, though in the work of Hayhurst and Sugden concentrations were measured in conjunction with a mass spectrometer, and in that of Hayhurst and Telford [83], solely with a mass spectrometer. These measurements, as has already been noted, are subject to systematic error.

For higher ionization levels, photometric measurements can be used. Jensen and Padley [84], for potassium, were able to work in the regime where both optical and microwaves could be used and obtained good agreement between the two; Kelly and Padley [85] compared optical and probe measurements with less success for the same metal. At these higher ionization levels, however, there is the possibility of interference from the back (recombination) reaction, which is not always allowed for. Instead, it is assumed that a straight line graph is an indication that the back reaction is negligible. While linearity is certainly a necessary condition, it may not always be sufficient, and, indeed, one sometimes in review papers comes across experiments that have had to be rejected because of neglect of the effects of the back reaction and the consequent systematic error introduced.

Hollander [86], in work published publicly in, among other papers, Hollander, Kaff and Alkemade [87], used a photometric technique for measuring the variation of atomic alkali concentration with height in carbon monoxide/oxygen/nitrogen flames. By adding an electron-donor element (caesium) in the case of potassium and sodium seeded flames, he was able to suppress their ionization and compare alkali atom concentrations with and without suppression. This gave the ion concentration, from which a comparison was made with the levels expected theoretically from the Saha-Boltzmann

equation. From the lag in the establishment of equilibrium, Hollander calculated the finite ionization and recombination rate constants for caesium, potassium and sodium.

The presence of natural flame electrons from hydrocarbon flames gives rise to very similar curves to the ones Hollander observed, created by the relaxation towards equilibrium. Hollander himself seems of the opinion that this similarity precludes the use of his technique for measuring ionization rates in hydrocarbon flames and indeed quotes no values except those found in carbon monoxide flames.

All the difficulties discussed in this section may be avoided by using the technique described below, which is generally applicable at temperatures below ca. 2000 K in hydrocarbon flames, and thus extends the range over which ionization and recombination parameters may be measured.

2.2.2 The saturation current density method

The only way to determine the point by point ion production rates directly, i.e. without inferences based upon ion concentration measurements corrected for diffusion and recombination, is by use of the saturation current measurement technique. Using the electrodes employed for the ion density determination, one simply reverses and increases the voltage applied across the flame reaction zone and its attendant burnt gases (see Fig. 3.1) until the current drawn ceases to increase; all the ions produced are, in this case, withdrawn from the system before they have a chance to recombine (see Fig. 5.4). Thus the current obtained, referred to as the saturation current, measures directly the rate of charge generation in the space between the electrodes. If the voltage

is further increased, the current again begins to rise with the onset of secondary ionization, resulting from electrons accelerated in the field to energies above the ionization threshold (close to the ionization potential) of the neutral gases present. (See Fig. 5.4 again). Eventually, as the voltage and field are increased even further, arc or spark breakdown ensues. The focus of attention is, however, on the saturation current plateau region, where an increase of voltage has no measurable effect on the current.

Most saturation current density measurements have been carried out on a Botha-Spalding porous disc burner [88]. This allows the stabilisation of a flat flame in a plane normal to the direction of the gas flow over a wide range of volumetric flow conditions even at atmospheric pressure. The sintered disc itself acts as a heat sink. A slight decrease in flow velocity of the reactants causes the flame front to come closer to the burner, more heat is lost to the burner, the final flame temperature drops and, in consequence, so does the burning velocity. Hence a new equilibrium position is set up. The reverse arguments apply in the case of a small increase in reactant flow velocity, until a new equilibrium position is again set up, this time further away from the burner. Saturation current densities can therefore be measured as a function of flame temperature for the same reactants, and global activation energies measured either in terms of the charge produced cm^{-2} s^{-1} or, in hydrocarbon flames, charge produced per carbon atom consumed per second, plotted against the reciprocal of temperature.

Where metallic seed material is to be introduced into

a flame, normally some other type of burner is used since it is difficult to get the seed material through the pores of the disc without blocking them. In the present work, a Meker burner is used. Instead of a flat flame, a series of small interconnected cones is produced, but similar stability criteria exist to those in the Botha-Spalding disc case, thereby allowing a sufficiently wide range of flame temperatures to be produced from the same gas mixture. Local mixing ensures uniformity across a cross section parallel to the burner top a short distance above the apices. Since it is this region downstream of the reaction zone that is of primary interest in this work, non uniformities in the reaction zone are not of any importance there.

If we limit ourselves to an essentially unidimensional region of length l downstream of the reaction zone, in which charged species of both signs are produced at a rate q ions cm^{-3} s^{-1}, the general charge conservation equation for the positive species may be written:

$$q - \alpha n_+ n_e = \frac{1}{e} \frac{\partial j_+}{\partial x}$$

$$= \frac{\partial}{\partial x}\left\{ n_+ \mu_+ E - D_+ \frac{\partial n_+}{\partial x} + u n_+ \right\}$$

Here j_+ is the positive ion current, E the applied field, u the gas convection velocity (more or less constant), and x the distance co-ordinate. The equation is simplified by the assumption, implicit in it, that all the negative charge consists of electrons; the arguments are not affected materially if fuller equations including negative ions are used. The above leads to

$$\frac{1}{e} \int_0^l \frac{\partial j_+}{\partial x} \, dx = \int_0^l q \, dx - \int_0^l \alpha n_+ n_e dx$$

Two limiting cases may be distinguished. First, for a large field, $n_+ \simeq n_e \simeq 0$ so

$$(j_+)_1 - (j_+)_o = j_s = e\int_o^l q\, dx,$$

i.e. there is no charge recombination, and a saturation current of current density j_s is produced, equal to the rate of generation of charge, multiplied by the electronic charge.

The other is the case of a current tending to zero (which means in effect a small field), and a high ion concentration. Recombination involves the square of the ion density, electron and positive ion densities here being essentially the same, whereas convection, diffusion and electrically induced motion all involve n_+ to the power unity. The recombination process therefore predominates over these latter, leaving

$$q \simeq \alpha n_+^2$$

Until now, this technique has mainly been used to measure the activation energy for ion production in hydrocarbon-oxygen and -air flame reaction zones (Lawton [89], Lawton and Weinberg [90]).*

Since the publication of Lawton and Weinberg's paper, the value of the technique has become more appreciated. Much of

---

* Saturation currents were also obtained by Payne and Weinberg [91] in their work on increasing heat transfer rates by using the ionic wind effect but were not interpreted in terms of ionization rates. Saturation current measurement is employed in the flame ionization detectors used in gas chromatography; their current-voltage characteristics are described by Bolton and McWilliam [92]. The values of ionic mobility chosen by these latter authors are by no means convincing, and seem to have been adopted without any attempt at a critical evaluation of the differing values cited in the literature. This may account, at least in part, for the only fair agreement between theory and experiment for one of their mobility-dependent constants of integration.

Melinek's [93] thesis depends on this technique for the measurement of ionization energies of various systems, and the method has been used in conjunction with mass spectrometry, which identifies the various positive ions produced (Arrington, Brennan, Glass, Michael and Niki [94]).

Nesterko and Rossikhin [95] used the technique, again to measure activation energies, but did not appreciate the necessity for changing the temperature by varying the flow rate. Instead they changed the fuel/oxygen ratio, and since the saturation current drawn is in fact dependent on this ratio, the magnitude of their results for the ionization activation energy must be treated with caution. In common with the present work, some of their flames were seeded with ionizable material (sodium and potassium). They found the apparent activation energy in the burnt gas region for these metals to be only ca. 50 kcal $mole^{-1}$, which is only about half the ionization potential. Glushko, Tverdokhlebov and Chirkin [96], working with a low pressure C_2H_2-air flame, obtain ca. 20 kcal $mole^{-1}$ for lean and slightly rich flames, but something like twice that value for a smoking flame. No details, however, are given about the volume of burnt gases above the reaction zone, so it is not possible to gauge the contributions made within and above the reaction zone, and this latter result should be treated with caution. Much the same results are published in Tverdokhlebov and Chirkin [97]. A very controversial aspect of this work is the deduction of ion production rates by dividing the saturation current density by a value for the flame reaction zone thickness, arrived at either by some rather crude model (e.g. van Tiggelen and Vaerman [98]), or by observation of a

half-width from the steady state ion density profile in the absence of a field (Taran and Tverdokhlebov [99]).

Despite the introduction of an arbitrary or dubious reaction zone thickness, the quotient (see above) of the maximum ion production rate and the square of the maximum ion density (observed by small probes) does give in Taran and Tverdokhlebov's work a recombination coefficient very similar in size (2×10^{-7} cm^{-3} s^{-1}) to that observed downstream of the reaction zone in other work. Lead and bismuth salts were also added to the flame and the recombination coefficient downstream of the reaction zone, assuming no further ionization, was derived from the standard equation (see, e.g., Calcote [52])

$$D_a \left[\frac{\partial^2 n_+}{\partial x^2} - u \frac{\partial n_+}{\partial x} - \alpha n_+^2 \right] = 0$$

where D_a is the ambipolar diffusion coefficient, other terms having been defined previously.

The last point to be noted in this brief review of previous work with saturation current is that virtually nothing has been done in the way of measuring an increase of saturation current downstream of the reaction zone with the exception of certain parts of Melinek's thesis (Melinek [93(a)]). For a hydrocarbon-air flame, Melinek claims to have observed ionization downstream of the reaction zone in the absence of metallic seed, the ionization rate falling off inversely as the square of height. There is some doubt, however, because close proximity of the top electrode to the reaction zone may have caused some quenching and lowering of the final flame temperature; thus, as the electrode was moved away, the small increase in saturation current might

have arisen from a slight increase in temperature of the reaction zone.

Melinek et al [24] are on much firmer ground in dealing with ionization from a sooting flame, when they obtain in the burnt gas zone, an ionization activation energy (or, more correctly, work function) of 4.62 eV for soot particles, which compares particularly favourably with that for graphite (4.4 eV). In this experiment, the saturation current density is very low up to about half a centimetre above the reaction zone. From there onwards the burnt gases have the yellow luminosity characteristic of soot, and the saturation current increases linearly with distance by an order of magnitude over a distance of ca. 2 cm at 1784 K.

Similar to the above, but only semi-quantitative in nature, is Melinek's [93(b)] statement that the ionization, due to sodium introduced into one of his flames, approximately doubles as the distance of the upper electrode from the reaction zone is doubled.

The use of the saturation current technique for measuring activation energies in the reaction zone, using an Arrhenius expression is, by this time, firmly established, as long as the elementary precaution is taken to alter flame temperature by altering the flow rate rather than the equivalence ratio. Nothing more need be said on this score at present.

The intention of the present work is to develop the technique one stage further so that it is capable of determining, quite unambiguously and without the need for any dubious assumptions about reaction zone thickness, whatever that may be, an ion production rate. This is done by measuring quantitatively what

Melinek et al [24] measured qualitatively, i.e. the increase in ionization current above the reaction zone for a flame seeded with an alkali metal.

CHAPTER 3 THE EXPERIMENTAL APPARATUS

3.1 The flow system

While the apparatus constructed and used was of quite a simple design, it nevertheless conformed to a number of quite strict conditions. These are that the part of the flame being studied must be sensibly one dimensional in flow and uniform in temperature and ion density, especially if seeded, across any cross section, as well as both being stable over long enough periods of time to allow measurements to be made with ease, and being reproducible from day to day. In addition, faults which develop should become apparent as soon as possible, so that corrections may be made before too much time is wasted, and the whole apparatus must be capable of being cleaned and reassembled without great difficulty. A diagram of the apparatus developed is shown in Fig. 3.1; certain minor modifications to this circuit were sometimes necessary (e.g. the substitution of hydrogen for ethylene as a fuel in the annular flame which shielded the seeded central core upon which measurements were made); and, given this flow network, were easily introduced. This shielding technique, using an annular flame of the same composition and flow rate as the main central flame, to ensure uniformity of temperature and temperature-dependent parameters across a cross-section is quite standard (Sugden and Wheeler [44]; Knewstubb and Sugden [100]).

Flame instability caused by gas flow fluctuations was rare. Air was taken from a compressor manufactured by Whittaker Hall & Co., capable of delivering 900 litres per minute at pressures of up to 150 p.s.i. ($1.07 \cdot 10^6$ N m^{-2}). The air passed through an oil filter, pressure reducing valve and large ballast volume

(to even out possible fluctuations) before being dried and metered. Commercial-grade ethylene (99.85% purity) had to pass through a similar circuit (except that the oil filter was absent) before being metered; because of its large Joule-Thomson effect, it was also necessary to heat the ethylene cylinder head to ensure a steady flow. No such difficulties were found with nitrogen (used in small quantities as an additive), so it was passed directly from the cylinder through a valve to a capillary flow meter (marked C.F.M. on Fig. 3.1). This and the other capillary flow meters were calibrated using a bubble meter (Exner [101]) under the pressure conditions encountered in practice. Where the flow conditions were not quite as critical, viz. in the annular sheathing flame, or where the volumetric throughput did not need to be known with such accuracy, rotameters were used; these were calibrated in the same way as the capillary flow tubes, and are marked "ROT." in the figure.

Manometers 1 and 2 read the same to within one torr while manometer 3 read within one torr of atmospheric pressure. Any blockage in the flow system was shown up immediately by the departure of one or more of the manometers from its set value.

Most of the flames studied had the same unburnt composition, so, in order to burn the gas at different temperatures, it was necessary to bleed off a certain fraction of the unburnt mixture, thereby reducing the volumetric throughput to the burner (see chapter 2). This was done before some of the mixture passed through an atomiser of standard design, whose reservoir contained sodium or potassium carbonate solution, or a mixture of the two in sufficient strength to cause measurable ionization in the hot gases produced by the flame. A fine mist of this solution was

carried along by the atomiser gas flow before being united with the main body of the gas (which had not been bled off) in a mixing chamber. This chamber was found necessary since a T-junction quickly blocked up from salt depositions.

The combustible mixture then went into the central cylinder of a brass Meker burner, cooled by a continually circulating current of water driven at constant speed by a small pump. Rather than have a burner constructed from a bundle of hypodermic needles, as was the case in the two papers quoted above in which shielded flames were used, here the top of the burner consisted of a disc and annulus, each drilled with regularly spaced 3/64"-diameter holes. This avoided any problem there might otherwise have been due to the blocking up by salt deposits of small bore tubes.

Both independently fed sections of the burner contained a sufficient number of small glass balls to provide a uniform gas flow. In the central cylinder was a metal gauze to prevent any of the balls falling down and blocking the entrance to the burner. If the height of any of the flame cones on the burner became more than about 3 mm, the glass beads were rearranged to even out the flow and ensure a uniform cone height. What might be called the "characteristic" temperature of each flame was measured by a sodium D-line reversal technique (see below) with the beam incident on the centre of the seeded part of the gases at a height of 6 mm above the burner. Immediately this changed by more than $\pm 7^{o}$ K, the minimum observable change using the eye, rather than, say, more quantitative photoelectric means, the flow system was checked and corrected to bring the temperature back to normal.

The seeded part of the post-reaction zone burnt gas region

had to be maintained as a right circular cylinder. In the absence of any flow constraint above the burner, air entrainment would cause, instead, this region to be onion-shaped. A combination of a horizontal stainless-steel gauze of the same diameter as the burner, and an electrically-insulating chimney of slightly larger diameter, leading to an air exhaust system, brought the seeded burnt gas region back to the required shape. The gauze was suspended from a clamped metal rod which could be moved vertically against a Vernier scale, as could the chimney. The rod was electrically insulated by the clamp from earth so that a (flexible) high tension lead could be attached to it, thereby making an electrode of it; the other electrode was the metal burner itself.

3.2 The Electrical Circuit

Two major sets of measurements were made. In one a high potential ($\leq$10 kV) from a Brandenburg DC unit was applied across the flame in order to draw a saturation current. The other type of measurement goes to the other extreme and draws, by comparison, a very small current from the flame. This means that the charged species, instead of being collected at the electrodes, recombine within the flame, so measurements are made under conditions approaching as closely as possible the ideal of no electrical disturbance of the flame gases. These current-voltage measurements yield the positive ion density within the hot gas region. Stable characteristics were best obtained by applying the H.T. output from the Brandenburg across a high resistance ($5 \cdot 10^8$ or $1 \cdot 10^9$ ohms) in series with the flame and increasing or decreasing the applied voltage slowly. Previous measurements of the current-voltage characteristics of flames (Lawton [89]; Lawton and Weinberg [90];

Peeters, Vinckier and van Tiggelen [7]; Melinek [93]) have relied on a point-by-point plot of current against voltage. This technique was abandoned in this work partly because it is too time-consuming, but more seriously because it was not sensitive enough to show the relationship between saturation current and inter-electrode spacing at some of the lower temperatures used. A much better method is to use an X-Y plotter whose scale may be varied to give a maximum separation between adjacent readings while still keeping the whole of one set of readings on a plot of size 15 x 10 inches.

Besides rapid random fluctuations in the amount of seed material entering the flame, there are also longer-term instabilities, due to changes in volumetric throughput (if the compressor becomes overheated), changes in the atomiser, the build up of seed deposits in the flow system or burner system etc. The X-Y plotter allowed a full set of flame characteristics to be obtained in about one minute, thereby enabling us to measure the variation with height of parameters which, on a point-by-point measuring basis, would appear either to remain constant or would be within the range of error involved on one individual saturation current reading. Thus changes over a distance of 1 centimetre of ca. 1.2% in the saturation current could be observed, which meant an extension of around 30% in the temperature range studied.

The X-Y plotter used was an EAI 1130 Variplotter which had scales ranging from 1 mV per inch at an input impedance of 25 kilohm to 400 mV per inch at 1 megohm on both abscissa and ordinate. The abscissa also had another scale of 500 mV per inch at 25 kilohm up to 20 V per inch at 1 megohm, and a time base scale of from 0.5 to 20 sec per inch. A zero-bias was also used whenever any specific part of the current-voltage characteristic had to

be studied in more detail. The Variplotter was, in effect, used to measure the voltage across a small resistor in series with the flame and hence the current through the flame gases, and, when in series with a resistor much larger than its own maximum input impedance, to measure the voltage applied across the flame gases. The resistors used were calibrated, using resistors guaranteed to $\pm$ 1% with a standard cell, to an overall accuracy of $\pm$ 2%.

A diagram of the circuit is also to be found in Fig. 3.1.

3.3 Temperature measurement apparatus

Since in any case the flames were being seeded with alkali metal salts to provide a source of ionization in the hot gases, the method that lent itself most readily to the measurement of temperature was the spectrum line reversal technique, using the sodium resonance doublet lines at 589.0 and 589.6 nm. This method, by now standard, was first used practically at the turn of the century (Kurlbaum [102]; Fery [103]) although, in the former of those papers, it was the carbon particles in a fuel-rich flame which were matched to a variable background source, an optical pyrometer being used alone without need for a spectroscope.

The experimental procedure of the present work followed the course outlined by Gaydon and Wolfhard [104(a)]. A disappearing filament-type optical pyrometer, previously calibrated against a black body in the red part of the spectrum, is used, with a red filter, transmitting light of mean wavelength 655 nm, to measure the brightness temperature of the centre of the strip of a tungsten strip lamp. This is then related by the standard calibration to the true temperature of the lamp, which is the temperature a black body would have were it emitting the same

amount of light at that wavelength. An ammeter was put in series with the tungsten strip lamp so that the temperature of the strip could be determined uniquely by reference to the current through it. (This method is preferable to measuring the voltage across the lamp, which could be liable to change were contact resistances to appear in the circuit.)

Light from the tungsten strip was focussed on to the axis of the hot gases by means of a lens, L_1 (see Fig. 3.1). This image, together with the light from the hot gases (largely sodium resonance light), formed the object for a second lens, L_2, which gave an image on the slit of a spectroscope S. An aperture, A, was placed in the image plane of L_1, as formed by L_2, so that the solid angles subtended at L_2 by the flame gases and the image of the background strip are equal. If light emanating from the flame gases were to subtend a greater solid angle at L_2 (and hence the spectroscope slit) than light from the background source, then the measured flame temperature would have been too high. The positioning of the aperture outlined avoids this error. At all times, care had to be taken to keep the lenses dust-free otherwise the apparent temperature of the hot gases would be higher than the actual.

The sodium resonance doublet lines could usually be seen, by looking through the eyepiece of the spectroscope, against the background continuum provided by the strip lamp, either yellow in emission (indicating the background was cooler than the flame) or black in absorption (indicating the opposite). When the lines merged indistinguishably with the background then the two were at the same temperature, which could be ascertained by reference to the current-temperature calibration graph for the lamp.

Maximum contrast between the lines and continuum, and hence maximum accuracy, was achieved by adjusting the slit width of the spectroscope.

Certain errors creep into the method, however. First, although the lamp was calibrated for the red (655 nm) it was actually used in the yellow (589.0 and 589.6 nm). At the temperatures involved this means overestimating the flame temperature by about 15 to 20 K. However, this error is cancelled out to within a degree or two by the fact that there is a loss of light from the background lamp at two lenses, whereas light from the flame is lost at only one (Gaydon and Wolfhard [104(b)]).

Another error is due to the fact that the hot gas region is not optically thick, and so there is some emission of radiation from the flame which leads to a depopulation of the excited states of the sodium atoms as compared with full thermodynamic equilibrium. Gaydon and Wolfhard, relying on a quenching cross section for sodium resonance radiation by nitrogen of $14.5 \cdot 10^{-16}$ cm^2 measured by Norrish and Smith [105], found the effect of this to be equivalent to a lowering of temperature, assuming Maxwell-Boltzmann statistics, of 3.3 K. They pointed out, however, that Boers, Alkemade and Smit's [106] lower value for the cross-section for this quenching reaction led to an error of around 8 K at atmospheric pressure. This later value ($7 \cdot 10^{-16}$ cm^2 at 2200 K) was confirmed by Jenkins [107]. A table of quenching cross-sections from his paper for the gases which concern the present work is shown below (Table 3.1). Both Jenkins and Boers, Alkemade and Smit derived their results by observing the fluorescence of sodium in a flame.

TABLE 3.1

Gas	Temperature	Quenching cross-section ($cm^2 \cdot 10^{16}$)
N_2	1400 - 1800	6.95 ± 0.15
Ar	1400 - 1800	0.1
O_2	1800	12.3 ± 0.5
CO_2	1400 - 1830	17.0 ± 0.4
CO	1400 - 1830	11.9 ± 0.4
H_2O	1600 - 1800	0.5 ± 0.3

An average value, weighted according to the partial pressures of the gases present, of the quenching cross-section for this work is $7.5 \cdot 10^{-16}$ cm^2, and therefore the likely error is that the temperature has been underestimated by about 8 K.

In the present work, the burner could be moved both vertically and at right angles to the optical bench on which all the optical equipment was clamped. Temperature profiles were therefore obtained as functions of distance from the centre (uniform temperature) and height above the burner. A typical profile across a diameter is shown in Fig. 3.2. Slight irregularities of about $\pm$ 10 K ($\pm$ $\frac{1}{2}$%) were unavoidable and the 8 K error, referred to previously, was taken into account when measuring the average temperature at a given height. Temperature fell off with height quite rapidly due to the cooling effect of the gauze electrode, but at a given height it was found that the temperature was constant whatever the height of the electrode above it, with the sole constriction that the interelectrode separation did not exceed approximately 3 cm, this being the separation at which aerodynamic instabilities set in.

3.4 Measurement of the alkali concentration in the flame

With a couple of modifications, the method adopted to measure the sodium and potassium concentrations in the flame gases was that used by Gautier [108], Godard and Seyer [109], and, more recently, Knewstubb and Sugden [100]. The technique must measure the total amount of alkali passing through the burner in a given time; this cannot be equated to the amount being sprayed by the atomiser, since the mist settles out in non-negligible quantities at all points downstream of the spray.

For this calibration, only the central part of the Meker burner was used, the entrance to and exit from the surrounding outer annulus burner being sealed off. Dried air from the laboratory bench supply was passed through the atomiser, and along the same flow system as was used when flames were being burnt, into the burner at rates equal to the total throughput of all three gases (air, fuel and additional nitrogen) for each of the various flames studied. Usually the pressure head across the atomiser was kept, for a given throughput, equal to that used for the corresponding flame. To satisfy these conditions, the capillary flow tube normally used for measuring the air throughput was recalibrated so that, for each of the four different throughputs at one atmosphere and room temperature, we knew the differential height of the manometer for any given absolute pressure up to 340 torr above atmospheric, there being a constant pressure head of 260 torr across the capillary flow meter.

All this was necessary, since the air, having gone through the spray or its by-pass, was then sent through a half metre long column containing glass or quartz wool saturated with distilled water and placed on top of the burner, with a leak-free

joint between them. This, of course, introduced another pressure drop of up to 50 torr into the system. The glass wool filter was there to trap the sodium and/or potassium salts introduced by the atomiser; it was saturated since boiling distilled water had first been used to wash the wool, in order to get rid of a fine dust from the wool, together with other impurities. The alkali carbonate laden air passed through the filter for periods of up to ninety minutes. At an appropriate time, the air supply was turned off, the joint broken quickly and the seed material washed down into a 5-litre beaker with a further four litres of boiling distilled water, before samples were stored temporarily in polythene bottles prior to being analysed. An attempt was made to dispense with the filters, and just pass the gases through water. It was found that water alone is insufficient to trap more than a few per cent of the alkalis. Recently, this effect has also been noted by other authors (Johnson and Smith [110]).

The authors of the three papers referred to at the beginning of this sub-section (3.4), all, after having proceeded in principle as in the present work, then titrated for a halogen (chlorine, or bromine in the case of Knewstubb and Sugden).

Here a carbonate was used, so consequently a different method had to be used, and instead of measuring the halide concentration, we measured the alkali concentration. This explains the use of quartz wool in the measurements for sodium concentration, since boiling water leeches out sodium from ordinary glass wool.

The solutions prepared were analysed in a flame photometer for atomic alkali concentration. The instrument used was an EEL (Evans Electroselenium Ltd.) Flame Photometer Mark II, having

maximum linear full scale deflections corresponding to 5 p.p.m. of sodium and 10 p.p.m. potassium when the relevant filters were used with the inbuilt photocell. When necessary, solutions were diluted to bring them into the relevant linear regime of the flame photometer.

Certain checks were made in these measurements. As noted above, when glass wool is used, the observed sodium concentration is too high due to its being leeched out from the wool. So the amount of salts trapped in the tubing downstream from the atomiser, in the burner and in the rotameter were also measured. These gave the real proportion of sodium to potassium entering the flame (the same as in the seeding solutions), and also when the potassium concentrations in the glass wool, burner, tubing and rotameter were added to that which had collected in the smoothing volume of the atomiser, downstream from the spray itself, a figure was obtained consistent with the loss in alkali from the atomiser reservoir due to the action of spraying.

The main sources of error here appear to be in erratic functioning of the atomiser (which is just as likely of course when the seed is being fed into the flame), and in loss of seed through its dropping down into the burner or being blown by the air stream out of the top of the tube. To obviate these last two sources of error, spaces were left of approximately 10 cm at the top and 5 cm at the bottom of the half metre length tube; the middle 35 cm or so were packed with enough quartz or glass wool to trap all but at most 1% of the alkali seed. There was, due to the air stream, a layer of distilled water up to 5 cm thick on top of the wool, but only negligible amounts of this were blown, as spray, out of the column and lost. Nothing was usually

lost at the bottom of the column, since even if a considerable time elapsed between turning off the air supply and beginning the washing of the wool, the water just saturated the lowest part of the wool, which had over the course of this experiment been dried out by the air stream, instead of running down into the burner.

Results consistent to $\pm$ 8% (standard deviation quoted) were obtained from the flame photometric analysis of the solutions from the glass and quartz wool, and are tabulated below.

TABLE 3.2

Flame corresponding to volumetric throughput used	Final flame temperature (^{o}K)	Atomic alkali concentrations, p.p.m.	
		Na	K
A	2025	31.6	0
B	1957	9.8*	33.6
C	1890	5.6*	169
D	1818	12.5*	375

*Inferred from the potassium concentration

The final flame temperatures are calculated from extrapolations back to the reaction zone of the measurements of temperature versus height in the downstream region.

DIAGRAM OF APPARATUS

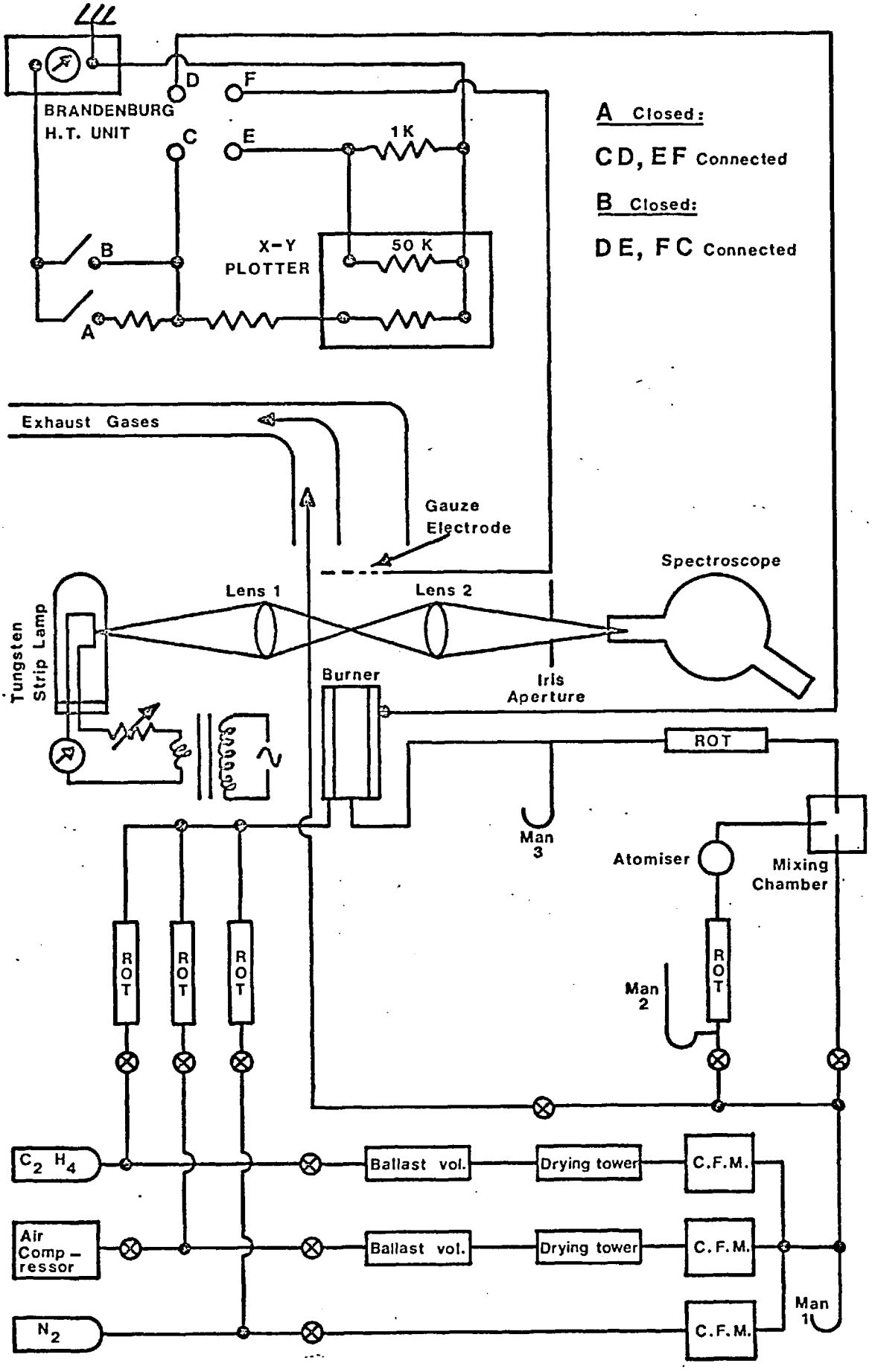

FIG. 3.1

TEMPERATURE PROFILE ACROSS A DIAMETER – FLAME C.

(Height 6 mm above the burner)

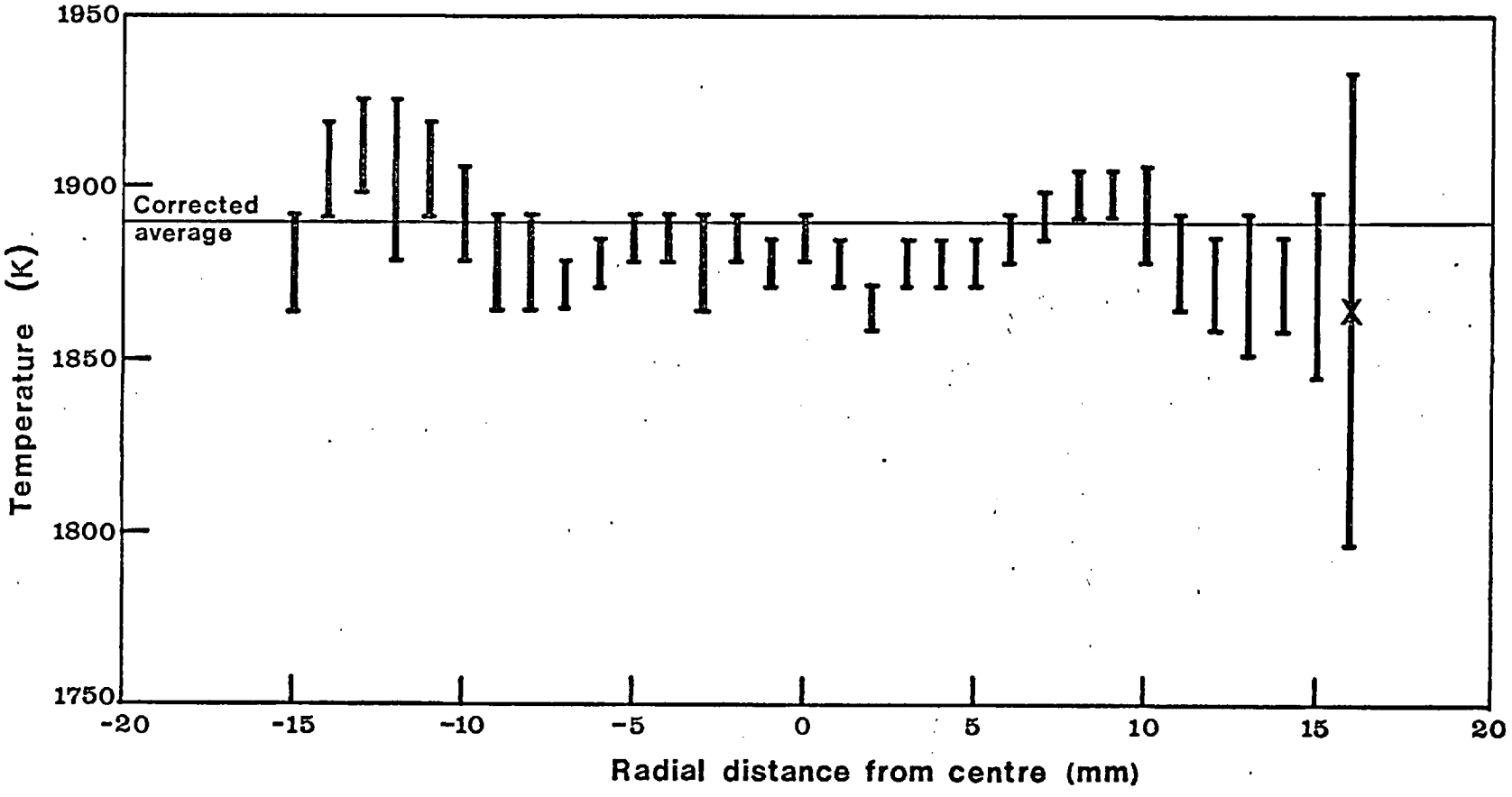

FIG. 3.2

CHAPTER 4 THE CHEMI-IONIZATION ACTIVATION ENERGY

It was found in practice that there was a more or less continuous range of temperature, extending over somewhat more than 300 K, in the hot gases produced by the four flames studied in detail. This afforded the opportunity of observing the magnitude of parameters of interest at any given temperature within this range, rather than just at the final flame temperature of each of the reaction zones. If plotted solely against these latter temperatures, the recombination coefficient for charged species and the ionization rate coefficient, at least, would yield totally false temperature dependencies; in addition to which enormous difficulties would arise in the interpretation of these restricted data. This comes about due to the production in the reaction zones, at least for the lower temperature flames, of certain slow-decaying radicals in quantities in excess of their thermodynamic equilibrium values, a phenomenon which will be discussed more fully later.

First, however, we shall deal with those readings and data directly necessary to the calculation of the activation energy for the production of charged species, before going on to ion density measurement, recombination coefficients and ionization cross-sections.

4.1 Composition of flames studied

In all, eight flames were studied at atmospheric pressure, their temperature range being determined by the necessity of having a saturation current plateau rather than a continuous increase of current with increasing voltage until secondary ionization sets in, and also of having measurably different

saturation current plateaux at different heights of measurement within the hot gases. If the temperature is too high the former condition is violated, and, if too low, the latter.

By trial and error, a fuel-lean flame composition was found which could provide flames burning at three different temperatures within this quite narrowly defined range. These differences were achieved by varying the volumetric throughput and hence the heat transfer rate to the burner, as explained previously. For each flame a sheath of similar composition shielded the inner core, on which measurements were made, from the atmosphere; its temperature was altered in the same way as the core's temperature. A hydrogen-air or carbon monoxide-oxygen sheath, both of which produced no measurable ionization compared with a hydrocarbon-air flame, was burned when measurements were being made on the unseeded core.

For these constant composition flames, the ethylene and air throughputs were fixed at a given value, so that when a lower temperature flame was needed, all that had to be done was to bleed off a given fraction of these gases. The volumetric throughput through the atomiser was kept constant at about two litres per minute (corrected to room temperature and pressure). A little extra nitrogen was added to some of the flames to provide a more uniform temperature profile in the core.

Table 4.1 gives the reactant compositions for the alkali metal-seeded flames studied (flames A-D), and an additional higher temperature unseeded CO-sheathed flame (E), and the volumetric throughput for these flames reduced to atmospheric pressure and room temperature (295 K). The equivalence ratio is defined as

the fuel:oxygen ratio present divided by that at stoichiometry.

TABLE 4.1

Flame designation	Equivalence ratio,	% N_2	Volumetric throughput, ml s^{-1}	Final flame temperature (^{o}K)
A	0.97	79.1	145	2025
B	0.73	78.1	128	1957
C	0.73	78.3	87	1890
D	0.73	77.3	66	1818
E	0.90	76.3	145	2082

4.2 The saturation current, ion yield and activation energy

The three seeded flames studied at atmospheric pressure having the same equivalence ratio afforded us the opportunity of measuring the global activation energy for the production of natural flame ions by burning the same flames without seed. In order to study a reaction zone of apparently uniform temperature, however, it was necessary to dispense with the ion-producing ethylene air shielding flame and instead burn a hydrogen-air flame whose ionization was completely negligible. The reaction zone temperatures of the ethylene-air inner disc flame were measured (by an extrapolation back from sodium D line reversals at different heights above the reaction zone) as 1957 K (flame B), 1890 K (flame C) and 1818 K (flame D), all to about $\pm$ 10 K or half a per cent. These three flames minus their alkali seed are flames F, G and H corresponding to B, C and D respectively, thus making up the eight atmospheric pressure flames referred to

at the start of section 4.1.

Total saturation currents were measured, in flames F, G and H, and, knowing the composition and volumetric throughput of the reactants, the ratio of ion pairs produced to carbon atoms introduced was calculated. The logarithm of this ion-production ratio was then plotted against the reciprocal of final flame temperature to give an activation energy, since we may write

$$\frac{N}{n_c} = AT^b \exp\left[\frac{-(E_a)_1 e}{kT}\right]$$

where N is the number of ion pairs produced per second, n_c the number of carbon atoms fed in per second, A and b constants, the latter of order unity, e the electronic charge and k Boltzmann's constant. A graph of $\ln \frac{N}{n_c}$ vs $1/T$ is a good straight line (Fig. 4.1) whose gradient, as may readily be appreciated, gives the activation energy for the process of ionization.

In measuring saturation currents, it was noticed that, for the hottest two flames, the saturation current increased with decreasing electrode height when the gauze anode was within about 1.5 cm of the reaction zone. Also the saturation current plateau became less well defined, developing a marked slope. These readings were ignored for this part of the work, an interelectrode separation of greater than 1.5 cm being used. For measurements with seed material, the current corresponding to a given electrode height for the unseeded flame was subtracted from the total saturation current, thereby ensuring that only the contribution of the seed material was considered.

Order of magnitude calculations on this saturation current-electrode separation dependence were carried out, using data

given by von Engel [111] on positive ion emission from hot bodies. The results were consistent with von Engel's suggestion. It should be noted that positive ion emission is made easier by the deposition of alkalis from the seeded flames on the anode, perhaps forming there some amalgam of lower work function than the electrode material itself.

A few words should perhaps be said on the use of the final flame temperature (or, rather, its reciprocal) as the abscissa for Fig. 4.1. Van Tiggelen has maintained (e.g. Peeters, Vinckier and van Tiggelen [7]) that it is possible to define a mean temperature, T_m, of the reaction zone

$$T_m = T_o + 0.74\ (T_f - T_o) \qquad \text{(van Tiggelen [112])}$$

where T_o and T_f are the initial and final temperatures, and that all natural (i.e. chemi-) ionization activation energies should be related to this mean temperature. However, as Weinberg pointed out (discussion appended to reference 8, q.v.), the experimental work of Melinek (Boothman, Lawton, Melinek and Weinberg [24]) shows that this mean temperature, at least for many hydrocarbon-air flames, corresponds numerically with that temperature, T_{CO}, at which CO and H_2O are produced. Further, in the same paper, Melinek, by using various additives, even such powerful inhibitors of flame propagation steps as bromine, to alter T_{CO} by up to 150 K while keeping T_f constant, showed that this led to negligible changes in the saturation current density. This insensitivity rules out T_{CO} as a useful temperature for the measurement of ionization activation energies, and because of the numerical coincidence, appears to rule out van Tiggelen's T_m also.

In contrast, however, there is certain evidence to link the

ionization step with the final flame temperature. Calcote's [52] analysis of a low pressure flame shows that the ion concentration peaks near the downstream edge of the reaction zone, in the position where Fristrom, Avery and Grunfelder [113] found that the most important flame species had levelled off to their final values, and the final flame temperature had been reached. Wortberg [78] found a similar result, as did Calcote, Kurzius and Miller [20]. Porter et al [53] found the maximum ion density reached a peak after the attainment of the final flame temperature, and at the same time shed some doubt on the most widely held mechanism for chemi-ion production.

Taran and Tverdokhlebov [99], using double probes in a 14-torr acetylene-air flame, found a coincidence of peak heights of both ion density and electron temperature, the latter being only a very slight peak. If Bell, Bradley and Jesch's [114] findings that the peak electron temperature occurs before the peak gas temperature is equally applicable to acetylene-air flames the picture becomes confused once again.

Since T_f is the most easily measurable temperature, and in the absence of any other well-established temperature, it seems safest to use T_f in dealing with measured activation energies for ionization. This statement, perhaps more than most, may have to be modified in the light of future research.

Since previous authors (Lawton [89], Melinek [93], Glushko and Tverdokhlebov [115]) have used saturation current densities rather than ion yields per fuel molecule or carbon atom consumed, comparisons are somewhat difficult between their and the present results. (The flames here, being composed of many small cones,

do not lend themselves at all easily to a direct measurement of flame area.) To attempt to obviate this difficulty, use may be made of results published by Kaskan [116], coupled with the argument below.

The ion production ratio, N/n_c, may be written, for flames of constant composition, as

$$N/n_c = A_1 \exp \frac{(-E_a)_1}{kT}$$

However, $N/n_c \propto \frac{I_s}{AS_u}$, where S_u is the burning velocity and A the flame area, or, writing this in another way $\frac{N}{n_c} \propto \frac{j_s}{S_u}$

j_s may be written as

$$j_s = A_2 \exp \frac{-(E_a)_2}{kT}$$

and S_u as $S_u = A_3 \exp \frac{-(E_a)_3}{kT}$

where in each case we have ignored the possible weak temperature dependence of the pre-exponential factor. From these equations we may write

$$A_1 \exp \frac{-(E_a)_1}{kT} \propto \frac{A_2}{A_3} \exp \frac{-\{(E_a)_2 - (E_a)_3\}}{kT}$$

Since this holds at all values of T,

$$(E_a)_1 = (E_a)_2 - (E_a)_3.$$

$(E_a)_1$ has been measured and, from Kaskan's graphs we find that for an ethylene-air flame of $\phi = 0.78$, quite close to our value of 0.73,

$$S_u = A_3 \exp -\left(\frac{1.04e}{kT}\right)$$

(This actually involves an extrapolation since the high temperature end of Kaskan's data overlaps only slightly with the low temperature,

1818 K, end of the present readings.) That is to say that the "activation energy" measured for the variation of burning velocity with temperature is 1.04 eV or 100 K joules per mole. This corresponds to Melinek's statement (Melinek [93(c)]) that the activation energy for the production of N/n_c is about half that for j_s, since a graphical interpolation of his results leads to $(E_a)_2$ = 222 k joules per mole at $\phi = 0.76$ for the variation of $\log j_s$ with $1/T$. In the present case, it appears, by adding the measured $(E_a)_1$ to Kaskan's value of $(E_a)_3$, that $(E_a)_2$ = 330 k joules $mole^{-1}$ (see Table 4.2). An interpolation of Lawton's [89,90] results, however, leads to $(E_a)_2$ = 163 k joules per mole, in closer agreement with Melinek.

The explanation for this may lie in the fact that while Lawton and Melinek both used a Botha-Spalding porous disc burner ostensibly giving a flat flame, the present work was on a Meker burner with a corrugated flame front. In all the investigations the temperature a few millimetres downstream of the reaction zone was uniform to $\pm \frac{1}{2}\%$. This, however, may hide more than it reveals especially in the present work due to quenching effects at the bases of the small flame cones. If this were the case then due to the exponential variation noted, the number of ions created per carbon atom consumed would be much less near the base of the cones than at the top. This effect is correspondingly greater as the temperature decreases, leading to a higher apparent activation energy than would be the case for a completely homogeneous flame front.

It has been suggested that measurement of the saturation current density could, when more empirical data have been amassed,

lead to a method of measuring final flame temperatures. Lawton [117] has in fact done this using the same system as for his activation energy measurements. The above, however, introduces a note of caution into the matter by pointing out that, for the moment at least, this method is only valid for a completely uniform reaction zone. Any irregularities, present in nearly all flames of practical interest, will necessarily introduce errors in temperature measurement. It is suggested, therefore, that although Lawton's temperature measurement is probably valid, one cannot use his arguments to deduce the temperature of a flame on another burner, although the flames burnt in the two cases may appear to be the same.

As a further note of caution, one may note the work of Fox and Kihara [118], who found that even porous discs do not give anywhere near such a homogeneous reaction zone as had formerly been assumed. Temperature gradients are present along a burner diameter, and, on the assumption that gases emerge at the local temperature of the disc surface, it is readily seen that, owing to the dependence of gas viscosity on temperature, the volumetric throughput per unit area of the disc is also dependent on the local disc temperature. This destroys the assumed unidimensionality of the reaction zone, even though it still appears planar to the eye.

It is, therefore, difficult to compare results obtained by different people, even if they use nominally the same burner system. Quite apart from minor inhomogeneities in the disc burners, as are always present, the results obtained are now seen as quite heavily dependent upon disc diameter, the volumetric

flow and the temperature and flow of the cooling water to the disc, and possibly other parameters.

A summary of the measurements on the flames with $\phi = 0.73$ is given below in table 4.2, upon which Fig. 4.1 is based.

TABLE 4.2

Flame	Final flame temp. (^{o}K)	I_s (μA)	Ion yield $(N/n_c) \times 10^7$
F	1957	50 ± 5	10.14
G	1890	30 ± 4	6.14
H	1818	9.5 ± 0.5	3.49

The log of this ion yield, plotted in Fig. 4.1 against the reciprocal of the final flame temperature, yields a good straight line, with correlation coefficient of (-) . 99997, although such a good fit is somewhat fortuitous in view of the errors involved in reproducing the flame from day to day.

The gradient corresponds to an ionization activation energy of 54 kcal mole^{-1} (i.e. 227 k joule mole^{-1}).

The unseeded flame, E, for which it was just possible to measure a saturation current, had an ion yield of $1.50 \cdot 10^{-6}$ per carbon atom at $\phi = 0.90$ at 2082 K. Because of the different value of ϕ, this and the unseeded equivalent of flame A are not included in Fig. 4.1; perhaps rather surprisingly, however, they do not lie very far from the extrapolated straight line plot of the results from flames F, G and H. Boothman and Lawton in Boothman et al [24], using a Botha-Spalding burner, showed that

ion yields are independent of pressure (results in Fig. 4 of that paper are presented in terms of saturation current density vs. pressure), so that work may be extrapolated to atmospheric pressure. Including results not published in that paper, the ion yield was $2.24 \cdot 10^{-6}$ ions per carbon atom consumed ($\pm$ 6.6% standard deviation) over a pressure range 47-103 torr at $\phi = 0.87$; below 47 torr quenching becomes important so that the yield decreases to $1.72 \cdot 10^{-6}$ at 30 torr. The flames at each pressure were on the point of lift-off, i.e. free-burning, so the temperature of all these reduced pressure unseeded flames was the same.

It is seen, then, that ion yields in various flames having the same sort of final flame temperature, but burning on two different types of burner, do have similar ion yields. The similarity should not, however, delude one into accepting exact comparability between two or more systems, however alike they may superficially appear to be.

NATURAL CHEMI-IONIZATION ION YIELD PER CARBON FUEL ATOM CONSUMED

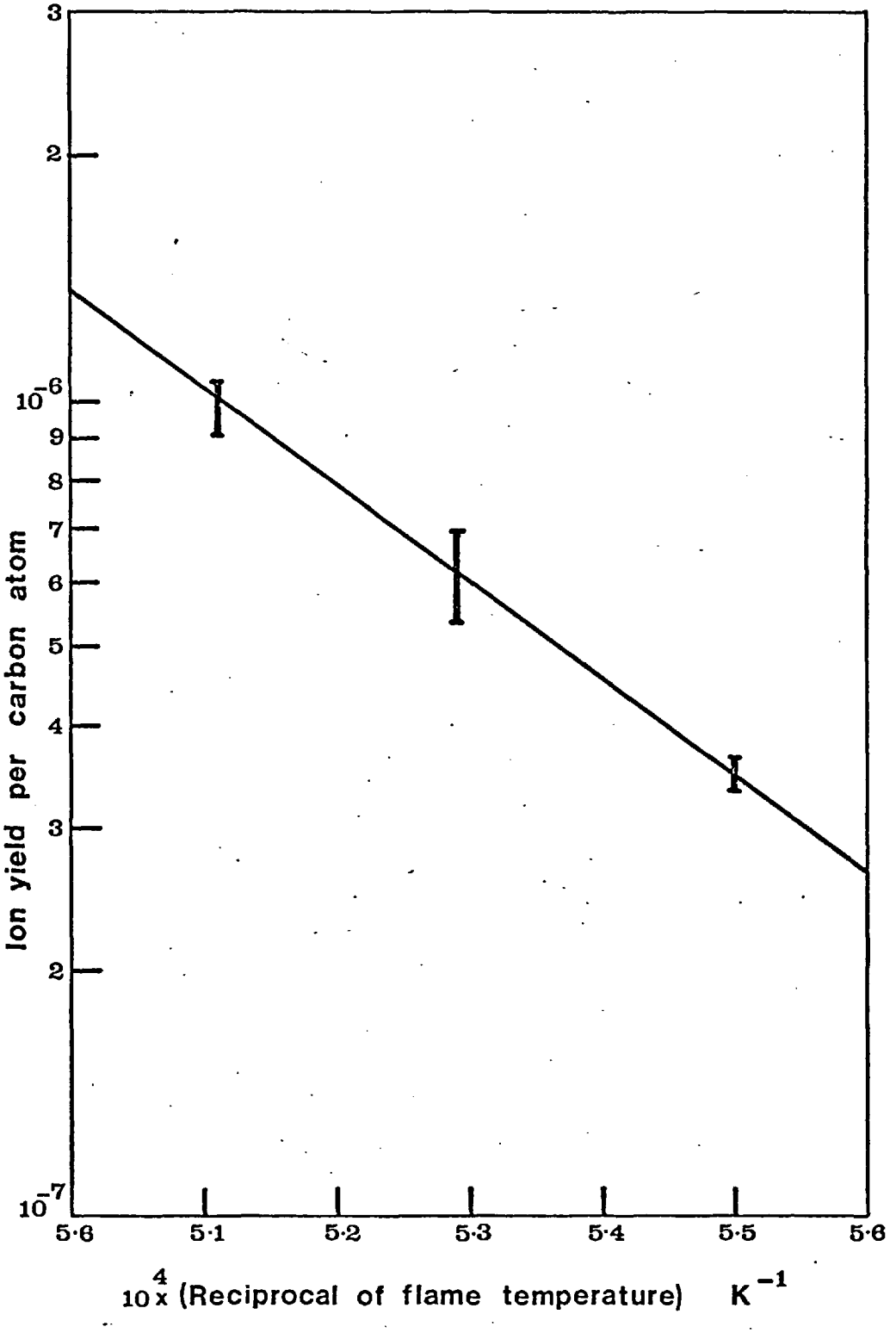

FIG. 4.1.

CHAPTER 5 DERIVATION OF EXPRESSIONS FOR VARIOUS PARAMETERS AND INTERPRETATION OF THE DATA

5.1 The current-voltage and voltage-distance graphs

In measuring the steady state ion density and hence the conductivity of flame plasmas, it is essential that the flame be as little disturbed as possible by drawing a current from it. Any current drawn must therefore be much less than the saturation current.

Families of curves of current versus voltage applied across the flame gases were traced out on the X-Y plotter, each curve being taken at one particular height of the gauze cathode above the burner anode. A typical such specimen is shown in Fig. 6.1. Each family may then be made the subject of a cross plot of applied voltage versus distance at a given constant current (Fig. 6.2). From these new families of voltage-distance curves, it should, in principle, be possible to derive the conductivity, σ, of the flame gases since $j = \sigma E$, where j is the current density and E the field $\left(E = -\frac{\partial V}{\partial x}\Big|_j\right)$.

Although the voltage readings from these graphs indisputably represent the voltage across the system necessary to draw a given current at a given height, one must ask whether the voltage gradients implied by these readings are the same as those in the bulk of the undisturbed plasma. (By 'undisturbed' is here understood those parts of the plasma not influenced by any electrode sheath, such as is described by Langmuir and post-Langmuir probe theories.)

If indeed this is the case, and the effect of the electrode sheaths may either be ignored or subtracted out as remaining

constant for a constant current density, j, the volume conductivity, σ, of the plasma may be written as

$$\sigma = \frac{-j}{\left.\frac{\partial V}{\partial x}\right|_j} = e \sum_i \mu_i n_i$$

where e is the electronic charge, μ the mobility, n the charge density, and the subscript 'i' refers to the type of charged species. When used in this context, the subscript 'e' will refer to electrons, '-' to negative ions and '+' to positive ions. The above equation reduces to

$$\sigma = \frac{-j}{\left.\frac{\partial V}{\partial x}\right|_j} = \mu_e n_e e$$

since $\mu_e >> \mu_+ \simeq \mu_-$ and, even after allowing for electron attachment n_e is still comparable in size with n_+ and probably greater than n_-.

This interpretation leads to values of α, the recombination coefficient for positive and negative species, of from $7 \cdot 10^{-6}$ to $4 \cdot 10^{-5}$ cm^3 s^{-1} within the temperature range 1700 to 2000 K. Such values would lead to insuperable difficulties of interpretation at the theoretical level, as well as giving rise to inconsistencies both within the corpus of this present work and also, external to it, since measurements of α by other methods at temperatures only a few hundred degrees higher have yielded, for the electron-positive atomic ion recombination in the presence of a third body, results that are three or four orders of magnitude lower. Internally, to explain the apparent low ion density, one would be forced to assume that free alkali metal atoms, A, were being mopped up by OH radicals, formed in quantities up to a few per cent of the total number of molecules present, by the

reaction A + OH → AOH. Further, there seems to be no explanations of sudden jumps of about a factor of two in the graph of α against temperature, or in the shape and intercepts on the axes of the current-voltage graphs. Last of the major objections is that if the apparent ion density or conductivity is plotted against the current at which it was measured, there is a rise to a maximum value, followed by a slow decline. In terms of a simple theory of an inter-electrode space dominated by electron conduction, there is again no satisfactory explanation for this, since as j increases, the apparent value of α should decline monotonically.

There is then a decisive body of evidence pointing to the rejection of this view of a plasma completely undisturbed by the presence of electrodes and having a uniform field in the hot gas region directly related to the observed voltage-distance curves.

We shall now consider in detail the motion of charged species in the flame plasma using for part of the analysis a line of approach similar to that developed (Thomson and Thomson [119(a)] and later, Loeb [35(b)]) for the case of a body of gas at uniform temperature, between electrodes at the same temperature as the gas, where ions are created, recombine and move under the influence of a small applied electric field. The approximation, used to achieve a solution in the two works cited, that positive and negative species mobilities are equal, cannot of course be used here since one species is electrons.

5.2 The Ion Density

5.2.1 Conditions for measuring the ion density

Before any voltage is applied across the plasma, positive and negative species both move together with velocity

equal to the sum of convective and diffusional velocities. An electrode placed in the path of the gas will collect electrons and ions of either sign. Reference may be made here to Figure 5.1.

At first, the current at the cathode is negative (region A of Fig. 5.1) since, due to the higher mobility and, therefore, higher velocity of the electrons, they arrive at the electrode first, thereby creating an electrostatic charge and consequent field which retards further electrons and accelerates positive species so that the two subsequently arrive in equal numbers. On further increasing the negative voltage to the electrode, the current measured by an ammeter in series passes through the zero point (a), after which an excess positive charge is collected (region B). An equal negative charge is collected at the upstream burner-anode, thus maintaining overall charge neutrality. On increasing the magnitude of the negative applied voltage even further, the negative ion and electron contribution to the current is cut down to zero at the cathode (point b).

It is apparent that the two processes are at work when the current increases from zero; these are illustrated by the current-voltage graphs (Figs. 5.1 and 6.1). At first, as the current increases from zero, the predominant process is the one described above - the relatively rapid elimination from the cathode of negative species. To a first approximation, this section of the current-voltage characteristic is a straight line. Closer observation reveals a slight curve, convex to the voltage axis, due probably to a spread of velocities in the sheath region. It may be noted here that a point-by-point plot of the characteristic would conceal this curvature.

As the voltage is further increased, there is a

recognisable "elbow" (b in Fig. 5.1) in the current-voltage characteristic at the point where negative species concentration in the cathode sheath drops to zero. After this, further increases in the voltage lead to slower increases in the current than is the case before the elbow is reached (region C). The process at work in the current increase is now solely that of withdrawal of positive ions from the plasma at the cathode before they have had chance to recombine to reform neutral species.

The value of σ given by

$$\sigma = \frac{-j}{\partial V / \partial x \big|_j}$$

is seen from the above arguments to be related to a net positive charge collected. In the first part of the characteristic the net is not the same as the absolute density because of the collection of negative species also. After the "elbow", the ion density again begins to drop due to the removal of ions from the plasma. Herein lies the similarity to the Langmuir probe, where there is also an "elbow" that defines the voltage at which a "pseudo-saturation" sets in. It does not, of course, in either case represent a true saturation effect, which only happens when all ions are withdrawn before they have a chance to recombine.

Our task is to find the ion density in the plasma before it drops due to the removal of ions after "pseudo-saturation". It will be demonstrated here that the apparent ion density increases from zero with increasing current up to a maximum, coinciding with the "elbow", approximating at this point to the 'undisturbed' ion density value, and then declines slowly. However, a correction for the finite current value at the "elbow" must be used. At a given electrode height, x, since in the

steady state set up, the rates of production and disappearance (by recombination and withdrawal) of charge must be equal, the equation of charge conservation for positive species is

$$eq(x) - e\alpha n_+^2 = ed\frac{}{dx}\left[n_+\left(\mu_+E + u - \frac{D_+dn_+}{n_+dx}\right)\right] \qquad (5.19a)$$

This may be integrated from the reaction zone to the electrode:

$$e\int_o^x q(x)dx = e\int_o^x \alpha n_+^2 + en_+\left(\mu_+E + u - \frac{D_+dn_+}{n_+dx}\right)$$

The term on the left hand side is equivalent to the saturation current density drawn at a height x, i.e. j_s. The production rate, q(x), comes from measurement of the gradient of the saturation current density vs. electrode height graphs (figs. 5.2 and 5.3), the value of j_s at a given height being the average of many plateau values of the current-voltage characteristic, as is seen for some settings of the electrode for flame B in fig. 5.4. The first term on the right hand side refers to that part of the charge which recombines within the plasma, the remaining one being the current withdrawn under the conditions prevailing at the elbow of the current-voltage characteristic. The main part of this is the convective term in 'u', which remains constant, while the left hand term increases with height; thus the correction factor to be applied to account for a withdrawal of current is greatest at the lowest electrode heights, being of the order of 10% there and falling to 1 or 2% at the highest electrode settings.

Symbolically, the above equation may be written

$$j_s = j_{rec} + j_n$$

where $j_n << j_s$, j_n being the current at the elbow and j_{rec} a notional current accounting for the charge which recombines in the plasma. The maximum apparent ion density measured would correspond to a current of $j_s - j_n$, so this density must be multiplied by a correction factor $j_s/(j_s - j_n)$, seen in Table 6.3, page 112.

5.2.2 The cathode as a plane probe

Unsuitability of existing theories

Were absolute rigour to be observed, it would be

steady state set up, the rates of production and disappearance (by recombination and withdrawal) of charge must be equal, diffusion being negligible, we have

$$q_x = \left(\frac{dn_+}{dt}\right)_{rec,x} + \left(\frac{dn_+}{dt}\right)_{j,x}$$

where $\left(\frac{dn_+}{dt}\right)_{rec,x}$ is the rate of disappearance of charge by recombination and $\left(\frac{dn_+}{dt}\right)_{j,x}$ is the rate of withdrawal of ions due to the current, both at a height x. The production rate, q_x, comes, of course, from a measurement of the gradient of the saturation current vs. height graphs (Figs. 5.1 and 5.2), the value of j_s at a given height being the average of many "plateau" values of the current-voltage characteristic, as is seen for some electrode settings of flame B in Fig. 5.3.

$$q_x = \frac{1}{e}\frac{\partial j_s}{\partial x}\bigg|_{0,rec} = \frac{\partial n}{\partial t}\bigg|_{0,rec} \quad \text{ions cm}^{-3}\ \text{s}^{-1}$$

the subscripts meaning zero charge recombination.

We have, then,

$$j_s = j_{rec} + j$$

where $j \ll j_s$. The maximum apparent ion density would give rise to a current of $(j_s)_x - j_x$ rather than $(j_s)_x$, so to obtain the true steady state ion density in the undisturbed plasma region, we should multiply the one obtained by $\frac{j_s}{j_s - j}$, which may increase the measured ion density by up to ca. 20%, though usually much less.

5.2.2 The cathode as a plane probe

Unsuitability of existing theories

Were absolute rigour to be observed, it would be

necessary to consider the gauze cathode as, from a distance, a plane probe and, close up, a three dimensional grid, immersed in a plasma, whose steady state ion density could be derived from the current-voltage characteristics of the probe. Although probe theory is relatively well developed for spherical and cylindrical probes, with the reservations expressed in Chapter 2, the same cannot be said for their planar equivalents. The case of grids is not dealt with. Indeed, the only theory which attempts to come to terms with a situation somewhat like the present one is that due to Toba and Sayano [120], who use the method of matched asymptotic expansions.

However, as they themselves admit, the theory is basically only semi-quantitative and its main function is to elucidate the mechanisms at work in the sheath regions; any predicted ion density is not necessarily correct to better than a factor of two. The main differences between the situation studied by Toba and Sayano and the present work are that here the convective flow of the gases is important, there is the possibility of negative charge existing in two forms (ionic and electronic) of widely different mass and mobility and diffusion characteristics, and there is the existence of temperature gradients in the electrical sheath, cutting the charge generation rate down effectively to zero near the electrode. All of these points would have to be taken into consideration in modifying Toba and Sayano's approach to describe the present voltage, field and ion density profiles, but such a task is outside the scope of this thesis. We shall, therefore, sacrifice much of the mathematical rigour in order to have a probably more accurate measurement of the ion density.

5.2.3 Calculation of ion density in the present work

Consider what happens at that current defined by the "elbow" of the current-voltage characteristics. Only positive ions are collected at the cathode, and, similarly, only negative species at the anode.

The general expression for current density, j, is given by

$$\frac{j}{e} = n_+\left(\mu_+ E + u - \frac{D_+}{n_+}\frac{dn_+}{dx}\right) + n_e\left(\mu_e E - u + \frac{D_e}{n_e}\frac{dn_e}{dx}\right) + n_-\left(\mu_- E - u + \frac{D_-}{n_-}\frac{dn_-}{dx}\right) \quad (5.1)$$

At the "elbow", since the current at the cathode due to negative species is zero, the "elbow" current, denoted by j_n, may be written as

$$\frac{j_n}{e} = n_+\left(\mu_+ E_s + u - \frac{D_+}{n_+}\frac{dn_+}{dx}\right) \quad (5.2)$$

where E_s is the field at the edge of the cathode sheath. This, of course, leads on subtraction of (5.2) from (5.1)

$$0 = n_e\left(\mu_e E_s - u + \frac{D_e}{n_e}\frac{dn_e}{dx}\right) + n_-\left(\mu_- E_s - u + \frac{D_-}{n_-}\frac{dn_-}{dx}\right) \quad (5.3a)$$

Equation (5.3a) may be rearranged to yield

$$E_s = \frac{1}{(n_e \mu_e + n_- \mu_-)}\left[u(n_e + n_-) - \left(\frac{n_e D_e}{n_e}\frac{dn_e}{dx} + \frac{n_- D_-}{n_-}\frac{dn_-}{dx}\right)\right] \quad (5.3b)$$

This may now be simplified by finding expressions for the derivatives with respect to distance of the ion densities.

From the graphs of saturation current versus height (Figures 5.2 and 5.3)* it can be shown that a good approximation to the ion production rate term is

*These represent averaged values of saturation current plateaux from all traces such as those shown in Fig. 5.4.

$$\frac{1}{e}\frac{dj_s}{dx} = q = q_o \exp(-2\gamma x) \text{ ion pairs } cm^{-3} \; s^{-1} \qquad (5.4)$$

with, in three cases, a correlation coefficient of better than 0.996, and, in the other, one only slightly worse.

For the potassium carbonate-seeded flames

$$\gamma = 0.46 \pm .01$$

and, for the sodium carbonate-seeded one,

$$\gamma = 0.23$$

Naturally, γ is dependent on the temperature-distance relationship, and will be different from these values for flames with other electrode characteristics.

The standard way of writing an expression for q is in the Arrhenius form, viz.

$$q = q_o \exp(-E/RT)$$

Temperature downstream of the reaction zone, however, falls off in such a way as to make equation (5.4) correct enough within the limits of correlation coefficient quoted.

Over the range of temperature (50-100 K) present in the gases from each of the flames studied, the recombination coefficient, α, does not vary greatly, and, to a first approximation, may be considered constant. The simplified picture of ionization and recombination processes dealt with in Chapter 2 gives the expression

$$q = \alpha n_+^2 \qquad (5.5)$$

For present purposes, this is adequate, but certain correction factors to this, the most important of which is due to the convection velocity of the gases, will be dealt with later. However, using (5.5) and combining it with (5.4) yields

$$n_+ = \left(\frac{q_o}{\alpha}\right)^{\frac{1}{2}} \exp(-\gamma x)$$

$$= (n_+)_o \exp(-\gamma x) \qquad (5.6)$$

On differentiation with respect to x, equation (5.6) becomes

$$\frac{dn_+}{dx} = -\gamma n_+ \qquad (5.7)$$

Equations (5.1) to (5.3) deal with both negative ions and electrons as well as positive ions. It is, therefore, necessary to find an equivalent to (5.7) for the negative species.

Again assuming negligible electrical disturbance of the flame gases, charge neutrality is maintained:

$$n_+ = n_e + n_- \qquad (5.8)$$

We shall further assume that the proportions of electrons and negative ions to positive ions remains constant for each flame, i.e.,

$$\beta = \frac{n_e}{n_+} = \text{constant} \qquad (5.9a)$$

and, therefore

$$1 - \beta = \frac{n_-}{n_+} = \text{constant} \qquad (5.9b)$$

In actual fact, β might tend to rise with increasing x (i.e. decreasing temperature), but to be offset against this is the fact that the main species to which electrons attach, viz. the hydroxyl radical, itself decays with increasing x towards its equilibrium value. Added to this cancelling out is the other much lesser effect that electrons attach at a finite rate, so it may be assumed that the assumption of constant β is not at all a bad one. In this case,

$$\frac{dn_-}{dx} = -\gamma n_- \qquad (5.10a)$$

and $$\frac{dn_e}{dx} = -\gamma n_e \qquad (5.10b)$$

This pair of equations, together with (5.8), may now be substituted back into equation (5.3b) to yield

$$E_s = \frac{un_+ + \gamma (n_e D_e + n_- D_-)}{n_e \mu_e + n_- \mu_-} \qquad (5.11)$$

For small fields, Einstein's relation is true:

$$D = \frac{\mu kT}{e} \qquad (5.12)$$

so, on substitution of (5.12) into (5.11), and using (5.9a) and (5.9b) to write the resultant in terms of ,

$$E_s = \frac{u}{\beta\mu_e + (1-\beta)\mu_-} + \frac{\gamma kT}{e}$$

However, the denominator of the first term on the right hand side here is just really an average value of μ for the negative species, so writing this as $\bar{\mu}_-$, we obtain

$$E_s = \frac{u}{\bar{\mu}_-} + \frac{\gamma kT}{e} \qquad (5.13)$$

As $\beta \to 1$ (i.e. in the limit of no electron attachment),

$$E_s \to \frac{u}{\mu_e} + \frac{\gamma kT}{e} \qquad (5.14)$$

Substitution of (5.7) and (5.13) into (5.2) yields, on rearrangement,

$$n_+ = \frac{j_n/e}{u\left(1 + \frac{\mu_+}{\bar{\mu}_-}\right) + \gamma\left(D_+ + \frac{\mu_+ kT}{e}\right)} \qquad (5.15)$$

Einstein's relation may be used again, and, on remembering that $\bar{\mu}_- \gg \mu_+$, at least in flames of the temperature and composition used here, (5.15a) becomes

$$n_+ = \frac{j_n/_e}{u + 2\gamma D_+} \qquad (5.15b)$$

Strictly speaking, since a current j_n has been drawn from the plasma, the above should be corrected accordingly to allow for this, the corrected value being (see section 5.2.1)

$$n_+ = \frac{j_n}{e(u + 2\gamma D_+)} \cdot \frac{j_s}{(j_s - j_n)} \qquad (5.16)$$

Expression (5.16) will be used to calculate the ion density from the curves obtained. In all cases, u is at least an order of magnitude greater than $2\gamma D_+$, using the values of D_+ calculated in Appendix A, so the effects of mobility and diffusion on the calculation of ion density come in, as does the finite current effect, only as first order correction factors.

5.2.4 The field in the plasma and the ionic velocities

Although (5.13) gives the field at the plasma/cathode sheath, this expression is valid only there and only for conditions at the "elbow". The more general expression for the field in the plasma itself, E_p, is derived from (5.1). Using (5.6), (5.9) and (5.10), (5.1) becomes

$$j/_e = (n_+)_o \exp(-\gamma x) \left[(u + \mu_+ E_p + \gamma D_+) + \frac{\beta}{1+\beta} (\mu_e E_p - u - \gamma D_e) + \frac{1}{1+\beta} (\mu_- E_p - u - \gamma D_-) \right]$$

Rearranging, using Einstein's relation, and, rewriting in terms of $\bar{\mu}_-$, we obtain

$$E_p = \frac{j \exp(\gamma x)}{e(n_+)_o(\bar{\mu}_- + \mu_+)} + \frac{\gamma kT}{e} \frac{(\bar{\mu}_- - \mu_+)}{(\bar{\mu}_- + \mu_+)} \qquad (5.17a)$$

$$\text{or} \quad E_p = \frac{1}{e(\bar{\mu}_- + \mu_+)} \left[j/n_+ + \gamma kT(\bar{\mu}_- - \mu_+) \right] \qquad (5.17b)$$

By imposing the condition (5.2), i.e. conditions at the "elbow", and making the appropriate substitutions, it is easily shown that (5.17) reduces to (5.13) at the plasma/cathode sheath boundary. Equations (5.17) show the plasma field may be thought of as comprising two terms, one approximately constant, and the other rising exponentially with distance, the field becoming strong enough at the plasma/cathode sheath boundary to turn back the negative species. Upstream from this plane, where the field is weaker, negative charge drifts along in the same direction as the convection velocity, u, thereby reducing the current from the positive ion current value to its resultant (measured) value. The positive ion current decays in an approximately exponential fashion since that is the mode of decay of the positive ion density, whereas the positive ion velocity remains fairly constant.

Equation (5.17a) may be used to calculate, from (5.1), the ion and electron velocities in the plasma. If μ_+ is neglected cf. $\bar{\mu}_-$ (see Appendices A and B), the three resultant velocities are seen to be (ignoring smaller terms):

$$v_e = u - \frac{\mu_e j}{e n_+ \bar{\mu}_-} \qquad (5.18a)$$

$$v_- = u - \frac{\mu_- j}{e n_+ \bar{\mu}_-} \qquad (5.18b)$$

and

$$v_+ = u + \frac{\mu_+ j}{e n_+ \bar{\mu}_-} + 2\gamma D_+ \qquad (5.18c)$$

The predominant term is u in the expressions for v_+ and v_-.

This analysis leaves out the question, irrelevant to our purposes, of what happens near the reaction zone and between there and the burner/anode. The ion current distributions there must be quite complicated because of the non-planar nature of the reaction zone, and the important role played by electron attachment upstream of the reaction zone (i.e. in the unburnt reactants). If we leave aside these complicating factors, we can sketch out schematically the current distribution, which turns out to exhibit quite a high degree of symmetry. This is shown in Figure (5.5).

5.2.5 The determination of j_n

From all the figures obtained of the type of which Fig. 6.1 is an example, one obtains values of j_n at the electrode heights marked simply by drawing tangents to the current-voltage curves on either side of the "elbow" of each characteristic; j_n is the current density corresponding to the current defined by the intersection of the pair of tangents for each characteristic.

As in the case of Langmuir probe characteristics, the two sections of the characteristic are not perfectly linear. However, the error introduced by treating them as such is only a few per cent at the ion densities encountered here.

A lower limit on the ion density is, however, introduced by such considerations, since as ion density decreases the corresponding "elbow" becomes more and more rounded, and, therefore, difficult to define.

This lower limit was not however reached in this work, being defined instead, as previously stated, by a difference in

saturation current density of ca. 1.2% between inter-electrode distances differing by 1 cm. Beyond this point saturation current differences were obscured by random errors due to fluctuations of seed material. It should be pointed out that even here, adjacent low-current current-voltage characteristics at different electrode settings, such as Fig. 6.1, were still quite separate from each other.

Historically, it has been judged safer to use graphs of voltage against electrode spacing to try to measure conductivity. Such an attempt here, however, fails because of the increase of cathode fall voltage with increasing height (i.e. decreasing ion density). One can instead make a cross plot of the current-voltage characteristics to give equivalent families of voltage-height curves at constant current, then write some expression for the ion density such as

$$n_+ = \frac{j/e}{u - \mu_+ \frac{\partial V_T}{\partial x} + \gamma D_+}$$

where V_T is the total voltage across the electrodes and, of course, $-\frac{\partial V_T}{\partial x}$ is some kind of artificial field.

As j increases this expression passes through a maximum before declining slowly. However, there seems no sound physical basis for relying on the change with height of the voltage across the electrodes to provide any convincing description of the undisturbed ion density at the edge of the cathode sheath. This expression gives answers that are quite consistently lower than those obtained from the intersections on the current-voltage families of graphs and unless or until a full description can be given of the cathode fall, there seems no way of rigorously

tying this expression up with equation (5.16).

It is, therefore, maintained that the best way of measuring ion density in the present case is as outlined at the start of this sub-section, and substituting j_n into equation (5.16), which is corrected for the withdrawal from the plasma of a finite non-zero current.

5.3 The recombination coefficient

It has already been stated earlier that, in the absence of losses due to convection, electric fields and diffusion, the rate of production of charge is balanced by its recombination in one or more three body processes. This may be written, if we ignore charge transfer reactions, as

$$q = \alpha n_+^2$$

if electrons and positive ions are the only species present, or

$$q = \alpha_1 n_+ n_e + \alpha_2 n_+ n_-$$

if there are electrons and negative as well as positive ions; α_1 and α_2 are the recombination coefficients for positive ions with electrons and negative ions respectively.

We shall now demonstrate that this is a fairly good description of the present situation and extend the equation to include correction terms.

Assuming, as above, that the ratio of electrons to negative ions remains constant, the equations of charge conservation become (again taking no account of charge transfer reactions):

$$q - \alpha_1 n_+ n_e - \alpha_2 n_+ n_- = \frac{d}{dx}\left[n_+ \left(\mu_+ E + u - \frac{D_+}{n_+} \frac{dn_+}{dx} \right) \right] \qquad (5.19a)$$

$$\text{and } q - \alpha_1 n_+ n_e - \alpha_2 n_+ n_- = -\frac{d}{dx}\Big[n_e(\mu_e E - u + \frac{D_e}{n_e}\frac{dn_e}{dx}) + n_-(\mu_- E - u + \frac{D_-}{n_-}\frac{dn_-}{dx})\Big] \qquad (5.19b)$$

By ignoring the very small dependencies of u and the various Ds and μ's on x, we obtain, on dividing through (5.19a) by μ_+ and (5.19b) by μ_e and carrying out the differentiation,

$$\frac{1}{\mu_+}(q - \alpha_1 n_+ n_e - \alpha_2 n_+ n_-) = E\frac{dn_+}{dx} + n_+\frac{dE}{dx} + \frac{u}{\mu_+}\frac{dn_+}{dx} - \frac{D_+}{\mu_+}\frac{d^2n_+}{dx^2} \qquad (5.20a)$$

$$\text{and } \frac{1}{\mu_e}(q - \alpha_1 n_+ n_e - \alpha_2 n_+ n_-) = -E\frac{dn_e}{dx} - n_e\frac{dE}{dx} + \frac{u}{\mu_e}\frac{dn_e}{dx} - \frac{D_e}{\mu_e}\frac{d^2n_e}{dx^2} - \frac{\mu_-}{\mu_e}(E\frac{dn_-}{dx} + n_-\frac{dE}{dx}) + \frac{u}{\mu_e}\frac{dn_-}{dx} - \frac{D_-}{\mu_e}\frac{d^2n_-}{dx^2} \qquad (5.20b)$$

Adding (5.20a) and (5.20b), we obtain

$$(\frac{1}{\mu_+} + \frac{1}{\mu_e})(q - \alpha_1 n_+ n_e - \alpha_2 n_+ n_-) = \frac{d}{dx}\Big[E(n_+ - n_e - \frac{\mu_-}{\mu_e}n_-) + \frac{u}{\mu_+}\frac{dn_+}{dx} + \frac{u}{\mu_e}\frac{d}{dx}(n_e + n_-) - \frac{D_+}{\mu_+}\frac{d^2n_+}{dx^2} - \frac{D_e}{\mu_e}\frac{d^2n_e}{dx^2} - \frac{D_-}{\mu_e}\frac{d^2n_-}{dx^2}\Big] \qquad (5.21)$$

If we now return to equation (5.1), divide it by μ_e and differentiate with respect to x, it becomes on rearrangement (j being constant of course):

$$\frac{u}{\mu_e}(\frac{dn_e}{dx} + \frac{dn_-}{dx}) - \frac{D_e}{\mu_e}\frac{d^2n_e}{dx^2} - \frac{D_-}{\mu_e}\frac{d^2n_-}{dx^2} = \frac{d}{dx}\Big[E(\frac{\mu_+}{\mu_e}n_+ + \frac{\mu_-}{\mu_e}n_- + n_e)\Big] + \frac{u}{\mu_e}\frac{dn_+}{dx} - \frac{D_+}{\mu_e}\frac{d^2n_+}{dx^2} \qquad (5.22)$$

On substitution for the L.H.S. of (5.22) in (5.21) we obtain

$$\left(\frac{1}{\mu_+} + \frac{1}{\mu_e}\right)\left(q - \alpha_1 n_+ n_e - \alpha_2 n_+ n_-\right) = \frac{d}{dx}\left[En_+\left(1 + \frac{\mu_+}{\mu_e}\right) + \left(\frac{1}{\mu_+} + \frac{1}{\mu_e}\right)\left(u\frac{dn_+}{dx} - D_+\frac{d^2n_+}{dx^2}\right)\right] \quad (5.23)$$

μ_+ may be neglected in comparison with μ_e, and if we define

$$\alpha n_+^2 = \alpha_1 n_+ n_e + \alpha_2 n_+ n_-$$

then,

$$\alpha = \frac{q}{n_+^2} - \frac{\mu_+}{n_+^2}\frac{d}{dx}(n_+E) - \frac{1}{n_+^2}\left(u\frac{dn_+}{dx} - D_+\frac{d^2n_+}{dx^2}\right)$$

Using (5.7), (5.17b) and Einstein's relation, this reduces to

$$\alpha = \frac{q}{n_+^2} + \frac{\gamma u}{n_+} + \frac{2\mu_+\gamma j}{n_+^2 e\mu_-} + \frac{2\gamma^2 D_+}{n_+} \quad (5.24)$$

This may be compared with the expression of Thomson and Thomson [119(b)] for gas flowing at ω cm^3 s^{-1} into a vessel of volume V and producing a steady state ion density n (the temperature throughout being uniform):

$$\alpha = \frac{q}{n^2} - \frac{\omega}{nV}$$

From the observed values of the measured parameters, and the calculated values of μ and D (see Appendices A and B), the only terms of (5.24) that need be considered are the first two on the right hand side. The convective term, $\frac{\gamma u}{n_+}$, varies from ca. 10% of q/n_+^2 at the higher temperatures, ion production rates and ion densities, to as much as 60% at the lowest temperatures. The other two terms, relating to mobility and diffusion, are at least an order of magnitude less than the convective term and may therefore be neglected. So, we have

$$\alpha = \frac{q}{n_+^2} + \frac{\gamma u}{n_+} \quad (5.25a)$$

Returning to the case of both electrons and negative ions, it is easily seen that (5.25) is equivalent to

$$\alpha_1 + (1 - \beta)\alpha_2 = \frac{q}{n_+}2 + \frac{\gamma u}{n_+} \qquad (5.25b)$$

This pair of equations, (5.25), will be used to calculate the recombination coefficient.

Thus, in this section, we have shown what might have been supposed intuitively, viz., that the application of a small voltage across the system does not disturb it unduly. The convective velocity term, however, must be taken into consideration as a corrective factor in the calculation of the recombination coefficient, but, for this calculation, axial diffusion is negligible.

5.4 Errors arising from radial diffusion

For the sake of completeness, some consideration should be given to the loss of ions by outward radial diffusion from the cylindrical column of seeded hot gases. With the given configuration, the calculation of this is, to say the least, complex and, in analytical terms, probably impossible. The problem of diffusion outwards from an unbounded cylinder, inside which is a uniform ion density and a constant ion production rate (equal to zero outside the cylinder) has been considered by Jaffe [121] (see Loeb [35(c)]). Here, however, there are axial gradients of temperature and various species concentrations upon which the ion density depends. Even were these capable of expression analytically, it seems likely that the ion and electron loss terms would still only be calculable by numerical integration.

A calculation, assuming no axial gradients, may be made in

order to give an order of magnitude estimate of the diffusion effects. At time t = 0, we assume a Gaussian density distribution, with density n_o at the axis and n at a distance, r, from the axis:

$$\frac{n}{n_o} = \frac{\exp(-r^2/b^2)}{\pi b^2}$$

where b is a constant related to the average displacement, r_o, from the origin at time t by

$$b = r_o\left(\frac{4}{\pi}\right)^{\frac{1}{2}}$$

If recombination does not alter the <u>form</u> of the curve from Gaussian, the solution of the differential equation for n is (where D_a is the ambipolar diffusion coefficient, equal here to ca. twice the positive ion diffusion coefficient: see Loeb [35d])

$$n = \frac{n_o}{1 + \frac{\alpha n_o}{8\pi D_a} \ln\left(\frac{4D_a t + b^2}{b^2}\right)} \cdot \frac{\exp\left(\frac{-r^2}{4D_a t + b^2}\right)}{\pi (4D_a t + b^2)}$$

Taking n_o as ca. 10^{11} cm^{-3}, typical lengths for the system and a time of 10 msec during which the ion density, in the absence of other effects, would be reduced to 20% of its initial value, then at a distance of 1.9 cm from the centre of the seeded column, i.e. ca. 4 mm from its edge,

$$n \leq 0.05\ n_o,$$

it being remembered that recombination still takes place while the species diffuse outward.

Similar conclusions result from a similar model starting again from a Gaussian distribution, and using Einstein's [122] analysis of Brownian motion, which gives for the ion density, n,

at time t and at a distance r from the centre of a volume in which the ion density is initially n_0,

$$n = \frac{n_0}{(4\pi D_a t)^{\frac{1}{2}}} \exp\left(\frac{-r^2}{4D_a t}\right)$$

The density at the edge of the "guard ring" flame is, from this expression, again the same order of magnitude as that from Jaffe's expression.

It is certain that very little is lost out of the system, since the above estimates are upper limits, the bulk of the ions being in the seeded column, with the axial density gradient having the effect of reducing even further radial diffusion outwards. As experimental confirmation of the negligibility of this effect, we note that the current-voltage characteristics at small applied voltages are not measurably altered if the system is enclosed by an insulating quartz cylinder of diameter only slightly larger than that of the burner itself. In the case of outward diffusion, this concentric cylinder would act as an electrostatic lens (Weinberg [123]) constraining the charged species to move more or less parallel to the axis. The lack of any such change in the characteristics implies that this was essentially the case anyway, and that radial diffusion, as assumed, is negligible.

5.5 Departures from equilibrium concentrations

5.5.1 Alkali hydroxide formation

The results of equation (5.16) for ion density lead to the conclusion (see ch. 6) that, except in flame A, the ion density present is somewhat less than the value expected from full thermodynamic equilibrium, unless one allows for alkali hydroxide formation. This departure from the theoretically

expected value is more marked for each successively lower temperature flame, although within the hot gases produced by one flame the ion density tends towards the equilibrium value as temperature decreases (i.e. as distance or time from the reaction zone increases).

A clue to this behaviour may be found in, for example, the work of Kaskan [124,125] on premixed hydrogen-air flames, both lean and rich, burning on a porous disc burner. The ratio of the OH concentration actually present to the equilibrium value will be called the overproduction ratio. It was found by Kaskan to be less in lean flames than in rich ones and to increase as the reaction zone temperature decreased; at one atmosphere, it varied from 2.6-3.0 at 1750-1840 K to 19 at 1370 K for an equivalence ratio of only just over unity (1.20). A rough extrapolation of Kaskan's data for the lean and slightly rich flames (Kaskan [125]) plotted against either T or T^{-1} indicates that we might expect full thermodynamic equilibrium in the production of OH at ca. 2050 K. (The mechanism for the production of OH is more complex than the above indicates, so not too much weight should be attached to the temperature quoted.)

Even after allowing for the different set of reactions in a hydrocarbon-air flame, it should not be surprising that, for the flames studied, there may be an overproduction of the hydroxyl radical in the reaction zone. In fact, such a phenomenon is observed in the work of Baxendale, Livesey, Roberts, Smith and Williams [126] for oxy-propane flames of equivalence ratio ca. 2 when the reaction zone temperature is below 2800 K. This overproduction leads, in our case, to a depletion of free alkali atoms, and thus to a diminution of the ion density to values below those predicted by full thermodynamic equilibrium.

There are two reactions by which alkali hydroxide may be formed. Sugden [127] and later investigators, e.g. Padley, Page and Sugden [128] and Jensen and Padley [45,84] all postulate, with undeniable justification, the reaction

$$A + H_2O \rightleftarrows AOH + H \qquad (5.26a)$$

leading to an equilibrium constant, K_{26}, given by

$$K_{26} = \frac{[A]\,[H_2O]}{[AOH]\,[H]} \qquad (5.26b)$$

Here A represents either of the two alkali metals used - K or Na.

In all these papers, the flames used were premixed $H_2/O_2/N_2$ ones with (taking Sugden's paper as an example) a hydrogen atom concentration of up to 1%, thereby facilitating the back reaction of (5.26a). In most of the flames studied in this work, the concentration, even after allowing for an overproduction of up to an order of magnitude, is only ca. 10 p.p.m., so one might suspect that reaction (5.26a) is not necessarily balanced.

The alternative reaction for AOH production is

$$A + OH + M \rightleftarrows AOH + M \qquad (5.27a)$$

where M is any third body. This has an equilibrium constant defined by

$$K_{27} = \frac{[A]\,[OH]}{[AOH]} \qquad (5.27b)$$

The equilibrium hydroxyl radical partial pressure varies from about $8 \cdot 10^{-4}$ at the highest temperatures to about $2 \cdot 10^{-4}$ at the lowest ones. Allowing for a super-equilibrium concentration, which will be demonstrated later, bringing the actual partial pressure up to 10^{-3} or more, there seems a reasonable chance that (5.27a) may predominate over (5.26a) as the alkali hydroxide producing mechanism.

In support of this, certain arguments of a qualitative nature may be advanced. Gaydon and Wolfhard [104(c)] state that if gas kinetic cross sections are an adequate description of the reactions, then, at flame temperatures, three-body reactions are about one thousandth as frequent as two-body ones. They further state that effective cross-sections for three-body reactions are likely to be greater than gas kinetic ones, and would be increased yet further by the formation of collision complexes. Since the complex $KOH.H_2O$ is known to be quite stable (Hayhurst and Sugden [28]), (5.27a) might indeed have a high cross section if, as is likely from the composition of the burnt gases, the third body is H_2O.

In addition, because of the nature of the electronic structure of their outermost shells, a reaction between A and OH might be expected to have a high cross section. On the other hand, the cross-section for the de-excitation of Na ($3p\ ^2P$) atoms by H_2O molecules (Jenkins [107]) is very low (0.5×10^{-16} cm^2 as compared with, e.g. $7 \cdot 10^{-16}$ for N_2 and $17 \cdot 10^{-16}$ for CO_2 instead of H_2O). Were the same order of magnitude correct for ground state alkali atoms reacting with water vapour, then again reaction (5.27a) would be kinetically favoured with respect to (5.26a).

Qualitatively, then, it is seen that reaction (5.27) is possibly more important than (5.26) in the present situation.

Rather more quantitatively we may refer to the reasoning put forward by Sugden (op. cit.). Θ_{27} is the ratio to which $\frac{[AOH]}{[A]}$ would tend were equation (5.27) dominant and Θ_{26} the same ratio if (5.26) dominated; the forward rate constants will be written k_{27} and k_{26} respectively.

For ternary recombination to dominate, Sugden derived,

by considering the growth of KOH from zero to its steady state value,

$$\frac{\Theta_{26}}{\Theta_{27}} >> \frac{K_{26}\, k_{-26}\, [H_2O]}{K_{27}\, k_{-27}\, [OH]}$$

which, on substitution, becomes

$$[H] << \frac{k_{-27}}{k_{-26}} \qquad (5.28)$$

Strictly speaking, if the same arguments exactly are to apply here, the growth of AOH must not change to a great extent the hydrogen atom concentration. This is usually true only if $[H] >> [A]$ and $[H] >> [AOH]$ which is not the case here. However, the work of Bulewicz, James and Sugden [129] shows that if there is a super-equilibrium production of H, O and OH radicals, then

$$[H] = \frac{[OH]\ [H]_e}{[OH]_e}$$

$$= (\text{const})\ [OH]$$

where the subscript e refers here to conditions at full thermodynamic equilibrium. $[A]$ and $[AOH]$ are both very much smaller than $[OH]$, so $[OH]$ may be regarded as constant for the purposes of the integration which Sugden carried out, and equation (5.28) is found to be applicable here despite the relatively low hydrogen atom concentration. Putting this another way, the H atom concentration is determined by the reactions relevant to the formation of water vapour rather than those pertaining to AOH formation.

k_{-26} is the velocity constant of a bimolecular reaction and may be written as $A_{-26} \exp(-E_{26}/kT)$ where the frequency factor may be taken as ca. 10^{-10} cm^3 molecule^{-1} sec^{-1} (Sugden, op. cit.). E_{26} for the reaction involving potassium is

(Kelly and Padley [60]) 142 kjoules $mole^{-1}$, using their recommended value for the dissociation energy of KOH, viz. 352 kJ $mole^{-1}$ and 494 kJ $mole^{-1}$ for the dissociation energy of H_2O. Taking a temperature of 1850 K (i.e. in the middle of our range) k_{-26} 10^{-14} cm^3 $molecule^{-1}$ sec^{-1}, even before allowing for a steric factor which would lower the value even more.

$k_{-27} \sim 4 \cdot 10^8 \eta \exp(-E_{27}/kT)$ where η is a factor of order 10^2-10^3 which allows for the fact that the third body in reaction 5.27 may be triatomic (H_2O or CO_2, both of which form about 10% of the burnt gases), thereby enhancing the efficiency of the reaction. Taking an average temperature for our range and Kelly and Padley's value for E_{27} (the dissociation energy of KOH),

$k_{-27} \sim 20$ to a factor of about 3.

The condition for termolecular reactions to dominate is then

$$[H] \ll \frac{k_{-27}}{k_{-26}} \sim \frac{20}{10^{-14}}$$

or $$[H] \ll 2 \cdot 10^{15} \qquad (5.29)$$

where, because of the steric factor referred to, this figure is probably a lower limit.

Even if we allow that at the lower temperatures investigated, H atoms are present at an order of magnitude greater than their equilibrium concentration, they are still there only at the level of ca. $3 \cdot 10^{14}$ at most, and probably the true figure is somewhat less.

It is seen therefore that condition (5.29) holds quite comfortably, so in the present case the dominant mechanism for

the production of AOH should be

$$A + OH + M \rightleftarrows AOH + M.$$

Freck [130] noted that for fuel-lean hydrocarbon-air flames at the lower temperatures he studied (1800 K upwards) there was a predicted drop in electron density, due partly to the depletion of alkali atoms by OH radicals and partly due to attachment of the electrons produced, again probably due to OH radicals. His predictions are in agreement with the findings of Brogan [131], although perhaps somewhat fortuitously so, because of the outdated thermodynamic data on alkali hydroxides and the high value used for the electron affinity of OH (see below for a discussion of this).

5.5.2 Chemical species concentrations and ion densities

In the analysis presented in this sub-section, we shall assume that a steady state exists in the hot gases above the reaction zone, the departure from equilibrium being determined by the excess OH production in the reaction zone. Results derived later are based on measurements taken at further than ca. 1 cm from the burner (i.e. about 6 msec downstream of the reaction zone for the hottest flame and to about 20 msec for the coolest one). Even this was not always sufficient for the creation of the steady state postulated as evidenced by the departure from linearity in Fig. 7.1. Ionization processes should, long before this, have reached equilibrium levels, since in the admittedly somewhat different situation of a shock-initiated C_2H_2-O_2 combustion systems, (Hand and Kistiakowsky [132], Matsuda and Gutman [133]) it was found that a time of only ca. 50-500 μ sec was needed for the ion and electron production rates to reach their equilibrium levels, with

a probable dependence of log (reaction time) on the reciprocal of temperature.

Five equations are written for five unknown parameters in terms of another five parameters which either have been measured or are calculable from statistical mechanics and the published data in the literature. Alkali metals are assumed to be present as three species: as free atoms, as the hydroxide and as atomic ions. Other species, including the monohydrate of the hydroxide (see above) may be neglected. So, if $[A_T]$ is the total atomic alkali concentration fed into the system,

$$[A_T] = [A] + [AOH] + [A^+]$$

Although $[A^+]$ is necessary for the solution of this set of simultaneous equations, in the above equation it is dwarfed by all the other species present (see Gaydon and Wolfhard [104(d)], for the fractional ionization at selected temperatures). The above equation then reduces to

$$[A_T] = [A] + [AOH] \qquad (5.30)$$

Alkali atoms ionize on collision with a sufficiently energetic neutral body, the reaction being written

$$A + M \rightleftarrows A^+ + e + M \qquad (5.31a)$$

This may be treated simply as a chemical change (Saha [134]) with equilibrium being determined in terms of the Saha-Boltzmann equilibrium constant, K_{31}.

$$K_{31} = \frac{[A^+][e]}{[A]} = \frac{g_{A^+} g_e}{g_A} \left(\frac{2\pi m_e kT}{h^2}\right)^{3/2} \exp\left(\frac{-E_i e}{kT}\right) \qquad (5.31b)$$

where E_i is the ionization potential of A, m_e the electronic mass, g the ground state statistical weight of the species indicated by the relevant subscript and h Planck's constant.

Some electrons attach to neutral species. It may be shown that the only species that need trouble us is OH, (see section 6.1.2 where the statistical mechanics expression in 5.3.2 will also be dealt with), so we may write

$$M + OH^- \rightleftarrows OH + e + M \tag{5.32a}$$

leading to

$$K_{32} = \frac{[e][OH]}{[OH^-]} = 8\left(\frac{2\pi m_e kT}{h^2}\right)^{3/2} \exp\left(\frac{-20,656}{T}\right) \tag{5.32b}$$

There is, of course, an alternative neutralisation reaction for A^+, viz.

$$A^+ + OH^- + M \rightarrow A + OH + M$$

but the equilibrium constant for this is contained by a combination of 5.31 and 5.32.

The field gradient in the plasma is small enough to allow us to assume, for the purposes of this analysis, charge neutrality at all points in the plasma.

$$[e] + [OH^-] = [A^+] \tag{5.33}$$

The fifth equation is (5.27b)

$$K_{27} = \frac{[A][OH]}{[AOH]} \tag{5.27b}$$

Equations (5.27b) and (5.30)-(5.33) inclusive are the necessary five referred to. The solution of the simultaneous equations is straightforward and yields

$$[A] = \frac{K_{27} K_{31} [A_T] - K_{32} [A^+]^2}{K_{31}(K_{27} - K_{32})} \tag{5.34}$$

$$[e] = \frac{K_{27} K_{31} [A_T] - K_{32} [A^+]^2}{[A^+](K_{27} - K_{32})} \tag{5.35}$$

$$[OH^-] = \frac{K_{27}([A^+]^2 - K_{31}[A_T])}{[A^+](K_{27} - K_{32})} \tag{5.36}$$

$$[OH] = \frac{K_{32}\,K_{27}([A^+]^2 - K_{31}[A_T])}{K_{27}\,K_{31}[A_T] - K_{32}[A^+]^2} \qquad (5.37)$$

$$[AOH] = \frac{K_{32}([A^+]^2 - K_{31}[A_T])}{K_{31}(K_{27} - K_{32})} \qquad (5.38)$$

It is, then, apparent that, in the steady state, the absolute concentrations of the various species of interest can be calculated from the observed parameters, $[A_T]$ and $[A^+]$, and the equilibrium constants of the relevant reactions.

CURRENT-VOLTAGE CHARACTERISTIC, DEMONSTRATING THE PRESENCE OF AN ELBOW

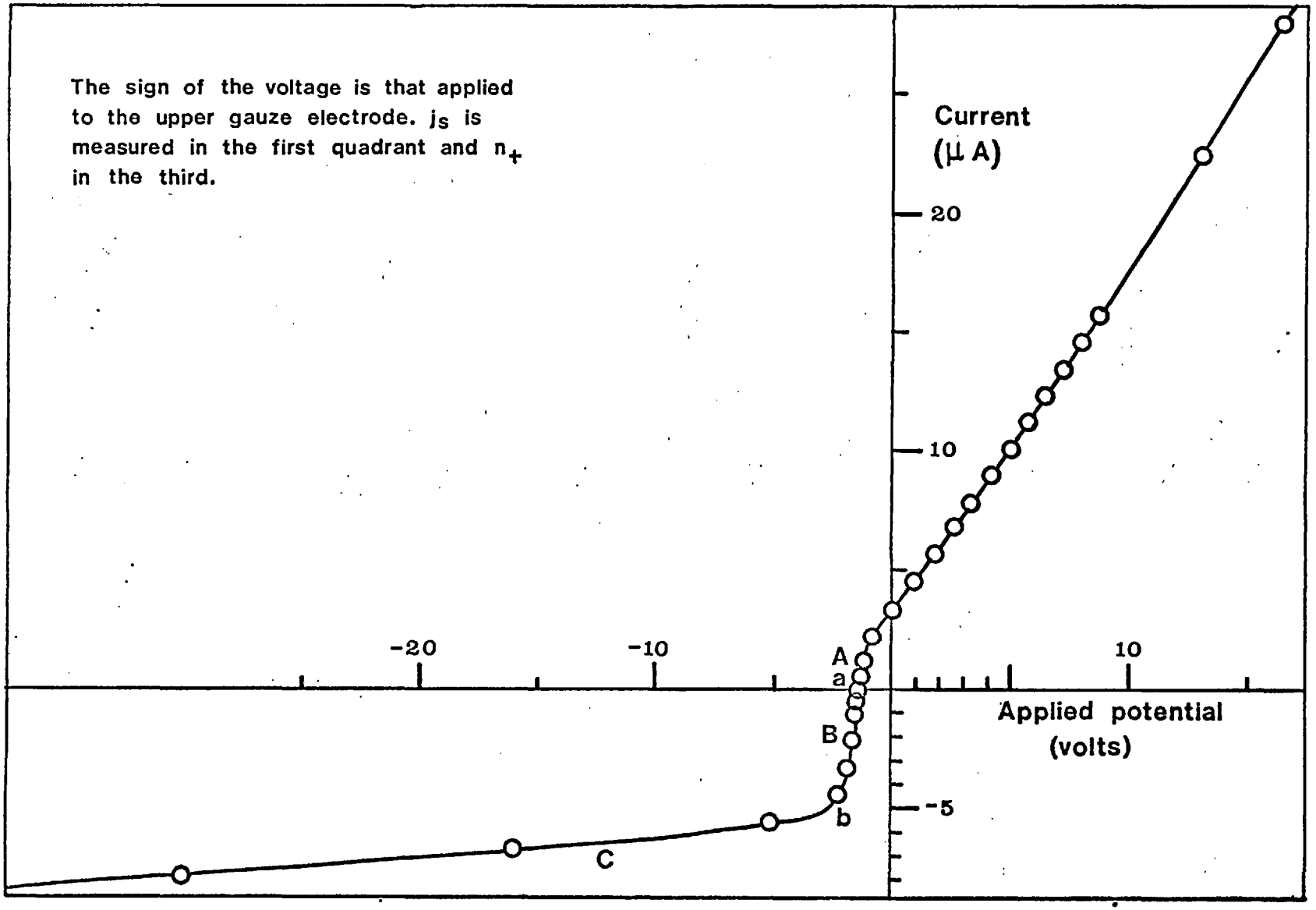

FIG. 5.1.

SATURATION CURRENT VS. ELECTRODE SEPARATION

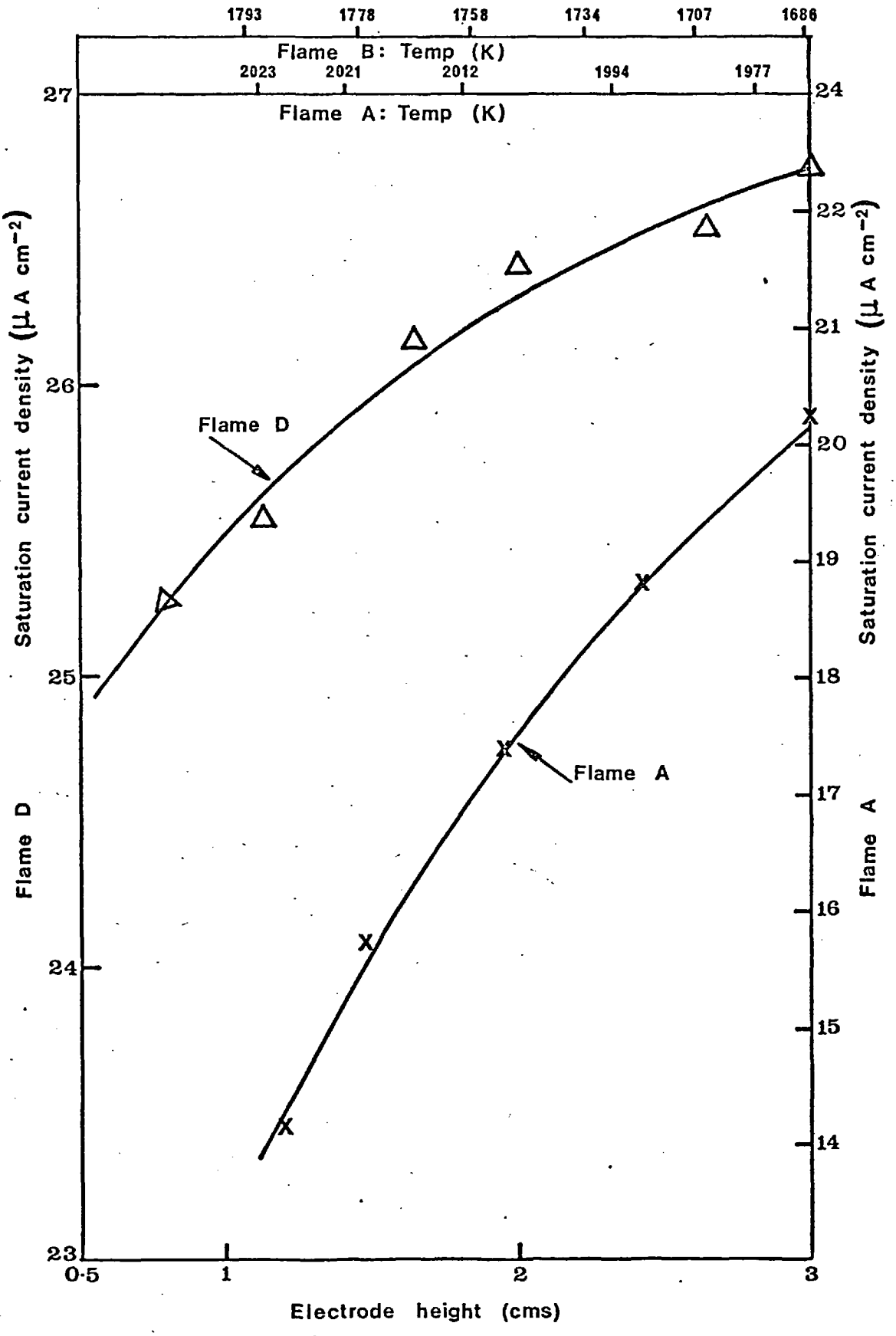

FIG. 5.2.

SATURATION CURRENT VS. ELECTRODE SEPARATION

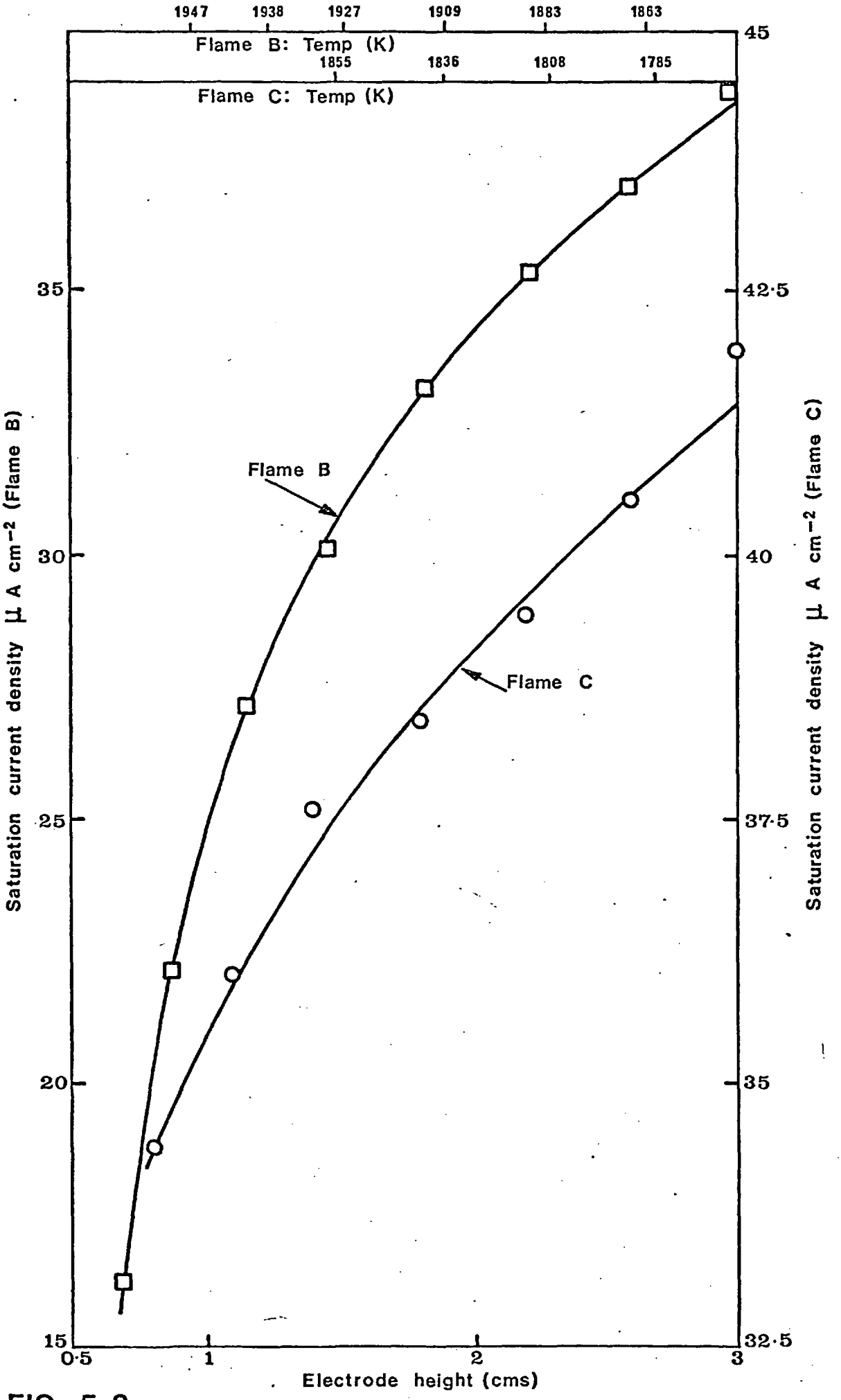

FIG. 5.3.

SATURATION CURRENT PLATEAU REGIONS FOR THE SEEDED ATMOSPHERIC PRESSURE FLAME B.

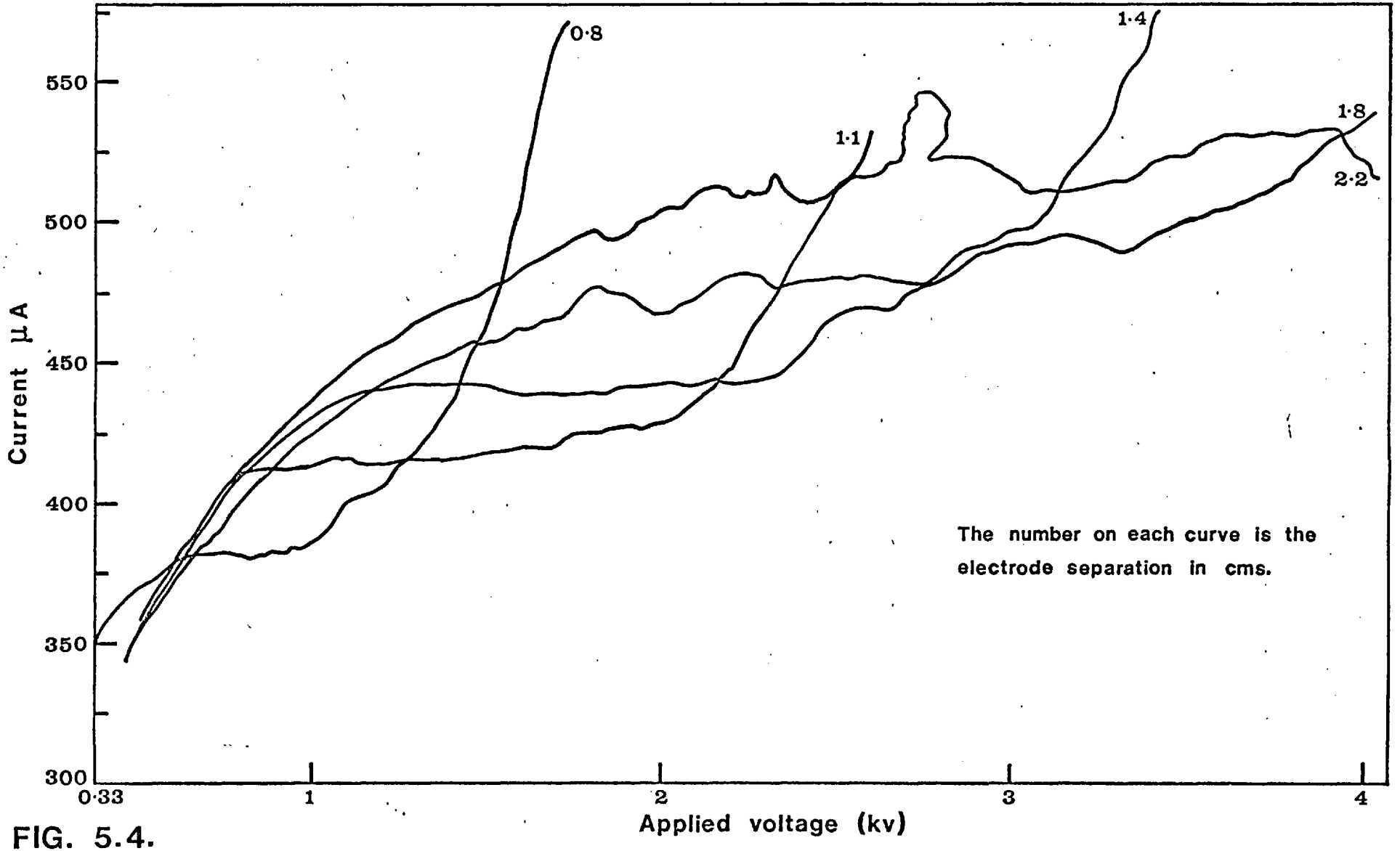

FIG. 5.4.

SCHEMATIC REPRESENTATION OF CURRENT DISTRIBUTION AT THE CURRENT AT WHICH ION DENSITY MEASUREMENTS ARE TAKEN

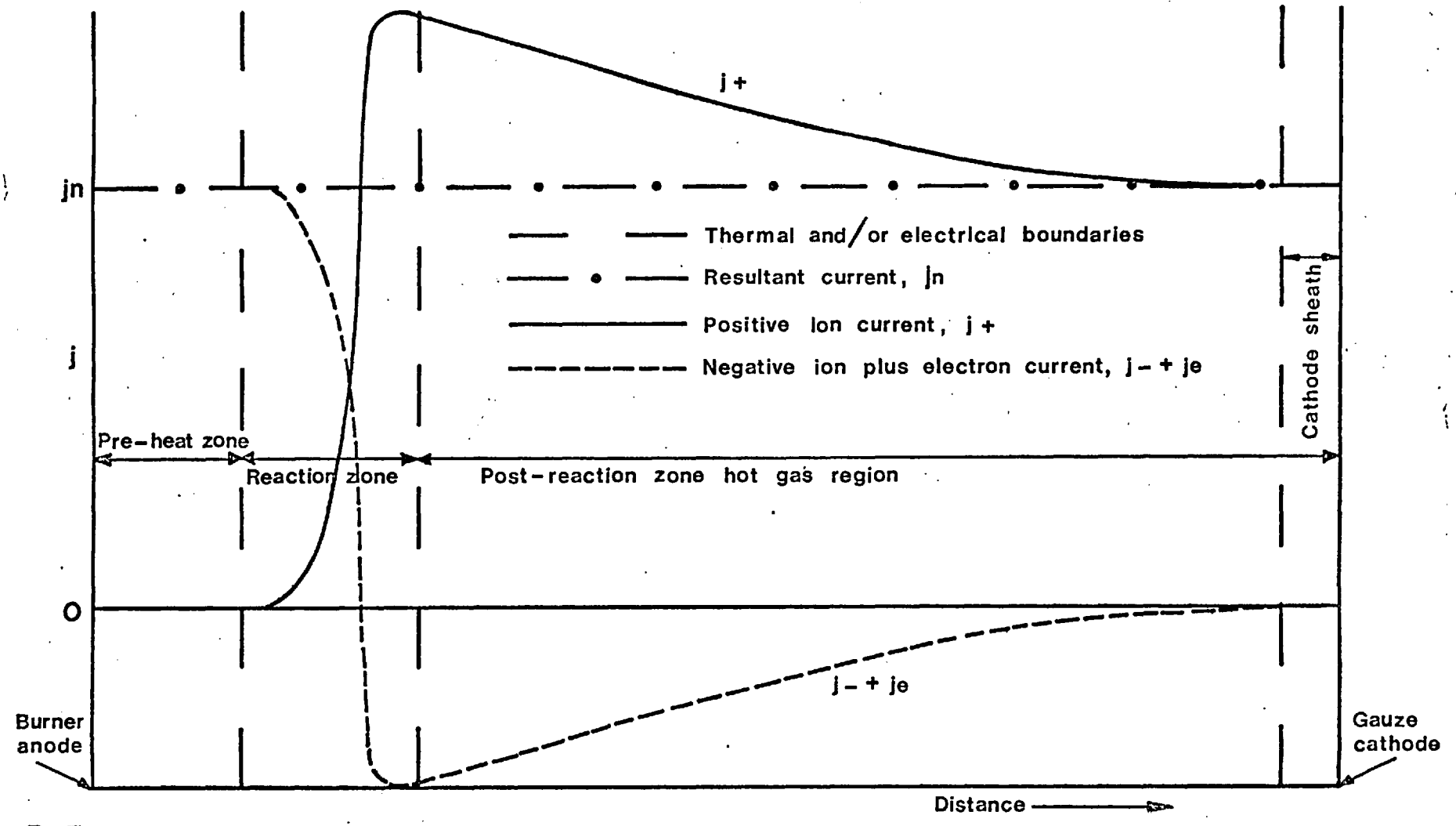

FIG. 5.5.

CHAPTER 6 EXPERIMENTAL RESULTS - RECOMBINATION COEFFICIENTS AND IONIZATION CROSS-SECTIONS

6.1 The ion density

On the basis of the theory developed in the preceding chapter, we are now in a position to use the graphs obtained to calculate positive ion densities. The current-voltage curves (Fig. 6.1) are used in preference to the less easily quantifiable voltage-distance curves (Fig. 6.2) in the manner described.

6.1.1 Equilibrium product species concentrations

Table 4.1 lists the reactant compositions and volumetric throughputs of the various flames studied. From these data, it is possible to calculate the equilibrium concentrations of the more important flame product species. These are shown in Table 6.1 for flames A to D for the temperatures at which the ion densities were measured.

Flame	Temp. (K)	Equilibrium species concentration (atmospheres)									
		$10^2 . N_2$	$10^2 . CO_2$	$10^2 . H_2O$	$10^2 . O_2$	$10^3 . CO$	$10^3 . NO$	$10^4 . OH$	$10^4 . H_2$	$10^5 . O$	$10^6 . H$
A	2025	78.9	9.93	10.1	0.51	2.2	1.35	9.4	4.8	5.7	42
	2021	78.9	9.93	10.1	0.51	2.2	1.3	9.3	4.8	5.6	41
	2012	78.9	9.95	10.1	0.51	2.0	1.3	8.9	4.5	5.2	37
	1994	78.9	9.98	10.1	0.50	1.8	1.2	8.1	4.0	4.5	31
	1977	78.9	10.0	10.1	0.49	1.5	1.2	7.4	3.5	3.9	26
B	1947	77.9	8.50	8.54	4.56	0.33	3.3	10.2	0.76	9.4	9.8
	1938	77.9	8.50	8.54	4.56	0.30	3.2	9.8	0.71	8.7	8.9
	1927	77.9	8.51	8.55	4.57	0.27	3.1	9.2	0.65	7.9	7.8
	1909	77.9	8.51	8.55	4.58	0.23	2.9	8.4	0.56	6.8	6.4
	1883	78.0	8.52	8.56	4.59	0.18	2.7	7.3	0.45	5.5	4.7
	1863	78.0	8.52	8.56	4.60	0.15	2.5	6.5	0.38	4.6	3.7
	1848	78.0	8.52	8.57	4.60	0.13	2.4	6.0	0.33	4.0	3.1

TABLE 6.1 THEORETICAL EQUILIBRIUM COMPOSITIONS

Cont'd....

Flame	Temp. (K)	Equilibrium species concentrations (atmospheres)									
		$10^2 \cdot N_2$	$10^2 \cdot CO_2$	$10^2 \cdot H_2O$	$10^2 \cdot O_2$	$10^3 \cdot CO$	$10^3 \cdot NO$	$10^4 \cdot OH$	$10^4 \cdot H_2$	$10^5 \cdot O$	$10^6 \cdot H$
C	1855	78.2	8.44	8.49	4.56	0.14	2.5	6.2	0.35	4.3	3.3
	1836	78.2	8.45	8.49	4.57	0.12	2.3	5.55	0.30	3.6	2.6
	1808	78.2	8.45	8.50	4.58	0.09	2.1	4.7	0.23	2.8	1.8
	1785	78.2	8.45	8.50	4.59	0.07	2.0	4.1	0.18	2.2	1.4
	1765	78.2	8.45	8.50	4.59	0.06	1.8	3.6	0.15	1.9	1.0
D	1793	77.2	8.84	8.89	4.80	0.08	2.1	4.45	0.20	2.5	1.5
	1778	77.2	8.84	8.89	4.80	0.06	1.95	4.1	0.18	2.1	1.25
	1758	77.2	8.84	8.90	4.81	0.05	1.8	3.5	0.14	1.7	0.9
	1734	77.2	8.84	8.90	4.82	0.04	1.7	3.1	0.12	1.4	0.7
	1707	77.2	8.85	8.90	4.83	0.03	1.5	2.6	0.09	1.1	0.5
	1686	77.2	8.85	8.90	4.83	0.02	1.4	2.2	0.07	0.8	0.3

TABLE 6.1 (Cont'd)

All data used in the compilation of Table 6.1 are taken from Rossini et al [135]. Later editions of the JANAF Thermochemical Tables do change some values, but not sufficiently to alter any of the arguments advanced here.

The OH : H ratio, as pointed out in the previous chapter, is high, thus lending qualitative support to the arguments produced there in favour of the reaction for hydroxide formation:

$$A + OH + M \rightarrow AOH + M$$

Another feature to be noted is that, because the flames were oxygen-rich and not hot enough for any substantial decomposition of the products, the CO_2 concentration is greater than the CO by a factor that ranges from ca. 300 to ca. 2000 in the three flames with the same equivalence ratio.

In contrast to the other radical species (see below), the NO concentration may be an overestimate, since NO is probably formed rather slowly (Marteney [136]). As against that, a super-equilibrium production of O or possibly N atoms may still lead to near equilibrium NO densities, and there is the possibility (Fenimore [137]) of the production of N leading to NO through the action of hydrocarbon fragments on the nitrogen molecule. Thus NO may be produced in super-equilibrium, equilibrium or sub-equilibrium (rising relatively slowly to equilibrium) concentrations. Whatever the case on these points and the NO concentration figures in Table 6.1, the existence of NO does not actually have any bearing on the following arguments.

It should be stressed that all the data tabulated in Table 6.1 are only equilibrium concentrations, rather than experimentally determined ones. They may be used to calculate

equilibrium atomic alkali concentrations, which, were they then to be used in conjunction with the ion production rate term tabulated later (Table 6.5) would then result in those curves in Figure 6.3, shown as $(k_i)_e = q/[A]_e$.

In this figure, the log of the ion yield divided by the equilibrium number of alkali atoms (under saturation current conditions) is plotted as a function of $^1/_T$. It might be expected that there would be one straight line plot for sodium and one for potassium, but, as is seen, there are separate curves for each of the flames considered. The departure from equilibrium is more marked at the lower temperatures, due to the increased over-production of flame radicals, but the curves are consistent with a tendency to collapse towards one common (equilibrium) line. Thus figure 6.3 amply bears out the arguments contained in section 5.5.1.

6.1.2 The theoretical equilibrium and the measured ion density

Having seen the effect of an overproduction of radicals on the maximum ion yield (i.e. under conditions of no recombination of ions) we now turn to the steady state ion density. Table 6.2 gives the thermodynamic data used for the alkali hydroxides. Kelly and Padley [60] have recently published data on them which challenge those used by, e.g., Jensen and Padley [45], and, more recently, Cotton and Jenkins [138]. Results presented later are based on the new data of Kelly and Padley (op. cit.), who accept a linear structure for alkali hydroxides as found by Acquista, Abramovitz and Lide [139], Acquista and Abramovitz [140], Kuczkowski Lide and Krisher [141], and Lide and Kuczkowski [142]. (The first

two of these papers use infra-red spectra and the last two microwaves.) These findings are confirmation of the early, perhaps somewhat fortuitous, assumption of a linear structure by Smith and Sugden [143] in some of the first 'modern', i.e. post-Wilson, experiments on alkali-seeded flames.

TABLE 6.2

MOLECULAR PARAMETERS

	NaOH	KOH	OH
r_{A-O} Å	1.93	2.18	-
r_{O-H} Å	0.96	0.96	0.96
10^{38} I gm cm^2	0.66	1.0	0.01463
ω_{A-OH} cm^{-1}	431	408	-
ω_{A-O-H} cm^{-1}	337	325	-
ω_{AO-H} cm^{-1}	3600	3600	-
ω_{O-H} cm^{-1}	-	-	3738
D_o^o(A-OH) kJ mole^{-1}	330	352	-

The main, and basically the only important difference between these values and those used by, for example, Cotton and Jenkins [138] and Jensen and Padley [45] lies in the value taken for the A-O-H bending frequency. These latter authors use 1300 cm^{-1}, which decreases the equilibrium constant for

$$AOH + M \rightleftarrows A + OH + M,$$

thereby also decreasing the predicted free atomic and ionic alkali concentrations. The revised data predict 2.2 . 10^{11} ions cm^{-3} at the highest temperature at which concentration measurements were made in flame B, compared with ca. 1 . 10^{11} ions cm^{-3} for

the old, and a measured concentration of ca. $3 \cdot 10^{11}$ ions cm^{-3}. Kelly and Padley's comment on this bending frequency appears to contain a misprint, the ω_{A-OH} stretching frequency being quoted instead of the correct ω_{A-O-H} frequency in one place.

In this table, values for the OH radical are taken from Chamberlain and Roesler [144], and the ω_{A-OH} numbers are, following Jensen and Padley, estimates using Gordy's [145] rule.

Table 6.3 lists, for each flame, values of j_n, the value of j at the "elbow" of the current-voltage curves, as determined by the intersecting tangent method described earlier, and the values used (see Appendix A) for the mobility and diffusion coefficients, related by the expression

$$D_+ = \frac{\mu_+ kT}{e}$$

The values of Y, found experimentally from the saturation current density versus electrode height, are, as already observed, 0.23 for the high temperature sodium-seeded flame, and $0.46(\pm 0.01)$ for the other three, potassium-seeded flames.

TABLE 6.3 TERMS USED IN CALCULATION OF ION DENSITY.

Flame	Electrode height (cm)	Temp. (K)	u ($cm\ s^{-1}$)	μ_+ ($cm^2\ V^{-1}\ s^{-1}$)	D_+ ($cm^2\ s^{-1}$)	$10^{-3}\ j_n$ ($e.s.u.\ cm^{-2}$)	$\frac{j_s}{j_s - j_n}$
A	1.12	2023	141	19.80	3.45	5.70	1.11
	1.42	2021	141	19.80	3.45	4.95	1.10
	1.82	2012	140	19.70	3.41	4.11	1.09
	2.32	1994	139	19.50	3.35	3.24	1.08
	2.82	1977	138	19.37	3.30	2.56	1.07
B	0.96	1947	99	16.75	2.81	12.45	1.20
	1.25	1938	99	16.65	2.78	10.02	1.13
	1.53	1927	98	16.50	2.74	7.50	1.09
	1.91	1909	97	16.35	2.69	5.37	1.06
	2.29	1883	96	16.15	2.62	4.05	1.04
	2.67	1863	95	15.95	2.56	3.30	1.03
	3.05	1848	94	15.82	2.52	2.95	1.02
C	1.50	1855	77	15.92	2.54	2.64	1.02
	1.90	1836	76	15.74	2.49	2.34	1.02
	2.30	1808	75	15.53	2.42	2.10	1.02
	2.70	1785	74	15.28	2.35	1.77	1.01
	3.10	1765	73	15.12	2.30	1.32	1.01
D	1.08	1793	50.5	15.40	2.38	2.31	1.03
	1.46	1778	50.0	15.27	2.34	2.13	1.03
	1.84	1758	49.5	15.05	2.28	1.86	1.02
	2.22	1734	48.8	14.86	2.22	1.53	1.02
	2.60	1707	48.0	14.62	2.15	1.26	1.02
	2.98	1686	47.4	14.45	2.10	1.02	1.01

The data of Table 6.2 lead to the following expressions for the equilibrium constant for reaction (5.27) (viz. AOH + M $\rightleftarrows$ A + OH + M):

for sodium,

$$K_{27} = 8\left(\frac{2\pi m_{Na} m_{OH} kT}{m_{NaOH} h^2}\right)^{3/2} \frac{I_{OH}}{I_{NaOH}} \frac{\prod_i {}^{NaOH}\left[1-\exp\left(\frac{-hc\omega_i^{NaOH}}{kT}\right)\right]}{\left[1-\exp\left(\frac{-hc\omega^{OH}}{kT}\right)\right]} \exp\left(\frac{-39663}{T}\right); \quad (6.1a)$$

and for potassium,

$$K_{27} = 8\left(\frac{2\pi m_{K} m_{OH} kT}{m_{KOH} h^2}\right)^{3/2} \frac{I_{OH}}{I_{KOH}} \frac{\prod_i {}^{KOH}\left[1-\exp\left(\frac{-hc\omega_i^{KOH}}{kT}\right)\right]}{\left[1-\exp\left(\frac{-hc\omega^{OH}}{kT}\right)\right]} \exp\left(\frac{-42307}{T}\right) \quad (6.1b)$$

The factor 8 at the beginning of each expression is simply the ratio of ground state statistical weights, viz.

$$\frac{g_A \cdot g_{OH}}{g_{AOH}}$$

It is these expressions, together with the equilibrium OH concentration from Table 6.1, which lead to the equilibrium atomic alkali concentration listed in Table 6.4, column 4. Column 5 of the same table is derived from column 4, by allowing for electron attachment to the equilibrium OH radical densities, a value of 1.78 eV (Smith and Branscomb [146], Branscomb [147]) being used for the electron affinity. Earlier values (Page [148]) are much higher, but these, coming from quite early microwave experiments, must be disregarded. They would, contrary to observation, predict near-total attachment of electrons to form negative ions even at the highest temperatures encountered here. A later value, due to Feugier and Queraud [149], of 2.13 eV is

open to the same type of objection. These latter authors use direct attenuation of microwaves, a method that has been generally discarded in favour of measurement of the Q-factor, to measure electron density, and compare this with the ionization level to be expected from complete thermodynamic equilibrium, using Saha's equation. The method is open to doubt and does not lead to any convincing reason for ignoring Branscomb's work.

Equilibrium concentrations for free atomic and ionic alkalis are derived from equations (5.27) and (5.30) to (5.33) inclusive. Using the subscript e to denote equilibrium values, we have, again utilizing the approximation $[A^+]_e \ll [A]_e$:

$$K_{27} = \frac{[A]_e [OH]_e}{[AOH]_e} \tag{6.2}$$

$$K_{31} = \frac{[A^+]_e [e]_e}{[A]_e} \tag{6.3}$$

$$K_{32} = \frac{[e]_e [OH]_e}{[OH^-]_e} \tag{6.4}$$

$$[A^+]_e = [e]_e + [OH^-]_e \tag{6.5}$$

and $$[A]_e = [A_T] - [AOH]_e \tag{6.6}$$

The solution of these for $[A]_e$ and $[A^+]_e$ is

$$[A]_e = \frac{K_{27}[A_T]}{[K_{27}] + [OH^-]_e} \tag{6.7}$$

and $$[A^+]_e^2 = \frac{K_{27}K_{31}[A_T]}{K_{32}} \cdot \frac{K_{32} + [OH]_e}{K_{27} + [OH]_e} \tag{6.8}$$

The latter reduces to the simple Saha equation if $[OH]_e$, and therefore electron attachment, and hydroxide formation, is ignored (i.e. in mathematical terms assumed equal to zero). $[A]_e$ would

then be the same as $[A_T]$, since $[A^+]_e \ll [A]_e$.

$[A^+]$, in column (6) of Table 6.4, is, of course, the same as n_+ of equation (5.16) and is calculated from that equation using the data already tabulated mainly in Table 6.3. Values of j_s for the small correction factor are taken from Figs. 5.1 and 5.2. Equation (5.16) is

$$[A^+] = n_+ = \frac{j_n \cdot j_s}{(j_s - j_n)\, e(u + 2\gamma D_+)} \qquad (5.16)$$

TABLE 6.4 MEASURED AND EQUILIBRIUM ION DENSITIES

Flame	Temp. (K)	Time after reaction zone (msec)	$10^{-13}[A]_e$ (cm^{-3})	$10^{-10}[A^+]_e$ (cm^{-3})	$10^{-10}[A^+]$ (cm^{-3})	$\frac{[A^+]}{[A^+]_e}$ %
A	2023	7	9.46	5.9	9.2	156
	2021	9	9.45	5.8	8.0	138
	2012	12	9.41	5.4	6.6	122
	1994	15	9.34	4.7	5.2	111
	1977	20	9.25	4.1	4.1	100
B	1947	8	3.71	22.2	30.8	139
	1938	11	3.56	20.4	23.3	114
	1927	14	3.40	18.5	16.9	91
	1909	18	3.15	15.6	11.9	76
	1883	22	2.78	12.1	8.9	73
	1863	25	2.53	10.0	7.3	73
	1848	29	2.33	8.5	6.5	77
C	1855	17	12.2	20.6	7.1	34
	1836	23	11.1	16.9	6.4	38
	1808	28	9.46	12.6	5.8	46
	1785	33	8.23	9.7	4.9	50
	1765	39	7.30	7.7	3.7	48
D	1793	18	18.6	15.6	9.4	60
	1778	25	16.8	13.1	8.7	66
	1758	33	15.3	10.6	7.7	73
	1734	41	12.6	7.8	6.4	82
	1707	49	10.4	5.6	5.3	95
	1686	57	9.17	4.3	4.4	102

The effect of electron attachment in the calculation of the equilibrium state ion density is not very great, being of the order of 10% at both ends of the temperature range.

An immediate point to note is that $[A^+]$ appears to vary from about 30% to about 150% of the equilibrium value. The cause of the observed sub-equilibrium concentration is the depletion of free alkali atoms by the hydroxyl radical through reaction (5.27):

$$A + OH + M \rightleftarrows AOH + M \qquad (5.27a)$$

The other line of argument is that, if (5.26) is balanced and predominates, then

$$\frac{[A]}{[AOH]} = \frac{[H]}{[H_2O]\,K_{26}} \qquad (5.26)$$

Sub-equilibrium values of $[A^+]$, and hence sub-equilibrium values of $[A]$, would then require $[H] < [H]_e$, whereas direct measurements (Bulewicz, James and Sugden [129], Kaskan [124;125] and Baxendale et al [126]) all lead to the conclusion, whether the flames by hydrogen or hydrocarbon, that $[H] > [H]_e$.

The above, almost a reductio ad absurdum, is strong evidence that reaction (5.27) is the dominant one for hydroxide production under the conditions prevailing here. This should not be taken to mean that (5.27) is necessarily fully equilibrated; indeed, if measured values of $[A_T]$ and $[A^+]$ and calculated values of K_{27}, K_{31} and K_{32} are substituted into equations (5.34) to (5.38) inclusive, it may be seen that, although there is numerical self-consistency, either $[OH]$, $[OH^-]$ and $[NaOH]$ in flame A or $[e]$, $[OH]$ and $[K]$ at the highest temperature in flame C come out negative.

6.1.3 The apparent "negative concentrations"

The reason for this "negative density" result in flame A is probably that the charge transfer reaction from the natural flame chemi-ions leads to alkali ion densities in excess of equilibrium. This is not in fact allowed for in the set of five simultaneous equations (5.34)-(5.38), so that the apparent atomic alkali concentrations from these equations turns out to be, not only in excess of equilibrium like the ion, but also, since there is little sodium hydroxide formation at these temperatures, in excess of the total alkali concentration fed in. To maintain consistency in the equations, the apparent alkali hydroxide concentration must then be negative since

$$[A_T] \simeq [A] + [AOH] \qquad (5.30)$$

This "negative hydroxide concentration" in its turn implies negative answers for $[OH]$ and $[OH^-]$ to keep K_{27} and K_{32} constant and positive.

As the temperature of measurement in flame A decreases, $[A^+]$, i.e. n_+, approaches from above its full thermodynamic equilibrium value, and at the lowest temperature there (1977 K) all concentrations deduced from the set of five simultaneous equations are compatible with full thermodynamic equilibrium, and not just a steady state.

In flame C, where a different trio of species give negative concentrations, a possible explanation seems to be a lag in the setting up of equilibrium in the reaction

$$K + OH + M \rightleftarrows KOH + M \qquad (5.27)$$

so that, in actual fact, there are at first more free potassium atoms than are indicated by the simultaneous equations.

At the final flame temperature of flame C (i.e. close

to the reaction zone) the hydroxyl radical concentration has begun to rise above its equilibrium value, implying that the apparent ratio $[e]/[OH^-]$ in the set of balanced equations must fall. In fact, it falls so much that, at the highest temperature, shortest time and highest hydroxyl concentration, it actually passes through zero to become negative, so in order to give self-consistent answers the balanced equations must give negative answers for the hydroxyl concentration.

In flame D, although the same thing must happen, the ion density produced in the flame itself is, because of the low natural flame ionization activation energy (see Chapter 4), as compared with the alkali metals, so much higher than the equilibrium alkali ion density (and, by charge transfer, the alkali ion density itself of course becomes much than its equilibrium value) that this effect again predominates over the one due to the over-production of hydroxyl radicals.

In general, one may say that the assumption of balanced reactions does come into conflict with the physical situation when only a short time has elapsed after the reaction zone. One approaches a balanced state only after longer times, and, in flame D, not at all.

6.1.4 Alkali superoxides

One other major reaction, not included in the scheme here, has been postulated. This is the three body formation of an alkali dioxide or superoxide, AO_2, which might be assumed to be similar, broadly speaking, to the HO_2 radical, which has in recent years been shown to be of significance in the combustion mechanism of hydrogen flames.

This reaction has been suggested, independently, by Haber and Sachsse [150], Bawn and Evans [151], and, more recently, Kaskan [152], McEwan and Phillips [153] and Carabetta and Kaskan [154]. A similar molecule, $(Cs)_x(O_2)_y$ is suggested by Bernard, Labois and Ricateau [155].

Kaskan, working with a fuel-lean hydrogen flame, found reaction (5.26) incapable of explaining his results, and, in a similar flame, McEwan and Phillips proposed the formation of NaO_2 to explain the decay of sodium atoms downstream of their reaction zone. These latter authors give a dissociation energy for the molecule of (65 ± 3) kcal mole^{-1}, which is also the figure that would be needed on the basis of Bawn and Evans' suggested structure if NaO_2 were to be formed in our flame A in concentrations similar to those of the free alkali atom. This, however, would imply a lowering of the ion density by a factor of ca. 2 in all flames (if a dissociation energy of 70 kcal mole^{-1} is adopted for KO_2), contrary to observation. Were this to occur, the solution for $[A]$, $[e]$ and $[OH]$ in equations (5.34), (5.35) and (5.37) would be negative at all temperatures considered. Further, the ionization cross-section, dependent on n_+ (see next section), would then be increased to a size which, although still credible, would, in the case of sodium, be quite substantially higher than that found by other methods.

The conclusion must therefore be that, in this work, alkali dioxides or superoxides are not formed in any significant quantities, and it is suggested that other mechanisms (perhaps reaction 5.27) might be operative in the fuel-lean flames where authors have postulated the existence of these molecules.

6.2 The ionization cross-section

6.2.1 Experimental determination of the ionization cross-section

Figures 6.3 and 6.4 (sodium) and 6.5 (potassium) are plots of the ionization constant, k_i (on a log scale) vs. the reciprocal of temperature, the former being the results of the present work and the latter pair including the results of other work. k_i is simply the quotient of q, the ion production rate term (see Table 6.5 below) and the atomic alkali concentration, and is shown in that Table together with the associated ionization cross-section as a function of T^{-1}, the values of T^{-1} corresponding to the values of T in Table 6.4.

Values of k_i shown in the graphs are, for flame A (sodium-seeded), based on equilibrium atomic alkali concentrations (which coincide with the steady state value from equation (5.34) at the lowest temperature of measurement - 1977 K), and, for flames B to D (potassium-seeded) on both the full thermodynamic equilibrium values and the steady state values from equation (5.34), adjusted as explained below in the case of flame D. The increasing lack of equilibrium may be seen from the slope of the graphs which ranges from 5.59 eV for sodium in flame A (within experimental error compatible with the ionization potential of 5.14 eV) through 3.82 eV (flame B cf. the potassium ionization potential of 4.34 eV) to 1.88 eV (flame D - completely incompatible with equilibrium). The four temperatures for which one obtains more or less the same ionization cross-section for potassium, on the hypothesis of a steady state, have a best straight line fit gradient of 4.00 eV. That hypothesis is therefore

consistent at these temperatures (1883, 1863, 1848 and 1785) with observation.

If $[N]$ is used to denote the total species number density at a temperature T, a gross ionization cross-section may be defined (Hollander [86], Hollander, Kalff and Alkemade [87], Jensen and Padley [84]) as

$$\sigma_i = \frac{k_i}{[N]} \left(\frac{\pi\mu}{8kT}\right)^{\frac{1}{2}} \exp\left(\frac{eE_i}{kT}\right) \qquad (6.9)$$

Here μ is the reduced mass of the alkali atom-gas molecule pair.

$$\mu = \frac{m_A \cdot m_g}{m_A + m_g}$$

where we have used an average for the mass of the gas molecule, m_g, weighted according to the partial pressure of each species. E_i is of course the ionization potential of the alkali, and other terms are standard ones.

Derived values of σ_i for Na and K are shown in Table 6.5. For potassium, it is seen that flame B gives the same results as flame C provided enough time is allowed to elapse in either flame to allow the setting up of the steady state described by equations (5.27) and (5.30) to (5.33). The temperatures at which this is valid are, as previously noted, 1883, 1863 and 1848 (flame B) and 1785 (flame C); at the next lower temperature after 1785, there is some doubt about the value of q since this was derived by extrapolation, so the corresponding cross-section is best ignored. The coincidence of the σ_i values measured in the two flames is sufficient to indicate that they are, possible systematic error apart, genuine. Flame D apparently gives much lower values for σ_i. It is the lowest temperature flame which has, one may be confident, the highest ratio of hydroxyl radicals

TABLE 6.5 IONIZATION CONSTANTS AND CROSS-SECTIONS

Flame	$10^{4}T^{-1}$ (K^{-1})	$10^{-13}q$ $cm^{-3}s^{-1}$	$10^{-13}[A]^{b}$ cm^{-3}	$\frac{q}{[A]}=k_i$ s^{-1}	$10^{12}\sigma_i$ cm^{2}	$10^{-13}[A]_e$ cm^{-3}	$\frac{q}{[A]_e}=(k_i)_e$ s^{-1}	$10^{12}(\sigma_i)_e$ cm^{2}
A	4.943	3.14	28.7[c]	-	-	9.46	0.332	3.17
	4.948	2.61	21.2[c]	-	-	9.45	0.276	2.71
	4.970	2.37	15.8[c]	-	-	9.41	0.252	2.82
	5.015	1.86	12.2[c]	-	-	9.34	0.199	3.08
	5.058	1.33	9.45	0.141	2.64	9.25	0.144	2.70
B	5.136	10.33	7.60	1.36	0.40	3.71	2.79	0.81
	5.160	7.26	4.78	1.52	0.49	3.56	2.04	0.66
	5.189	6.00	2.77	2.07	0.78	3.40	1.76	0.67
	5.238	3.94	1.64	2.40	1.17	3.15	1.25	0.86
	5.311	2.93	1.32	2.22	1.42	2.78	1.05	0.71
	5.368	2.04	1.18	1.73	1.58	2.53	0.81	0.74
	5.411	1.79	1.23	1.46	1.64	2.33	0.77	0.94
C	5.391	2.43	-0.004	-	-	12.2	0.199	0.20
	5.447	1.74	0.249	6.98	9.3	11.1	0.157	0.21
	5.531	1.11	0.953	1.16	2.36	9.46	0.117	0.24
	5.602	0.713	1.23	0.579	1.67	8.21	0.087	0.25
	5.666	0.64[a]	0.860	0.744	2.96	7.32	0.087	0.35
D	5.577	0.791	5.03	0.157	0.40	18.6	0.043	0.11
	5.624	0.564	6.05	0.093	0.30	16.8	0.034	0.11
	5.688	0.406	7.03	0.058	0.25	15.3	0.027	0.12
	5.767	0.364	7.77	0.047	0.31	12.7	0.029	0.19
	5.858	0.209	9.24	0.023	0.24	10.4	0.020	0.21
	5.951	0.163	9.25	0.018	0.26	9.17	0.018	0.26

a Doubtful extrapolation.
b From the solution of the five simultaneous equations describing the steady state.
c Greater than $[A_T]$ the total alkali concentration in all forms.

present to the equilibrium concentration and probably, initially, the highest ratio of ion density present to the steady state value. It would, therefore, not be surprising to find substantial electron attachment, obscured in the set of simultaneous equations describing the balanced steady state by the abnormally high ion density (see above). What the apparent σ_i values can yield is, however, a more accurate assessment of electron attachment than that given by the set of simultaneous equations in the case of flame D.

In order to bring the apparent σ_i values up to the one measured at the four temperatures specified above, the positive ion:electron density ratio must be somewhere in the range 6 to 8, rather than the 1.1 to 1.5 indicated by the solution of the set of five simultaneous equations. This will later be shown to have its repercussions on the recombination coefficient data of Table 6.7, explaining certain apparently anomalous features by relating them to recombination reactions between negative and positive ions rather than electrons and positive ions.

It is this numerical factor, mentioned above, that is used to adjust the values of σ_i in flame D to the average value found at the four temperatures in flames B and C for which valid results were obtained.

Table 6.6 lists both the literature values, and those found in the present work, for the ionization cross-section. The values listed from this work are, again, those found at the temperatures for which there seems reasonable justification for the assumption of a steady state (and hence the use of the set of simultaneous equations), or in the case of sodium (flame A) a state near enough to full thermodynamic equilibrium.

TABLE 6.6 IONIZATION CROSS-SECTIONS $cm^2 \times 10^{12}$

Authors	Kelly & Padley[156]; Jensen & Padley[84].	Jensen & Padley[157]	Hayhurst and Telford[83].	Kelly & Padley[85]	Hollander, Kalff & Alkemade[87]	Hayhurst and Sugden[28]	
$(\sigma_i)_{Na}$	2.7	3.1[a]	2.5; 2.6[b]	1.8[c] (10 - 20?)	4.3	9.1	2.4[a]
$(\sigma_i)_K$	2.3	2.6[a]	1.4; 2.1[b]	2.1[c] (10 - 20?)	1.8	2.6	1.5[a]
T	2440	2250	2025-2445	2080-2500	ca. 2200-2500	2005	2270
Method	Single rotating probe (both) Microwave (Na) Microwave, optical (K)	Microwave	Mass spec.	Single rotating probe/optical	Photometry	Microwaves	
Flame	$H_2/O_2/N_2$	$H_2/O_2/N_2$	$H_2/O_2/N_2$	$H_2/O_2/N_2$; $H_2/O_2/Ar$; $H_2/O_2/CO$	$CO/O_2/N_2$	$H_2/O_2/N_2$ plus trace C_2H_2	

Cont'd...

TABLE 6.6 (Cont'd)

Authors	Padley and Sugden [30]				King [158]	Knewstubb & Sugden [100]		Ashton & Hayhurst [159]	Present work	
$(\sigma_i)_{Na}$	1.3	1.9	2.9	5.5	1.0–1.3	1.7[a]	1.5[a]	2.5[d]	2.9	
$(\sigma_i)_K$	-	-	-	-	0.1–0.25	-	-	2.8[d]		1.6
T	2460	2360	2260	2160	1970	2400	2600	2000–2800	1980	1780–1880
Method	Microwaves				Probe with extrapolation to $(n_+)_e$	Microwave		Photometry. Average of many others	I-V characteristics from parallel electrodes	
Flame	$H_2/O_2/N_2$ plus trace C_2H_2				$C_3H_8/O_2/N_2$	$H_2/O_2/N_2$		Various $H_2/O_2/N_2$ flames	$C_2H_4/O_2/N_2$	

If no footnote, then either the result is quoted explicitly, or the flame composition is published, allowing us to calculate μ for the result.

a Our calculation from published value of α, using values of μ typical for a $H_2/O_2/N_2$ system.

b Our recalculation of Hayhurst and Telford's values, allowing for the fact that species other than H_2O are important in the ionization process.

c Our calculation from the data published for a flame similar to those studied in the present work. See text for comments on figures in parentheses.

d Calculated from Ashton and Hayhurst's published value of k_i, the average of their own and all other values previously published for hydrogen flames.

A number of explanatory comments are necessary on Table 6.6. These are best dealt with in the sequence in which the papers are listed.

Jensen and Padley's [84] 1966 paper lists the cross-sections as $9 \cdot 10^{-12}$ cm^2 and $8 \cdot 10^{-12}$ cm^2 for sodium and potassium respectively. In the text they point out that they assumed, at the time, that water vapour, constituting about one third of all the species present, was the only one which contributed significantly as a third body in the ionization process. Padley later corrected this view and, in Kelly and Padley [156], gave a revised value for σ_i (that shown in Table 6.6), bringing $(\sigma_i)_{Na}$ and $(\sigma_i)_K$ down by a factor of about three in each case, to allow for ionization with other species as third bodies. Hayhurst and Telford [83] quote the old value in the table in their paper, apparently having overlooked Jensen and Padley's [84] textual comments; the old value in that table should therefore be ignored.

The footnote comment on Jensen and Padley's [157] slightly later (1967) paper is self explanatory; it should however be noted that such assumed values of μ may not be fully accurate, but since in any case the expression for σ_i contains the square root of μ, any error involved is very small.

Hayhurst and Telford [83] do publish explicit results for σ_i, but based on the assumption that only water vapour is important as a third body in the ionization process. The values with footnotes under their name in the table are corrected values allowing for the other species present in their flames, and represent averaged quantities. Six separate measurements may be taken for both K and Na corresponding to the points on their graphs, and, naturally, there is a certain spread due to

experimental errors.

Kelly and Padley [85], by using flames varying widely in composition, are able to measure the relative efficacy of different third bodies in the ionization process. The footnoted value is what, according to their probe data, would be the cross-section for a flame similar in composition to those used in this work. However, in the same paper, Kelly and Padley publish graphs of k_i measured optically which yield results for k_i and σ_i nearly an order of magnitude greater than those quoted on the basis of probe work. Values of σ_i based on these optical studies are suggested in parentheses after their own quoted values. It has already been pointed out that Kelly and Padley's probe theory requires an alkali ion mobility more than an order of magnitude greater than that found by Bradley and Ibrahim [27] or that calculated and used in the present work (see Appendix A). Nevertheless, their value is unlikely to be greatly in error, since it is based on an empirical calibration valid for their temperature range; however, an extrapolation of the theory outside this temperature range would almost certainly be invalid. The "optical" value is probably invalid.

Padley and Sugden [30] present their results in the form of values at k_i at the temperatures indicated. They point out at the end of their paper that these imply more rapid variations of α with T (and σ_i with T) than is at all likely, so these results should be treated with caution.

King's [158] results may be discounted. Although his probe theory for the measurement of positive ion density, n_+, may be correct, his results depend on extrapolation of n_+ to the thermal equilibrium value $(n_+)_e$ the expression for α being

$$\text{arc coth}\ \frac{n_+}{(n_+)_e} = (n_+)_e\,\alpha\, t + \text{const.}$$

This extrapolation is not accurate enough to give the order of recombination, or, apparently, the correct order of magnitude for α. Parameters dependent on α, therefore, such as k_i and σ_i, should not be taken from this paper.

Ashton and Hayhurst [159] show graphs of $\log(k_i\, T^{-\frac{1}{2}})$ vs. T^{-1} from all published data for alkali ionization in hydrogen flames. They give a best straight-line fit to the data, irrespective of flame composition, of

$$k_i = (7.3 \pm 2)10^{13}\, T^{-\frac{1}{2}} \exp(-E_i/RT)\ s^{-1}$$

where E_i is the ionization potential of the alkali in question. Since the reduced mass of an alkali ion-gas molecule pair is dependent on composition and nature of the alkali, this implies different ionization cross-sections for each alkali (see equation (6.9)). The figures quoted in the Table under Ashton and Hayhurst's names are for reduced masses corresponding to the present flames. It should be noted that Ashton and Hayhurst's fit to the data, using a pre-exponential factor for the rate constant independent of the alkali, leads to the prediction that potassium should always have a higher cross-section than sodium. In most of the cases listed where determinations have been made of the cross-sections of both metals, the reverse is the case.

Results derived here, on the assumption (see above) of a steady state, but not full thermodynamic equilibrium, except in the case of sodium in the hottest flame (where the two appear to coincide, after making allowances for charge transfer effects in the earlier parts of the flame) are compatible with those found by other workers by a variety of other methods. The temperature

of measurement here is lower than that of any previous determination, except in the case of sodium, where it coincides with the lower end of Hayhurst and Telford's [83] range. Whatever the method used, the possibility of systematic error cannot be excluded, but the near identity of values obtained serves to reinforce the validity of all of them as long as they are used in a regime to which they are appropriate.

6.2.2 Theoretical estimates of σ_i

As might be expected from the four orders of magnitude discrepancy between the ionization cross-sections found here and the corresponding gas kinetic cross-sections, the process of ionization is far from simple. As further illustration of this point, the work of Cuderman [160] may be cited. A beam of monoenergetic ground state potassium atoms in the energy range 20-1000 eV was passed into a collision chamber having a target gas pressure of $1 \cdot 10^{-5}$ torr; the measured ionization cross-section varied from about 10^{-19} cm^2 at the lower end of the range to about 10^{-15} cm^2 (i.e. gas kinetic values) at the higher end.

The first attempt to come to terms with the anomalously high cross-section encountered in flames seems to have been that of Hollander, Kalff and Alkemade [87], who considered excited states of the alkali atom up to a level ~kT below the ionization potential, arguing that the further ~kT necessary for ionization could then be received in collision with another gas molecule. At flame temperatures, the number of excited states involved in this distance from ground up to within ~kT of the limit is ca. 200, which, were all these levels to be weighted equally, would bring the ionization cross-section down to ca. 200 $Å^2$ on the basis of their results.

Direct evidence of at least a two-stage ionization process is to be found in the shock tube experiments on noble gases of A.J. Kelly [161] and Harwell and Jahn [162]. The first step involves excitation to one of the four closely spaced energy levels, two of which are metastable, that consist the first excited state of the atom. No hypothesis is however put forward as to the means by which the atom is ionized from its excited state.

This problem has recently been approached by Matsuzawa [163] for the case of the rare gases, and Fowler and Preist [164] and Preist [165] for the case of alkali metals in flame gases. Both the first of these papers and the latter pair consider the means whereby energy may be transferred to an electron still bound to the alkali, but in a state with a high value of the principal quantum number. Both energy and momentum must, of course, be conserved, and a condition for this is derived in the latter pair of papers for molecular third bodies, viz.,

$$\Delta < (4J + 6)B_o < kT$$

where Δ is the distance of the energy level of the electron below the ionization level, J the rotational quantum number and B_o the molecular parameter that describes the spacing of the rotational energy levels of the molecule that transfers energy to the electron, being de-excited itself in the process. So, the distance below the ionization limit of the electron energy level from which ionization takes place is seen to be less than kT, a suggestion first put forward by Jensen and Padley [157].

Both rotational and vibrational de-excitations are considered, as are the effect of both dipolar and quadrupolar molecules, and in addition possible single rescatterings of the

electron or gas molecule are taken into account using the method of Chew and Low [166], first developed to analyse elementary particle reactions.

As the binding energy, Δ, approaches zero, the number of available states goes to infinity for an isolated atom; however, in an ionized gas, it remains finite (Ecker and Weizel [167]), so, in principle, it is possible to estimate the number of states from which ionization may take place. The mechanism, due to a broadening of the levels and consequent overlapping, is described by Preist [168], who estimates the number of states below this continuum, as do Inglis and Teller [169]. The former estimate yields 250,000 and the latter 20,000; these represent extremes, with the true number probably lying somewhere between. It is of interest that this number should vary as the electron density raised to a small negative power (-0.4 to -0.5); if this be the case, the ionization coefficient is, in the case where a saturation current is drawn, different from that where a negligible current is drawn, and a systematic error is thereby introduced into the method. In addition, different results for k_i would be measured by different workers, dependent on the electron density present in each case.

The cross-section for ionization from a given level may be derived using the Born approximation, which was shown to be a good approximation for polar molecules (Takayanagi [170]) and quadrupolar molecules (Gerjuoy and Stein [171]). The former, however, probably breaks down for water vapour since a condition for it to hold is that

$$2D \ll 1$$

where Dea_o is the dipole moment (1.85 e.s.u. or 0.724 in these

units for H_2O), a_o being the Bohr radius.

On taking all these things into consideration, the gross ionization cross sections are given by

$$\sigma_i = \left(\frac{\mu_j}{m}\right)^{\frac{1}{2}} \frac{2\pi Q^2 a_o^2}{15} \frac{4}{\sqrt{\pi}} \left(\frac{B_o}{kT}\right)^{\frac{1}{4}} 0.9\, \underline{N} \qquad (6.10)$$

for a quadrupolar molecule (Preist's [165] equation (17)) and

$$\sigma_i = \left(\frac{\mu_j}{m}\right)^{\frac{1}{2}} \frac{8\pi D^2 a_o^2}{3} \frac{Ry}{kT} \left(\frac{kT}{B_o}\right)^{\frac{1}{4}} \left(\frac{2}{\pi}\right)^{\frac{1}{2}} I(0)\, \underline{N} \qquad (6.11)$$

for a dipolar molecule (Preist's [165] equation (24)) where $\underline{N}$ is the total number of bound states in the atom, Ry is one Rydberg, and $I(0)$ is the value of an integral $I(\Delta)$, defined elsewhere in the paper, in the limit as $\Delta \to 0$.

When molecular constants are substituted into the quadrupolar expression, it is seen that something like 10^4 bound states of the atom are required to explain the cross-section observed by Jensen and Padley [84], and Kelly and Padley's [156] results are explained by taking a lower limit of $n = 20$ on the principal quantum number. Carbon monoxide is not nearly as efficient as the polar expression indicates, however, and the case of water vapour molecules is, as yet, shrouded in mystery.

The present results are explicable if the total number of bound states in the atom lie somewhere between the two estimates of Preist [168] and Inglis and Teller [169]. Since however the flame gases contained some 10% of water vapour, there seems little to be gained by calculating how many states would be necessary to provide a quantitative explanation of the experimental results. In addition, only the theory of Matsuzawa attempts to explain the unusually high efficiency of monatomic species, relative to molecules, as third bodies in the ionization

process; even that predicts results that are consistently too low. Other weaknesses in the alternative theory are referred to by Fowler and Preist temselves.

Hayhurst and Telford [83] criticise the assumption in the theory propounded by Hollander, Kalff and Alkemade [87] of a "ladder-climbing" model, with the various excited states being in thermodynamic equilibrium with the ground state, i.e. the equivalent of a unimolecular reaction at its high pressure limit, for which transition state theory may be applied. Standard transition state theory, however, (considering a loosely bound electron and positive ion as the transition state, having a partition function about two orders of magnitude above that of the ground state) leads to pre-exponential functions some three orders of magnitude above those observed. These authors, therefore, conclude that the assumption of thermodynamic equilibrium between excited states and the ground state is invalid.

Instead they propose the formation of a loosely bound ionic complex and a subsequent ionization process.

$$A + M \rightarrow A^+M^-$$

$$A^+M^- \rightarrow A^+ + M^-$$

$$M^- \rightarrow M + e$$

This leads to an activation energy slightly less than the ionization potential and a pre-exponential factor significantly larger than that for a normal collision frequency. The authors estimate that this would lead to an ionization cross-section about 800 times the gas kinetic value in the case of $M = N_2$.

However, if, for the reaction of an excited alkali with a gas molecule, the pre-exponential factor in the rate constant increases as the atom nears the ionization limit,

Hollander's scheme is capable of explaining the size of the cross-sections. This phenomenon of an increasing pre-exponential factor does however appear in Preist's [166] analysis; for the hypothetical case of an isolated atom, it should in fact go to infinity.

We may conclude, then, that the high cross-sections for ionization found experimentally are in accord with the, as yet, semi-quantitative predictions of Preist [165], and Fowler and Preist [164]. Their preliminary analysis suggests, if anything, that the surprising feature about most ionization cross-sections measured up to now is that they are on the low, rather than the high, side. If the present results are free from systematic error, which some others, it has already been argued, may not be, they would lend credence to this theoretical problem.

6.3 The electron-ion three-body recombination coefficient

Having found the positive ion density under conditions approaching the ideal, as regards electrical disturbance of the flame plasma, we are now in a position to calculate, by substituting values of n_+ from equation (5.16) into equations (5.25), the three body recombination coefficient, α, for the reaction

$$e + A^+ + M \rightarrow A + M$$

Table 6.7 lists, at the temperature of measurement, the terms which appear in equation (5.25a):

$$\alpha = \frac{q}{n_+^2} + \frac{u\gamma}{n_+} \qquad (5.25a)$$

where α is of course an average over both electron and negative ion recombination processes.

Because of the delay in the establishment of a steady state

TABLE 6.7 THE AVERAGE RECOMBINATION COEFFICIENT

Flame	Temp. (K)	$q \cdot 10^{-13}$ $cm^{-3}\ s^{-1}$	$\frac{10^9 q}{n_+^2}$ $cm^3\ s^{-1}$	$10^9 \gamma u/n_+$ $cm^3\ s^{-1}$	$10^9 \alpha$ $cm^3\ s^{-1}$
A (Na seed)	2023	3.14	3.7	0.35	4.1
	2021	2.61	4.1	0.41	4.5
	2012	2.37	5.5	0.49	5.9
	1994	1.86	6.9	0.62	7.5
	1977	1.33	7.9	0.77	8.7
B (K seed)	1947	10.33	1.1	0.15	1.2
	1938	7.26	1.3	0.20	1.5
	1927	6.00	2.1	0.27	2.4
	1909	3.94	2.8	0.37	3.2
	1883	2.93	3.7	0.50	4.2
	1863	2.04	3.9	0.61	4.5
	1848	1.79	4.2	0.66	4.9
C (K seed)	1855	2.43	4.9	0.50	5.4
	1836	1.74	4.3	0.55	4.9
	1808	1.11	3.3	0.60	3.9
	1785	0.713	3.0	0.69	3.7
	1765	0.64	4.7	0.91	5.6
D (K seed)	1793	0.791	0.89	0.25	1.1
	1778	0.564	0.74	0.26	1.0
	1758	0.406	0.69	0.30	1.0
	1734	0.364	0.89	0.35	1.2
	1707	0.209	0.74	0.41	1.1
	1686	0.163	0.86	0.50	1.4

referred to above, the most reliable values of α are those measured at the lowest temperatures in each flame (i.e. after allowing as long a time as possible to elapse after the reaction zone). Values of α determined in the earlier parts of the flame are invalid because the equations take no notice of the effects of charge transfer from a species, H_3O^+, arising from the flame itself, whose concentration is actually higher than the steady state alkali ion density.

The result at 1765 K (flame C) should, as noted, be discounted because of a possible dubious extrapolation of the ion production rate curve. The low values in flame D are accounted for by electron attachment and the consequent important role of the recombination reaction

$$K^+ + OH^- + M \rightarrow K + OH + M,$$

which also possibly accounts for why α at 1785 K (flame C) is less than at 1848 to 1883 K in flame B.

6.3.1 Parameters used in the determination of α.

The values of q, the ion pair production rate term, quoted in Tables 6.5 and 6.7, come from the saturation current density vs. distance graphs (see section 5.2.1 and Figures 5.1 and 5.2). Having established q, a graph of q vs. x then gives the positive ion density distance scaling factor, γ, as derived in section 5.2.3. The values quoted from the method outlined in that section are not quite the same as those which would be obtained by a plot of positive ion density, given in Table 6.4, column 6, against distance. However, this is not of great importance, since all the term in γ does is provide a correction factor which increases the value of the recombination coefficient

(column 9) by from 10% to apparently about 60%, but in this latter case there is substantial electron attachment, so equation (5.25a) gives a value of α quite far removed from that for electrons. In principle, one could use an iterative procedure of feeding a value of γ derived from the measured ion densities back into the expression for the ion density to obtain a "better" value for it, then repeat until the required degree of self-consistency had been obtained, but it is felt that overall accuracy does not warrant this. Besides altering only a first order correction factor, it is in any case very doubtful whether the ion density measurements are more accurate than the ion production rate, so the correction factor is better derived from the latter, and any error involved is likely not to add substantially to those already present. Charge transfer effects from natural flame ions and subsequent recombination in any case alter the ion profile just downstream of the reaction zone.

The charge transfer effect is shown in its most pronounced form in the ion density curves in flames A and B. In the former, the apparent value of γ is about twice that calculated from the ion production rate curves. In the latter, it is 0.77, as compared with 0.46 from the ion production rate curves, but, if only the ion densitites at the temperatures where a steady state is postulated are used, then the value of 0.77 comes down to 0.41, consistent with the other method of measurement of γ. In the other two flames, C and D, values for γ of 0.39 and 0.41 are obtained, indicating either a steady state in the ionization-recombination reactions, or the lack of one masked by other reactions involving potassium atoms that have not reached a steady state. This is plausible since one would expect

Coulombic forces to hasten the rate of an electrical three-body reaction as compared with a similar neutral one.

The other term which enters into the calculation of the correction factor, as well as, more importantly, into the calculation from the observed graphs of the ion density, is the burnt gas velocity, u. The magnitude of u is obtained from measurements of the total volumetric throughput of the gases and the cross-sectional area of those gases coming from the central part of the burner, the area being measured by casting an image of this central, luminous section on a screen. It was not necessary to check this value of u since it is known (Kelly and Padley [156]) that such calculations for a shielded flame on a Meker burner; i.e. like the present system, agree to ca. 4% with particle track measurements of gas velocity.

6.3.2 Experimental values of the recombination coefficient

The values of the recombination coefficient shown in Table 6.7 appear somewhat irregular, and the coefficient found for flame D is anomalously low if one is to take seriously the $|e|:|A^+|$ results obtained from the simultaneous equations. However, using a corrected value of this ratio, β_{corr}, that brings the apparent σ_i values of Table 6.5 up to $1.6 \cdot 10^{-12}$ cm^2, the average value found in flames B and C after the excess ion density has decayed to a steady state value, one may obtain a corrected value of α, which gives a good approximation to α_1, the value for electrons.

From chapter 5, we have

$$\alpha = \frac{q}{n_+^2} + \frac{\gamma u}{n_+}$$

$$= \beta\alpha_1 + (1 - \beta)\alpha_2 \qquad (5.25b)$$

or $$\frac{\alpha}{\beta} = \alpha_1 + \frac{(1-\beta)}{\beta}\,\alpha_2$$

This function appears in Table 6.8 for flames A, B and C with α as found from the simultaneous equations at the temperatures where it seems probable there is a steady state (i.e. where the assumptions behind the equations have not been violated). For flame D, the corrected value of α (as explained above) is used.

In flame A, attachment is seen to be negligible and α, therefore, corresponds almost purely to the electron/ion/third body reaction. Flame B shows a steady rise in α as temperature decreases, there being ca. 20% attachment. In flame C, α appears to drop with respect to the higher temperature flame B, but the corrected value, after allowing for electron attachment in the steady state, brings α back to a value consistent with B.

Using the apparent value of β, β_a, for flame D would lead to values of α/β less than those of flames B and C, and imply a negative value of α_2, the coefficient for the positive ion/negative ion/third body reaction. The corrected value of β, once again, however, assures compatibility of α/β with the higher temperature flames.

Since the factor $\frac{(1-\beta)}{\beta}$ changes by a factor of ca. 20-30 for the potassium seeded flames without any noticeable change in the recombination coefficient other than that which might be expected from temperature changes (Bates, Malaviya and Young [42]) one may reasonably conclude that the effect of α_2 lies within the range of random errors. If this is put, at 1800 K, as ca. $2 \cdot 10^{-9}$, then since, for flame D, $\frac{1-\beta}{\beta}$ has a minimum value of ca. 5, this means that an upper limit may be put on α_2, viz.

$$\alpha_2 \leq 4 \cdot 10^{-10}\ \mathrm{cm}^3\ \mathrm{s}^{-1}$$

TABLE 6.8 THREE BODY RECOMBINATION COEFFICIENTS FOR ELECTRON-POSITIVE ION REACTIONS AND NEGATIVE ION-POSITIVE ION REACTIONS (ORDER OF MAGNITUDE ESTIMATE)

Flame	Temperature (K)	α_a (a)	β_c (b) $= \beta$	$\frac{1-\beta}{\beta}$	$10^9\alpha$ ($cm^3\ s^{-1}$)	$10^9 \frac{\alpha}{\beta}$ ($cm^3\ s^{-1}$) $= 10^9 \left[\alpha_1 + \frac{1-\beta}{\beta}\ \alpha_2\right]$	$10^9\ \alpha_2$ (b) ($cm^3\ s^{-1}$)
A	1977	0.95	As β_{app}	0.05	8.7	9.1	
B	1883	0.80	As β_{app}	ca. 0.25	4.2	5.3	
	1863	0.79	"	"	4.5	5.7	
	1848	0.81	"	"	4.9	6.1	
C	1785	0.52	As β_{app}	ca. 1	3.7	7.1	
D	1793	0.66	0.16	ca. 5	1.1	6.9	$\leqslant 0.4$
	1778	0.72	0.14	ca. 6	1.0	7.2	
	1758	0.77	0.12	ca. 7	1.0	8.3	
	1734	0.81	0.16	ca. 5	1.2	7.5	
	1707	0.87	0.13	ca. 6.5	1.1	8.5	
	1686	0.88	0.14	ca. 6	1.4	10	

(a) From the set of simultaneous equations. (b) See text.

This, with OH^- as the negative ion compares with recombination coefficient values for negative halogen ions with potassium ions found by Hayhurst and Sugden [28] which range from $2 \cdot 10^{-10}$ (Cl^- and Br^-) to $3 \cdot 10^{-9}$ (I^-) at a temperature of 1800 K.

6.3.3 Present and other literature values of α

The values of $\alpha/\beta \simeq \alpha_1$ shown in column 6 of Table 6.8 are plotted, together with the results of other workers in Figures 6.6 and 6.7. There is good agreement for both the potassium and sodium results, despite the variety of method used to determine ionization constants and ion or electron densities.

It is possible that, for sodium, the results of Hayhurst and Sugden [28] are too high. Using mass spectrometry, they noticed the first hydrate of the sodium ion in a proportion such that

$$\frac{[Na^+]}{[Na^+ \cdot H_2O]} \simeq 60$$

A reasonable assumption is that, like the hydronium ion, H_3O^+, this hydrate has a dissociative electron-ion recombination coefficient in the range $(1 - 4) \cdot 10^{-7}$, in which case the measured coefficient would be higher than that for the electron/ion/third body reaction by ca. 20%. The Hayhurst and Sugden results would still then be a factor of ca. 3 above the present ones and most others at similar temperatures. Padley and Sugden's [30] results are believed to show a spurious temperature dependence, and King's [157] results may be discounted because of the dubious extrapolation in his probe theory already commented on.

In Figure 6.7 there is less likelihood of spuriously high recombination coefficient since the $[K^+]:[K^+ \cdot H_2O]$ ratio

is much higher (Hayhurst and Sugden, op. cit.).

Ashton and Hayhurst's [159] best fit to the hitherto available data for all alkalis in hydrogen/oxygen/nitrogen flames, regardless of their composition, is

$$\alpha_1 = (3 \pm 0.8)10^{-2}\ T^{-2}\ cm^3\ s^{-1}$$

This ranges from $7.7 \cdot 10^{-9}$ at 1977 K to $10.6 \cdot 10^{-9}$ at 1686 K.

Bates, Malaviya and Young's semi-quantal prediction at 2000 K for a mixture of nitrogen and 20% hydrogen is $5.1 \cdot 10^{-9}$; the same, following a classical method (Sayasov [40], Dalidchick and Sayasov [38,39]) leads to $8.7 \cdot 10^{-9}$ at the same temperature.

The Thomson [32] theory, where one of the bodies is an electron, is expressed in terms of the average fractional energy loss, f. It varies from ca. $2.1\ 10^{-7}$f at 2000 K to ca. $3.2.10^{-7}$f at 1700 K. As pointed out in chapter 2, the corresponding value from Natanson's [36] theory is higher by a factor 85/64 (i.e. ca. 30%). At the temperatures encountered here, and the corresponding electron mobilities (see Appendix B) the term $1/\alpha_H$ in the equation (see chapter 2)

$$\frac{1}{\alpha_N} = \frac{1}{\alpha_T} + \frac{1}{\alpha_H}$$

is completely negligible.

6.4 The overall accuracy

The measured values of q are probably good to ca. 15%, and the ion density measurements to about the same. The gross recombination coefficient has therefore an associated random error of ca. 20%. When this is separated out into its components, difficulties arise since the electron and negative ion densities have to be calculated on a steady state hypothesis, or adjusted

empirically where the equations break down. Nevertheless, the consistency shown in Table 6.8 gives reasonable confidence to expect that these calculations are not greatly in error, so α_1 is probably accurate again to 20% even in flame C. Flame D raises problems because of the empirical adjustment of the ionization cross-section to those measured in flames B and C and the increasing importance of the negative ion reaction; in other words there is a systematic error introduced here as well as a random one. The values shown for D of $\alpha/\beta \simeq \alpha_1$ may then be regarded as upper limits with the same random error as in the other flames.

The question of ionization cross-sections is somewhat different because of the exponential term. A temperature error of 25 K gives rise to an error of ca. 30% and one of 50 K to a factor of ca. 2. As explained in Chapter 3, allowances were made for systematic errors in temperature measurement, but Figure 3.2 does show certain unavoidable irregularities in the temperature profile. Since the ion production rate, electron density and positive ion density, as well as the temperature-containing exponential, come into the expression for the cross-section, the estimated error attached to the cross-section may be placed at ca. 50%.

6.5 Reduced pressure measurements

Attempts were made to measure the pressure dependence of α.

6.5.1 The reduced pressure apparatus

A 5 cm diameter, 2.5 cm high water cooled Egerton-Powling matrix burner was used in the low pressure housing used

in the paper of Boothman et al [24]. The matrix, formed by winding alternate plain and crimped metal tapes in a tight spiral to the diameter of a collar that fitted into the water cooling jacket, allowed the passage of a fine potassium carbonate spray from the atomiser used in the atmospheric pressure work. Beneath the matrix was a column of glass beads which, perhaps somewhat surprisingly and fortunately, did not impede the passage of the potassium carbonate spray. Neither the gas flow system nor the electrical circuit was different in any fundamental respect from the atmospheric pressure work.

An additional electrical circuit allowed ignition by means of a spark, applied between the upper gauze electrode and an additional wire one, from a 3 kV mains transformer. During ignition, the thermocouple used for temperature measurements was, for protection, retracted into a short metal cylinder built into the inside of the metal one of three side windows of the burner housing. Both electrodes and the thermocouple entered the housing through standard sliding seals, obtained from Messrs. Edwards (High Vacuum) Ltd., the former two vertically and the latter horizontally.

The flames, of approximately the same equivalence ratio as the potassium-seeded ones at one atmosphere pressure, were burned within the pressure range 160-600 torr. At the higher end of this range, the centre of the matrix became red hot, giving rise to concern that ion emission from it may vitiate ion density results. As might be expected, the gas temperature above this part was much lower than that nearer the circumference of the matrix. In addition to this, in some flames, there was actually a temperature inversion, caused by diffusion, so that

in some parts of the gases, temperature actually rose with height, rather than decreasing. The absence of a shielding flame is a further complicating factor.

Because of the temperature irregularities, and the exponential dependence of ionization rates on temperature, the relevant area of cross-section for the flame gases may not, indeed almost certainly does not, coincide with the area of the matrix.

6.5.2 Values of α at sub-atmospheric pressure.

In view of this, only qualitative (i.e. order of magnitude) estimates of α could be made. By applying the same line of analysis as at atmospheric pressure, α ranged in value from ca. $4 \cdot 10^{-9}$ at 470 torr, through ca. $1 \cdot 10^{-8}$ at 275 torr to, at 156 torr, ca. $2 \cdot 10^{-9}$ (units of cm^3 $molecule^{-1}$ s^{-1} in all cases).

Such values, when the associated error is taken into consideration, are not in contradiction with theory. Bates, Malaviya and Young [42], for example, predict that α may rise by an order of magnitude as the temperature drops from $2 \cdot 10^3$ K to $1 \cdot 10^3$ K. This, on taking into account the fact that, especially at the lower end of the pressure range, the temperature dropped to as low as ca. 1350 K (after thermocouple corrections had been added on), is enough to counteract the expected drop in α with pressure which is expected on the basis of three-body collision theory.

The reduced pressure estimates, although they do not add to the knowledge of the three-body recombination rate, do not contradict the existing theories, and, after allowing for the quite big errors involved, are compatible with them.

6.5.3 Three-body reactions at reduced pressure

Rather more important than this somewhat negative result are two observations made at reduced pressure which are not dependent on the gross irregularities of the system.

Figure 6.8 is a trace of the current-voltage characteristic for an unseeded ethylene-air flame at 242 torr, and shows the saturation current plateau region. The number by each curve refers to the height in cm of the electrode above the flame reaction zone, and is also therefore related to the time taken for charged species to reach the electrode (the higher the number the longer the time). The interesting part is the break in the curves at about 50% of the saturation value; the rise to saturation from then on is much slower (as a function of applied voltage), and in the highest electrode case, saturation barely sets in before secondary ionization. This transition can only be due to the existence of two negative species of widely different mobilities, viz. electrons and negative ions.

The sudden change in gradient is, then, quite elegant visual proof of the existence of an electron attachment reaction. It is also a demonstration of the speed with which it takes place. At lower electrode heights, it is debatable whether the effect is present, but at higher ones, the charged species has to travel through the gases for a time roughly proportional to the electrode height (if there is a more or less uniform field between electrode and burner) so attachment probably approaches some steady state value.

The effect was not noticed at atmospheric pressure, nor indeed in all the reduced pressure flames, and is dwarfed when an alkali seed material is fed into the flame. It is

suggested that the effect may be limited in its importance to the outer sections of the flame, where the absence of an annular shielding flame means that flame gases tend to mix (as is not the case in the atmospheric pressure work) with the surrounding recirculated combustion product gases.

Due to this, and the other imponderables and irregularities in the situation, no meaningful estimate can be made of the electron attachment rate, and the figure stands as a purely qualitative demonstration of the effect.

Despite the, in general, lower temperatures employed at reduced pressure, it was usually easier to obtain electrode height dependent saturation currents. As an illustration of this, Figure 6.9, showing saturation current plateaux as a function of height for a potassium seeded flame at 212 torr, may be compared with Figure 5.4, showing the same at atmospheric pressure, the latter being one of the better to decifer, the former quite average. In other words, there seems at reduced pressure, to be much more free atomic alkali (in comparison with the total alkali introduced) than at one atmosphere.

This may be taken as confirmation of a third-body reaction (whose rate is of course inversely proportional to pressure in this range) in the removal of free atomic alkali. Support is therefore found for the reaction

$$A + OH + M \rightarrow AOH + M \qquad (5.27)$$

at atmospheric pressure, with possibly the alternative reaction (5.26)

$$A + H_2O \rightarrow AOH + H$$

coming to predominate at reduced pressures.

CURRENT VS. APPLIED VOLTAGE TRACE AT LOW CURRENT (DETAIL)

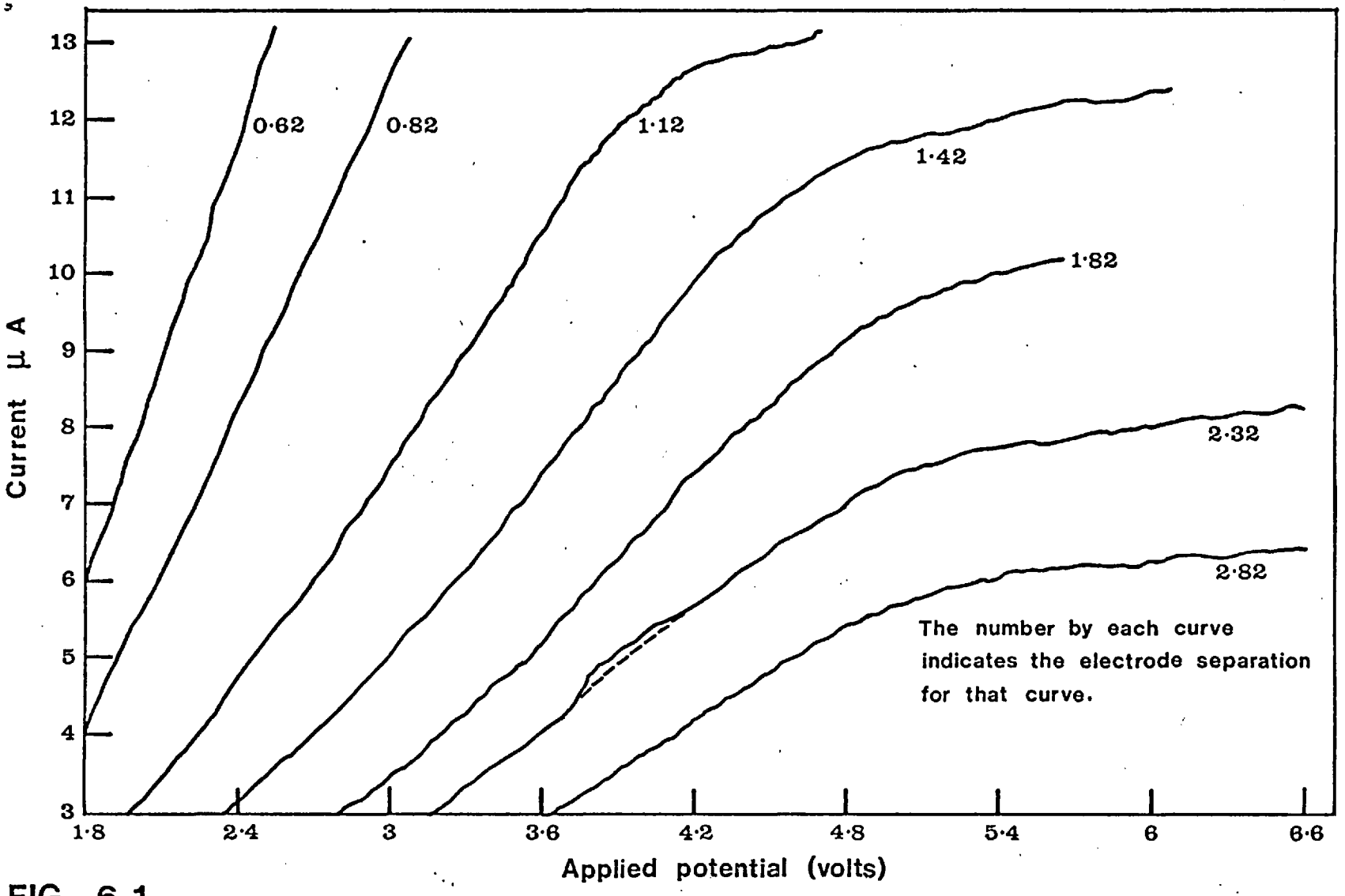

FIG. 6.1.

APPLIED VOLTAGE VS ELECTRODE HEIGHT AT CONSTANT CURRENT (Cross-plotted from Fig. 6.1.)

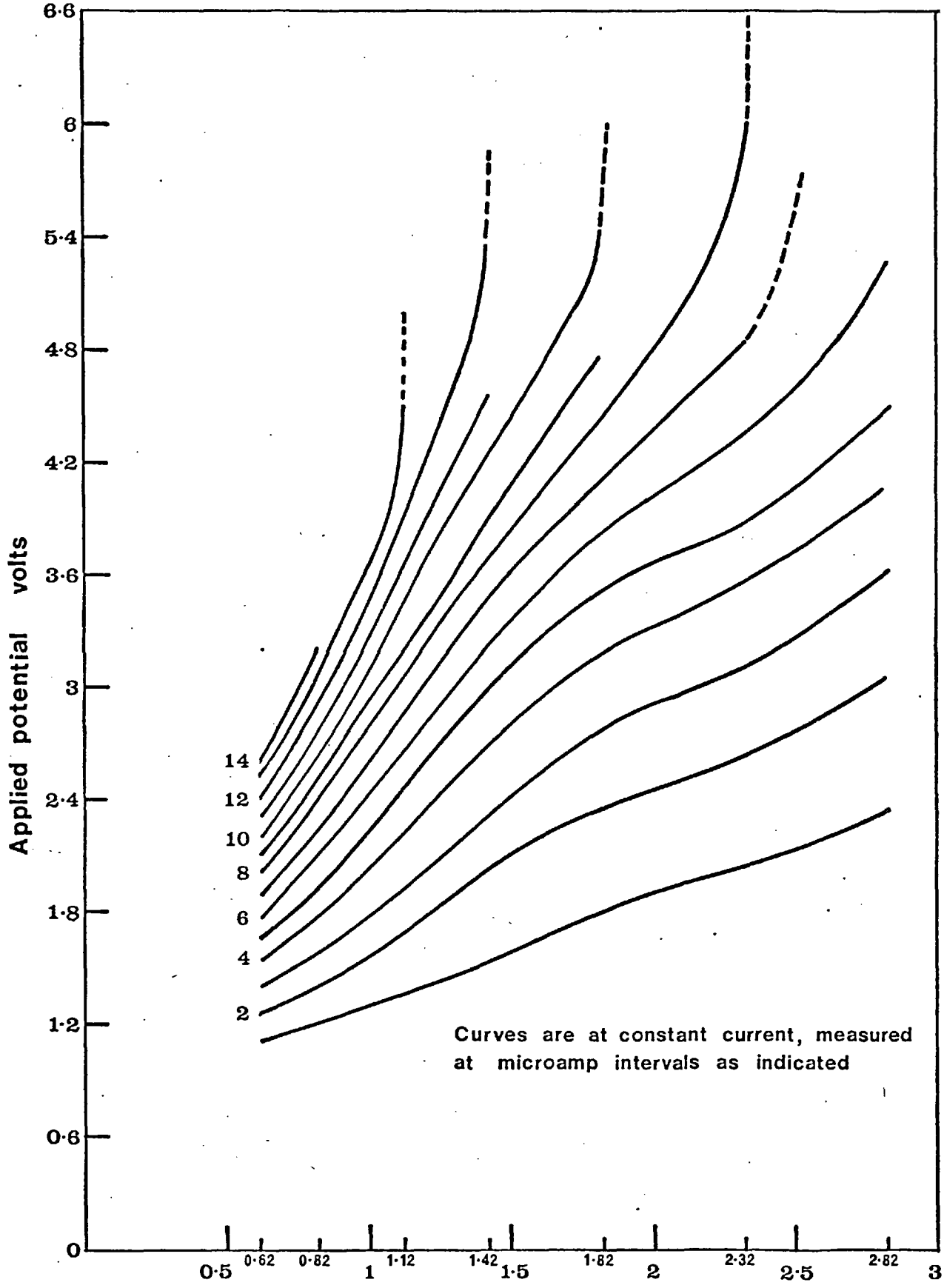

FIG. 6.2.

k_i and $(k_i)_e$ vs. $1/T$

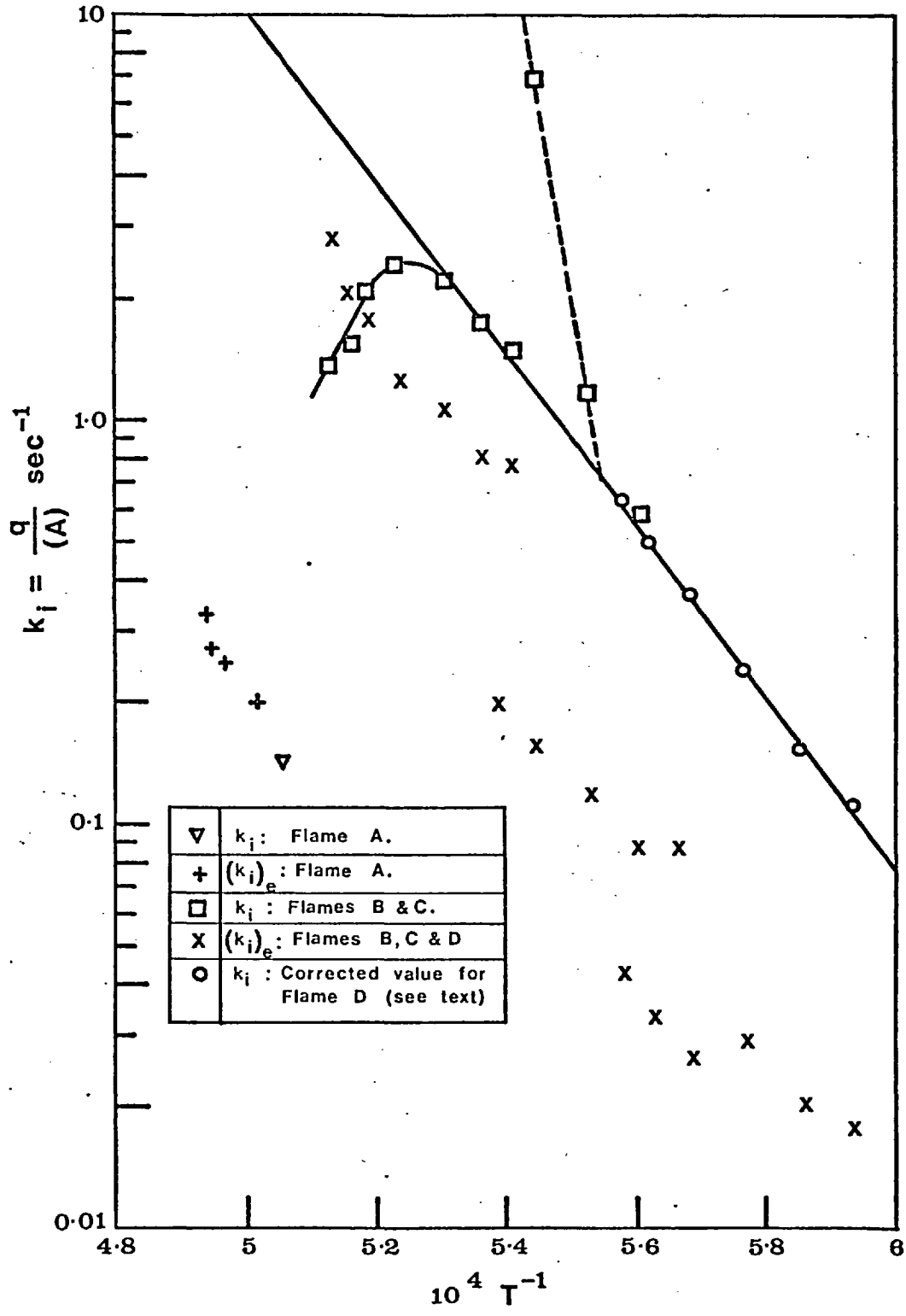

FIG 6·3

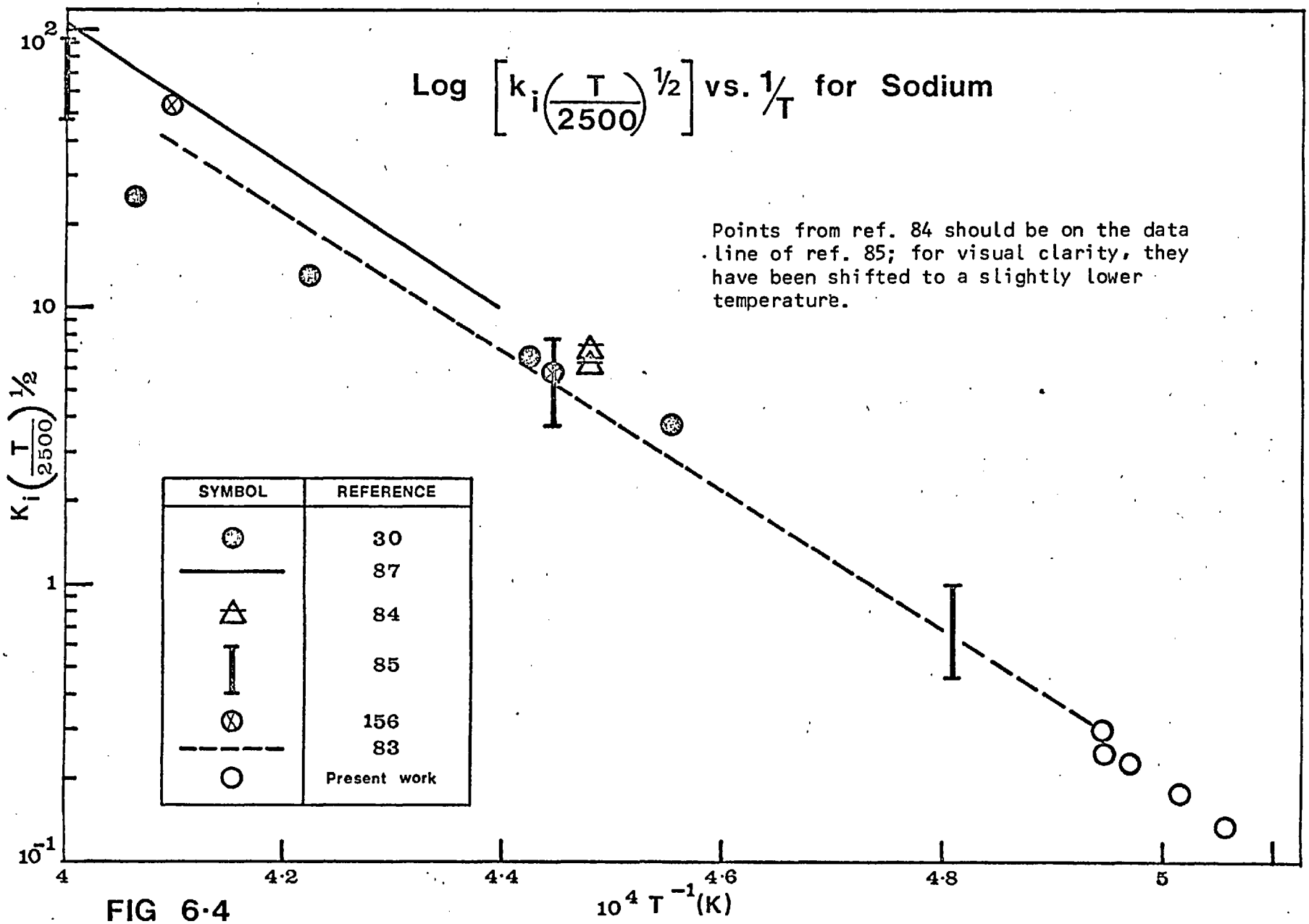
Log $\left[k_i\left(\frac{T}{2500}\right)^{1/2}\right]$ vs. $\frac{1}{T}$ for Sodium
Points from ref. 84 should be on the data line of ref. 85; for visual clarity, they have been shifted to a slightly lower temperature.
$K_i\left(\frac{T}{2500}\right)^{1/2}$
$10^4\ T^{-1}(K)$
SYMBOL
REFERENCE
30
87
84
85
156
83
Present work

FIG 6·4

Log $\left[k_i\left(\frac{T}{2500}\right)^{1/2}\right]$ vs. $1/T$ for Potassium

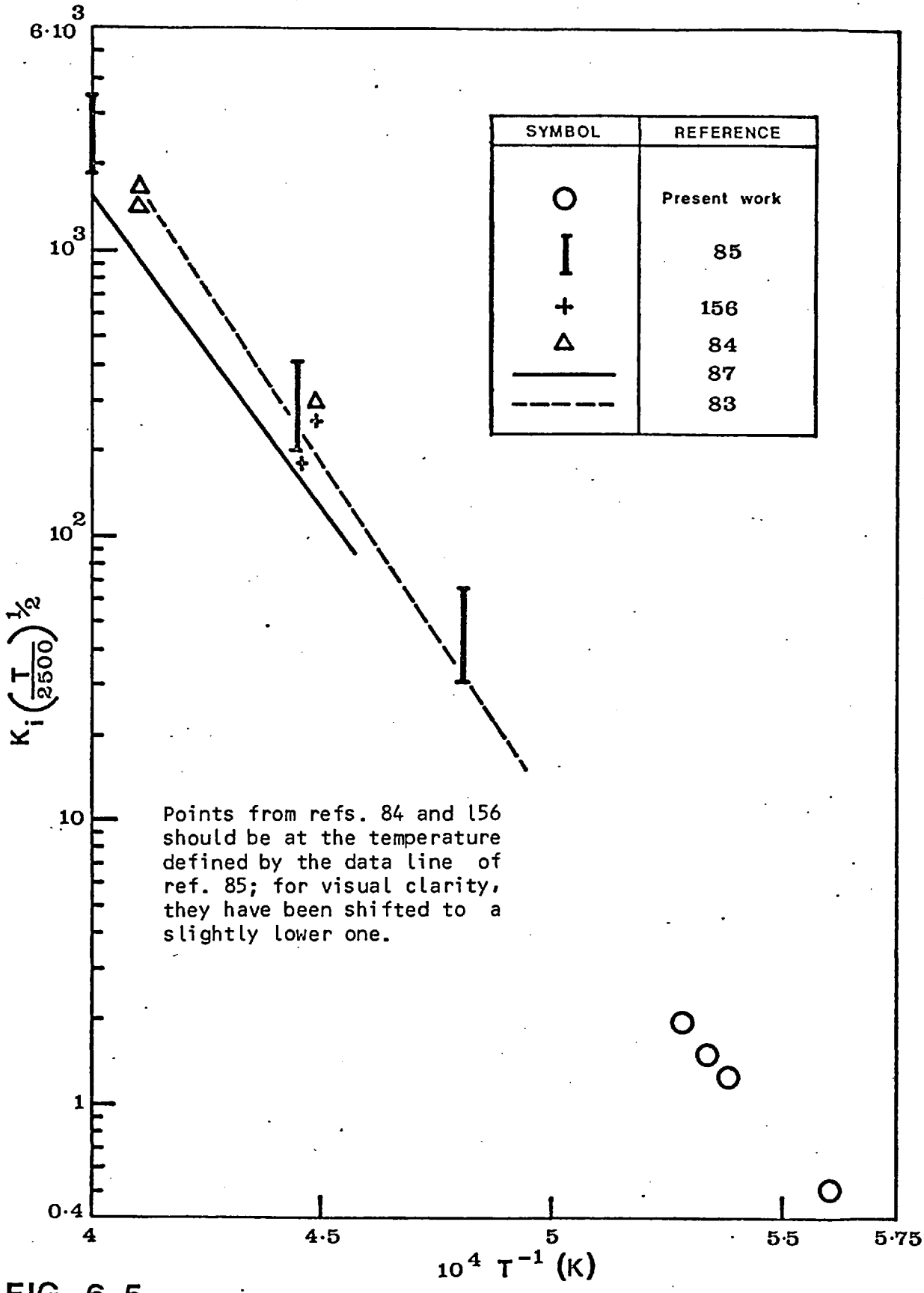

FIG. 6.5

RECOMBINATION COEFFICIENT FOR $Na^+ + e + M \rightarrow Na + M$

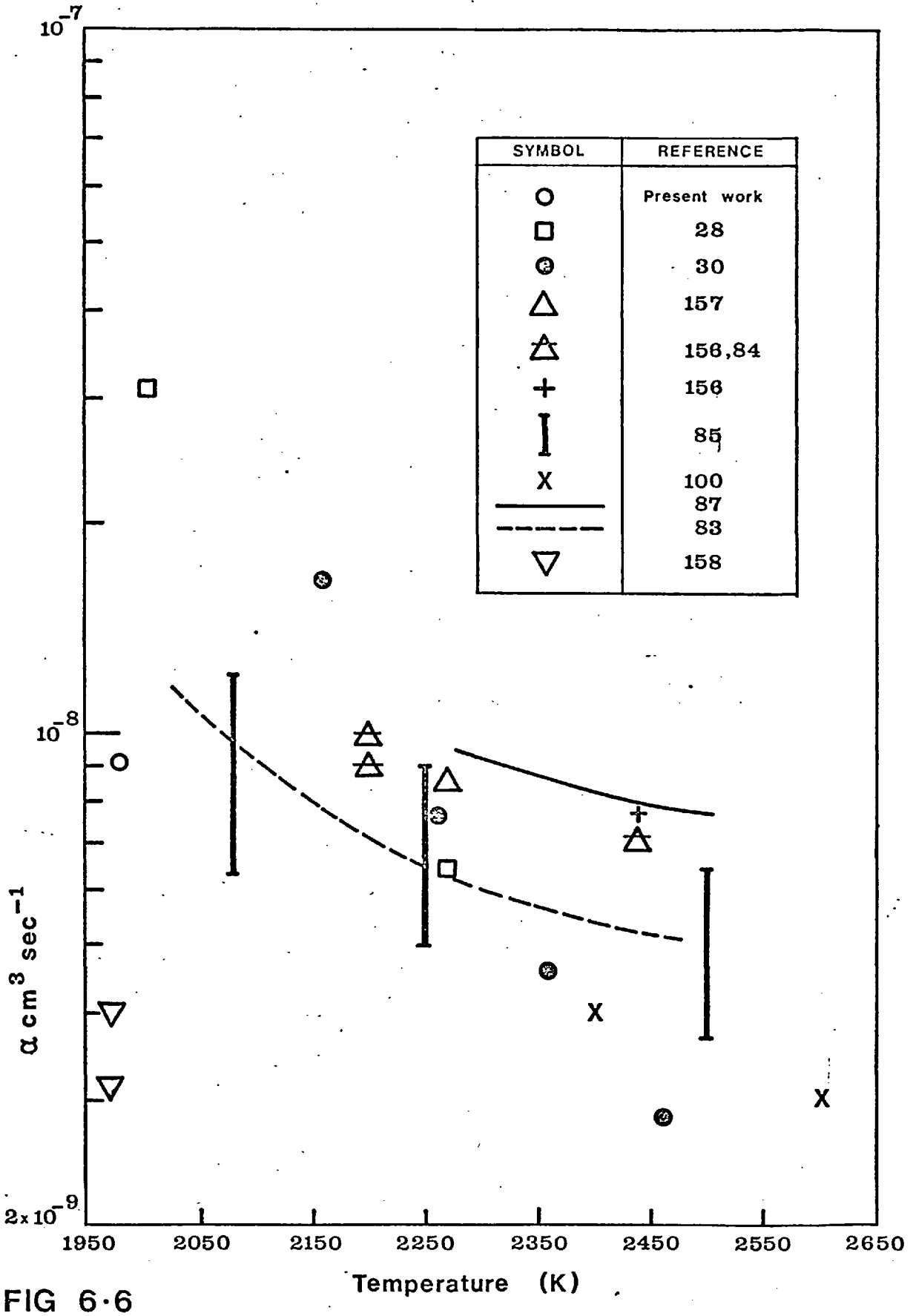

FIG 6·6

RECOMBINATION COEFFICIENT FOR $K^+ + e + M \longrightarrow K + M$

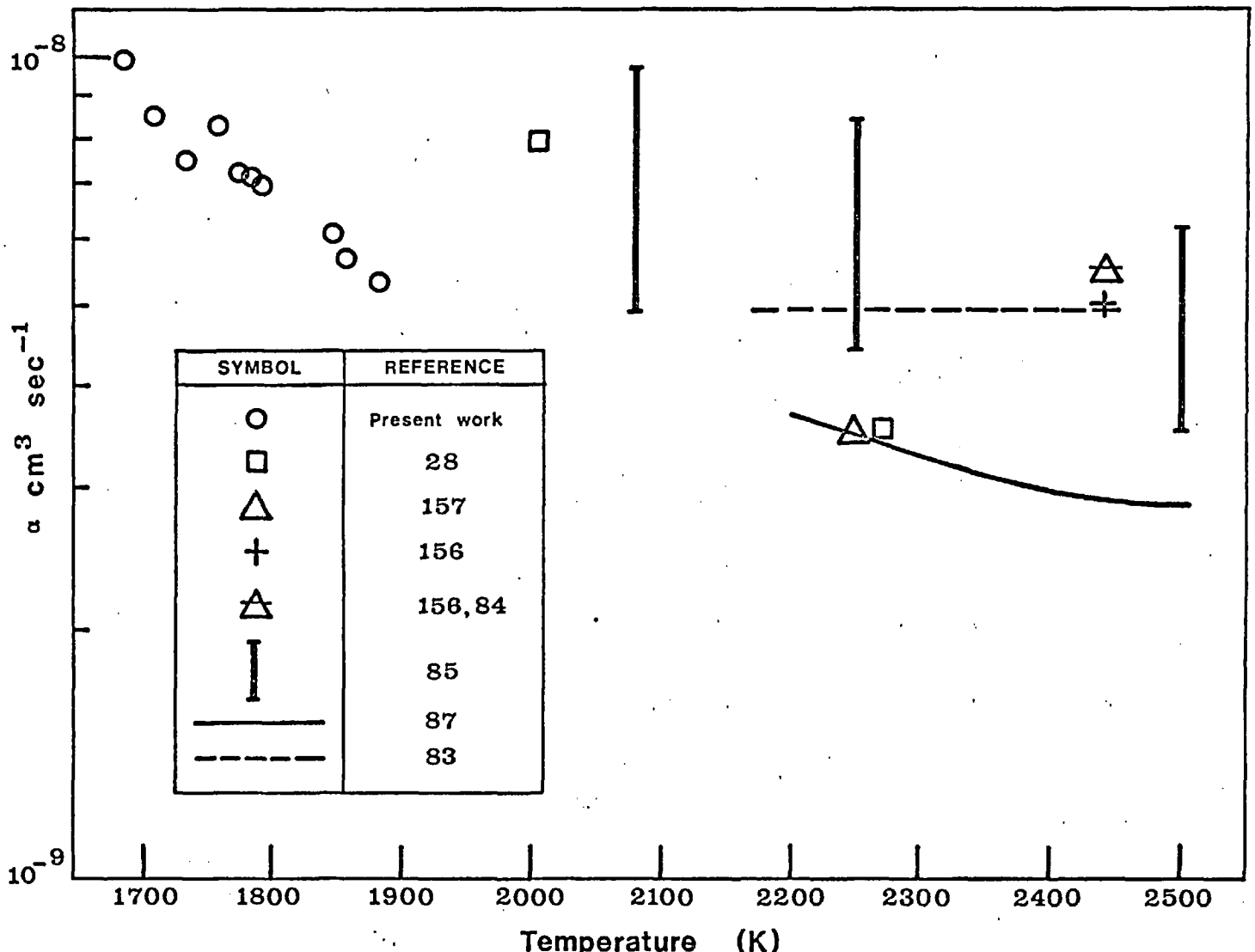

FIG 6·7

LOW PRESSURE 242 TORR UNSEEDED FLAME, DEMONSTRATING ELECTRON ATTACHEMENT.

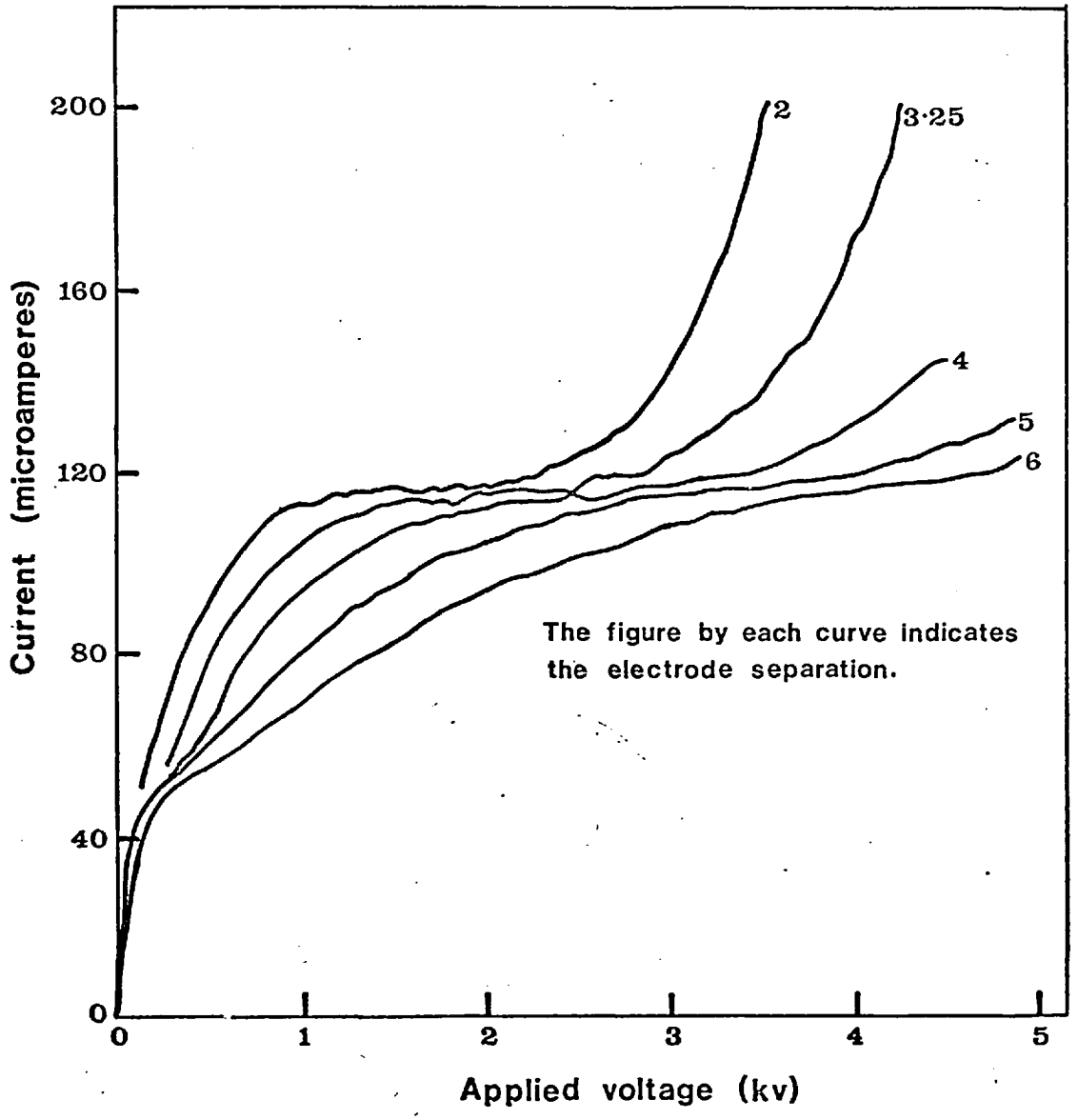

FIG. 6.8.

SATURATION CURRENT PLATEAUX FOR SEEDED 212 TORR FLAME

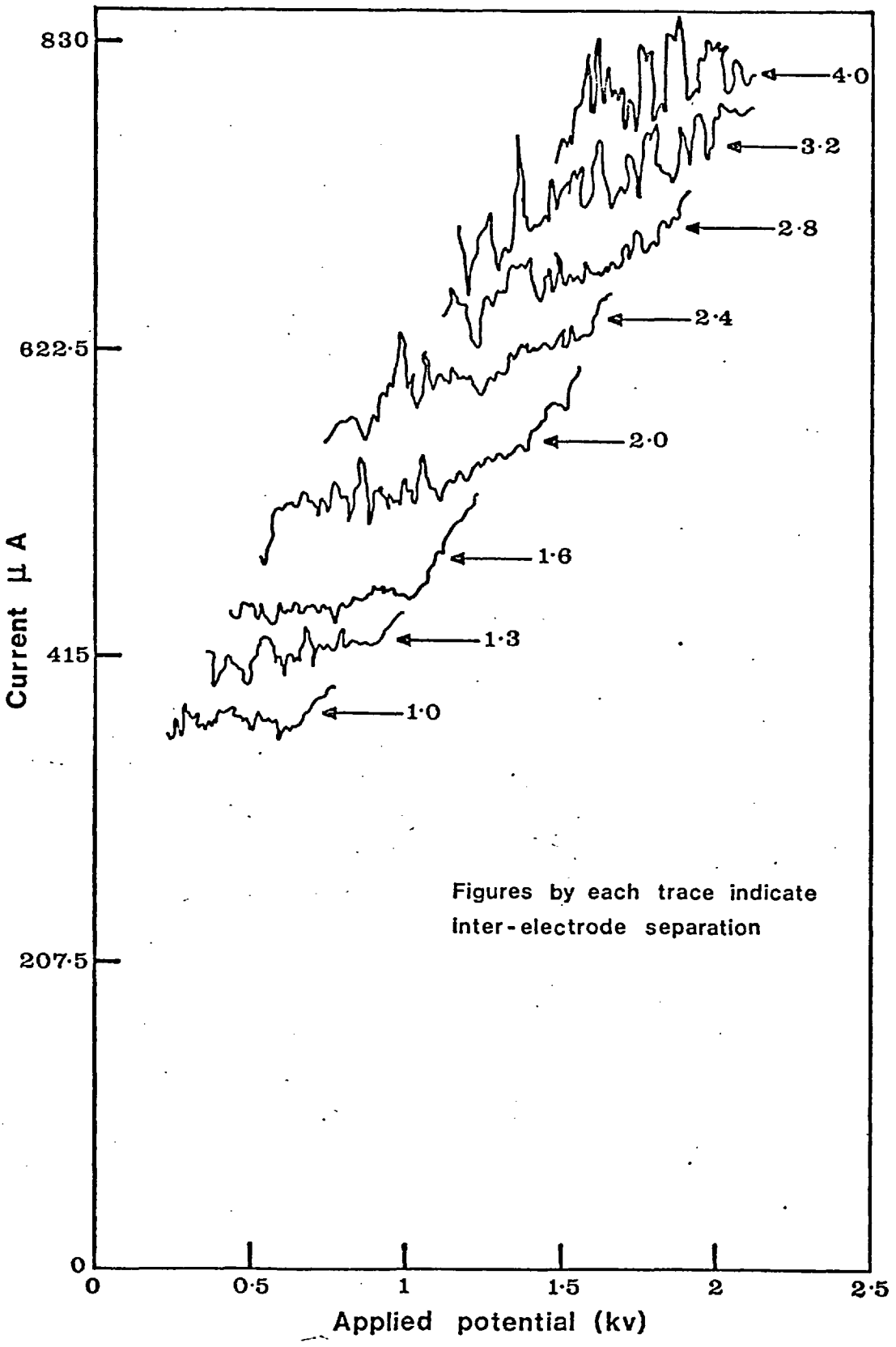

FIG. 6.9.

CHAPTER 7 OTHER RESULTS

7.1 The hydroxyl radical concentration

The five equations (5.34) to (5.38) give values for free alkali, alkali hydroxide, electron, and hydroxyl radicals with and without attached electrons on the hypothesis of a steady state. This clearly breaks down in the earlier parts of flames A and B where the ion density is above the steady state value; this could be due to charge transfer from H_3O^+ followed by relatively slow three body recombination, or the possible importance of the reaction

$$K + H_2O \rightleftarrows KOH + H \qquad (5.26)$$

in the early parts of the flame where the hydrogen atom concentration may be above equilibrium, or both. The two-body reaction, however, cannot dominate throughout, as already evidenced by the $(k_i)_e$ graphs in Fig. 6.3. The hydroxyl radical concentration, from equation (5.36), is therefore totally false in the early parts of flames A and B, apparently being negative in A and rising, with increasing time and distance from the reaction zone to a maximum in B rather than declining monotonically.

In flame C, the modulus of the apparent hydroxyl concentration is very high in the early stages, and may again be disregarded until the steady state is set up (as instanced by the equivalence of the measured ionization cross-section to that found in the latter stages of flame B).

In flame D, there is no steady state among the neutral species. What amounted to an empirical correction factor was introduced, as described, into the charged species relations. If this, and concentrations resulting from it, have the subscript "c" appended, viz.

$$\beta_c = (n_e)_c / n_+$$

and the apparent equivalent from the steady state equations the subscript "a", viz.

$$\beta_a = (n_e)_a / n_+$$

then, it is easily shown, since

$$n_e + n_{OH^-} = n_+$$

and

$$\frac{n_e \cdot n_{OH}}{n_{OH^-}} = K_{32}$$

that

$$(n_{OH})_c = \frac{(n_{OH})_a \cdot \beta_a(1 - \beta_c)}{(1 - \beta_a)\beta_c} \qquad (7.1)$$

Similarly, by using

$$\frac{n_{OH} \cdot n_K}{n_{KOH}} = K_{27}$$

and

$$[K]_T = n_K + n_{KOH}$$

it follows that

$$(n_{OH})_c = \frac{\beta_a}{\beta_c} \cdot (n_{OH})_a \cdot \frac{[K]_T - (n_K)_c}{[K]_T - (n_K)_a} \qquad (7.2)$$

The two are seen to be compatible only if

$$K_{31} = \frac{n_+^2}{[K]_T} ,$$

or, in other words, if there is no hydroxide formation, and therefore no electron attachment. In this case, of course, $\beta = 1$. This is mathematically trivial and, physically, both wrong and absurd.

Two possible conclusions may be drawn. First, although there may be a steady state electrically in flame D, there is definitely not one among the neutral species. In other words, equation (7.1)

may be true, but (7.2) is not due to the slow rate of neutral three-body recombination reactions as compared with the three-body electrical ones. The second possibility is that neither equation is adequate.

The correction factors do bring consistency to other electrical parameters (recombination coefficients and ionization cross-sections) thus giving indirect circumstantial evidence in favour of the former hypothesis, but against this is the fact that they lead to hydroxyl concentrations about 40 times the equilibrium value throughout flame D, i.e. partial pressures of 1.7% falling to 1%. These concentrations are perhaps excessive.

Equation (7.2) predicts hydroxyl radical concentrations of ca. 7 times the steady state values (themselves ranging from 4 times equilibrium to the equilibrium value furthest away from the reaction zone). As pointed out, however, (7.2) is unlikely to be an adequate description if (7.1) is not. Competition from, though not dominance of, the two-body potassium-water vapour reaction (5.26) is probably the likeliest explanation, with the real values for hydroxyl radical concentration lying between the two limits deduced above.

Table 7.1 lists the useful data one can extract from the steady state equations and compares them with the full thermodynamic equilibrium values. The subscript "s" refers to steady state values; "e", of course, to equilibrium. Values from equations (7.1) and (7.2) are listed for flame D at the highest and lowest temperature of measurement there to indicate the range within which the actual value may lie.

TABLE 7.1 THE HYDROXYL RADICAL CONCENTRATION

Flame	Temp. (K)	$10^{15}[OH]_s$ (cm^{-3})	$10^{15}[OH]_e$ (cm^{-3})	$\frac{[OH]_s}{[OH]_e}$
A	1977	2.5	2.7	0.90 ≃ 1
B	1883	6.8	2.8	2.4
	1863	6.2	2.6	2.4
	1848	5.0	2.4	2.1
C	1785	12.5	1.7	7.4
D	1793	10 - 70 (?)	1.8	6 - 40 (?)
	1686	7 - 40 (?)	1.0	7 - 40 (?)

7.2 Implications of a super-equilibrium hydroxyl radical concentration

The existence of a super-equilibrium concentration of OH, and other flame radicals, sheds light on a recent paper of Lawton [117].

Lawton, by measuring the negative species mobility in a flame of very similar composition (5.45% C_2H_4, 94.55% air) to those used here, and comparing that experimental value to a semi-theoretical one, came to the conclusion that, in order to account for the discrepancy between the two, electrons must have attached to a flame species, thereby lowering the average species mobility. Since he assumed that all neutral species were present in equilibrium concentrations, his only choice as a possible species capable of attaching electrons in the numbers necessary to explain

his results was water vapour. Certain comments may be made on his paper.

First, some of the values of the electron-molecule collision frequency, and, in particular, that for electron-water vapour collisions, have now been superseded since the publication of Frost's [172] 1962 paper (see Appendix B). This sheds doubt on the semi-theoretical electron mobility value used.

Second, the mobility evaluation method of Pack and Phelps [173] seems open to doubt for a flame such as this, where there are two terms, the electron-nitrogen and electron-water vapour molecule collision frequencies, which are similar in size; this makes convergence of the series slow if not impossible. In fact a numerical integration, using Lawton's data and equilibrium concentrations for a temperature of 1870 K, deduced by Lawton, leads to a value for electron mobility of 7600 $cm^2\ V^{-1}\ s^{-1}$, as compared with Lawton's value of 9000 from his series expansion. A numerical integration using the data of Appendix B, leads to a value of 5900 $cm^2\ V^{-1}\ s^{-1}$, compared with Lawton's measured value of 3600. Thus, even the very dubious assumption of 0.9 eV as the electron affinity of water vapour would not explain this, even though it appears to explain the figures in Lawton's paper.

Third, this value for the electron affinity of water value is eventually traceable to a paper of Platzman and Franck [174]. A discussion of it appears in Gray and Waddington [175], in which it is made clear that this refers to the trapping of an electron in a potential well created by the dipole moments of several water molecules in the liquid state. A straightforward extrapolation of this to electron affinity in the gas phase does not seem justified, especially as a mass spectrometric analysis of

negative ions in flame gases (Knewstubb and Sugden [176]) showed conclusively that negative water vapour ions were down in concentration by at least three orders of magnitude compared with negative hydroxyl ions. These remarks also apply to the assumption of H_2O^- by Jensen and Padley [84].

Fourth, the temperature used is open to question. Lawton's experimental set-up is similar to that used here, with, in his case, a massive water cooled electrode, rather than just a comparatively flimsy wire gauze. Since even the latter is observed to have cooled the burnt gases beyond the reaction zone, it may safely be supposed that this was even more the case in Lawton's work, where no direct temperature measurement was made, other than a measurement of the saturation current, for which, in effect, a temperature calibration in terms of reaction zone temperature had already been carried out on a similar apparatus. The temperature used in Lawton's paper, then, is almost certainly not as well defined as he claims, giving rise to a further source of error when the Saha-Boltzmann equation is applied.

Last, and what is challenged by the interpretation of the present results, is the stated assumption that the hydroxyl radical is present in equilibrium concentrations. As here, however, there is probably sufficient time for the reaction

$$e + X + M \rightleftarrows X^- + M$$

to become balanced.

Using a recalculated semi-theoretical electron mobility of 5900 $cm^2\ V^{-1}\ s^{-1}$ (data from Appendix B) and Lawton's measured value of 3600 $cm^2\ V^{-1}\ s^{-1}$, the ratio $\frac{n_e}{n_-} = \eta$ (Lawton's β) is given by

$$\frac{3600}{5900} = \frac{\eta}{1 + \eta}$$

or $\eta \simeq 1.6$

Since $K_{32} = \frac{[e]\,[OH]}{|OH^-|} = \eta[OH]$,

(the effect of other species, even O_2^-, being dwarfed by OH^-), then at 1870 K, $[OH] = \frac{2.54 \cdot 10^{16}}{1.6}$

or, $[OH] \simeq 1.6 \cdot 10^{16}$

Lawton's calculated equilibrium OH concentration is

$$[OH]_e = 1.9 \cdot 10^{15}$$

so $$\frac{[OH]}{[OH]_e} \simeq 8.5$$

Referring to Table 7.1, the same ratio, measured ca. 25-35 msec after the reaction zone, is over 2 for flame B (final flame temperature 1957 K), ca. 7 for flame C (final flame temperature 1890 K), and probably higher for D (final flame temperature 1818 K). An extrapolation, therefore, from B and C gives the right sort of figure to fit in with Lawton's measurements. Due to the errors involved both here and in Lawton's work, tne good agreement between the extrapolation from this work and Lawton's experimental findings is perhaps somewhat fortuitous. Nevertheless, one may conclude that there is now sufficient quantitative evidence to explain Lawton's results solely by reference to OH concentrations, without the need to invoke a mythical ground state negative water vapour ion.

7.3 The field in the plasma

Lawton [89] and Lawton and Weinberg [90] assumed a simple model to derive values for the voltage and field distributions in a non-seeded hydrocarbon flame whose only ionization came through the reaction

$$CH + O \rightarrow CHO^+ + e$$

Inter alia, electrons were assumed to have infinite mobility, so that even the smallest applied field would reduce the electron density to zero. For their purposes this model was successful, but Chapter 5 of the present work indicates that such assumptions have little relevance here, and would lead to glaring inconsistencies.

Instead, a finite value was assumed here for electron mobility, and a value of the field within the plasma, E, was derived:

$$E \simeq \frac{j}{e\, n_+ \beta \mu_e} + \frac{\gamma k T}{e} \qquad (5.17)$$

E is thus the sum of two terms: one proportional to temperature and the other rising roughly exponentially with distance if j is held constant. Obviously, this is far too general to be shown in graphical form, but in Table 7.2, selected values of E are shown in the final column. Currents are chosen that are typical of each flame in the region of the current-voltage characteristic where ion densities are measured; the relative magnitudes of the two terms are shown in columns 7 and 8. Other details are explained by the footnotes.

7.4 The fractional electron energy loss

Cottrell and Walker [177] published a graph of fractional electron energy losses, f, for collisions of electrons with selected common gases for energies up to 1 eV. The values at 0.15 eV, typical for the present work, are, for CO_2 ca. $4 \cdot 10^{-2}$, for O_2 $5 \cdot 10^{-3}$ and for N_2 ca. $5 \cdot 10^{-4}$ (the latter extrapolated from the 1.0-0.4 eV range).

From Chapter 6, Thomson's [32] theory predicts that at 2000 K, $\alpha_1 = 2.1 \cdot 10^{-7} f$ and at 1700 K, $\alpha_1 = 3.2 \cdot 10^{-7} f$, Natanson's [36]

TABLE 7.2 THE FIELD IN THE PLASMA (at selected currents)

Flame	T (K)	j ($\mu A cm^{-2}$)	β	$10^{-10} n_+$ (cm^{-3})	μ_e^c ($cm^2 V^{-1} s^{-1}$)	$\frac{10^2 \cdot j}{e \beta n_+ \mu_e}$ ($V\ cm^{-1}$)	$10^2 \cdot \frac{\gamma kT}{e}$ (Vcm^{-1})	E (Vcm^{-1})
A	2023	5	.95[a]	9.2	6400	5.6	4.0	0.096
	2021	"	"	8.0		6.4	4.0	0.104
	2012	"	"	6.6		7.8	4.0	0.118
	1994	"	"	5.2		9.9	3.9	0.138
	1977	"	"	4.1		12.5	3.9	0.164
B	1947	5	.80[a]	30.8	6500	2.0	7.7	0.097
	1938	"	"	23.3		2.6	7.7	0.103
	1927	"	"	16.9		3.6	7.6	0.112
	1909	"	"	11.9		5.1	7.6	0.127
	1883	"	"	8.9		6.8	7.5	0.143
	1863	"	"	7.3		8.2	7.4	0.156
	1848	"	"	6.5		9.2	7.3	0.165
C	1855	2	.52[a]	7.1	6200	5.5	7.4	0.129
	1836	"	"	6.4		6.1	7.3	0.134
	1808	"	"	5.8		6.7	7.2	0.139
	1785	"	"	4.9		7.9	7.1	0.150
	1765	"	"	3.7		10.4	7.0	0.174
D	1793	2	.14[b]	9.4	6100	15.6	7.1	0.227
	1778	"	"	8.7		16.8	7.1	0.239
	1758	"	"	7.7		19.0	7.0	0.260
	1734	"	"	6.4		22.9	6.9	0.298
	1707	"	"	5.3		27.6	6.8	0.344
	1686	"	"	4.4		33.3	6.7	0.400

a From the five equations describing the steady state.
b "Corrected" value; as stated in the previous section, there is still doubt as to whether this may be adequate.
c From Appendix B.

theoretical predictions being ca. 30% higher. The actual values from this work are ca. $9 \cdot 10^{-9}$ at 2000 K for sodium and ca. $1 \cdot 10^{-8}$ at 1700 K for potassium.

The implications of this are that, on the Thomson theory, the fractional energy loss for an electron in collision with a water vapour molecule is ca. 0.35-0.40, and, on the basis of Natanson's theory, ca. 0.25-0.30. This may seem large, but it does not seem inconceivable in the light of the water vapour molecule's huge dipole moment and large cross-section (see Appendix B) for collisions with electrons. Comparable figures are shown by Cottrell and Walker for CH_4 (ca. 0.3) and C_2H_4 and N_2O (both ca. 0.1).

Although there is doubt about the numerical factor in these relatively elementary recombination theories, they are probably not seriously in error, so the above estimates for water vapour are probably reasonably reliable.

CHAPTER 8 CONCLUSION

The work presented in this thesis contains a development and extension of the range of analytical techniques which can be applied to flames and hot gases in general.

Except for Melinek's [93] work, drawing a saturation current from a flame has been used solely in the attempt to measure the activation energy of the process that causes 'natural' ionization within the reaction zone of a hydrocarbon flame. Melinek measured the dependence upon the height of the measuring anode above the burner cathode of the saturation current in a smoking hydrocarbon flame. His results were found to be consistent with the ionization of solid carbon particles, whose work function was assumed to be very similar to that of graphite (4.4 eV). The present work, for the first time, avoids any possibility of agglomerates in the products by applying this technique to a fuel-lean hydrocarbon flame seeded with two alkali metals: sodium and potassium. After allowing for what was almost certainly positive ion emission from the anode, which was either not present or overlooked in Melinek's case, the measured ionization coefficient versus temperature graphs were found to have slopes consistent with the ionization of whichever was the predominant alkali atomic species in the two flames least affected by an over-production of hydroxyl radicals.

The ionization cross-sections found were some three orders of magnitude higher than the corresponding gas kinetic cross-sections. This is explained, at the moment semi-quantitatively, in the papers of Preist [165] and Fowler and Preist [164], although it seems likely that their analysis is, as yet, insufficient to account for the effects both of atomic species and those molecules

with a permanent dipole moment, especially those where Dea_o is comparable with, or greater than, 0.5. It seems, however, that for quadrupolar molecules, their explanation is probably valid. The number of the excited states from which ionization of the atom may take place, as well as the question of the existence of thermodynamic equilibrium in the higher excited states, is not yet fully understood, and it seems that further advance here is dependent on both a development of theory and the provision of more experimental results. If more work is to be carried out on this, special attention must be paid to the relationship between ionization cross-sections and both the density of free electrons present during measurement and the composition of the hot flame products. For the exact results required, it will not be enough to assume an equilibrium composition, since the effect of species such as the hydroxyl radical, which as a polar molecule may play an important part, may be either neglected or underestimated.

By varying the volumetric throughput while keeping the equivalence ratio of the flames constant, a value was found for the activation energy of the reaction zone ionization process, which is likely (Fontijn, Miller and Hogan [15], Bulewicz and Padley [16]) to be

$$CH(X^2\Pi) + O \rightarrow CHO^+ + e$$

The value found was 50–100% higher than those quoted for similar flames (though without the few per cent additional nitrogen used here) by Lawton and Weinberg [90], Lawton [89] and Melinek [93]. There are however differences even between the results of Lawton and Melinek, both of which were carried out on a Botha-Spalding porous disc burner. Two reasons may be advanced for these discrepancies, which are further added to if the results of some

Soviet researchers, referred to in Chapter 4, are also taken into account.

The first, coming from the work of Fox and Kihara [118], is the fact that porous discs do not give anywhere near such a homogeneous reaction zone as has been assumed until the publication of their recent paper, leading to the consequence that it is extremely difficult to compare results obtained by different people, even when they use nominally the same burner system (see Chapter 4).

The other major reason is that the ionization coefficient is dependent, as recently shown by Preist [165], on the free electron density present. Different systems may again be different in this respect. It should further be noted that, this being the case, the ionization coefficient itself and therefore any measured activation energy, is likely to be altered by the tool of measurement, i.e. the application of an electric field which removes charged species.

The present results represent, in all probability, something of an extreme in regard to this question of activation energies. In order to be able to seed the flame, a Meker burner had to be used, which gives a flame reaction zone consisting of a network of small cones. It cannot be claimed, therefore, that the zone is even as homogeneous as those produced on Botha-Spalding burners, which, as is argued above, do not themselves produce a totally homogeneous reaction zone. Whereas for the latter type it is possible, though as now seems likely rather dubious, to define a flame area for all but a flame about to "blow-off", it is quite impossible to define such for a Meker burner. This is why the current work defines activation in terms of ion yield per

molecule of fuel consumed, whereas others define it on the basis (still probably dubious) of saturation current density.

The conclusion to be drawn is that for the process of ionization in a reaction zone, activation energies should be defined only for specific systems. If this is adhered to then the various results obtained are probably equally valid, other factors being equal, though the concept of activation energy for this process loses its universal validity.

A mathematical approximation, based on physical principles, was found to describe the dependence of saturation current of a seeded flame on electrode height. When this is extrapolated back to the assumed reaction zone position, there is no clear evidence for unusually high ionization of alkali metals in the reaction zone. Since there is, as explained, doubt about where one should define the reaction zone, this should be taken as a null result.

A new method has been developed to measure positive ion density. The method gives an average across a cross-section prependicular to the gas flow, rather than an average at a point or across a diameter (spherical and cylindrical probes respectively) or within a volume usually defined by two parallel planes at right angles to the flow (microwave cavity methods).

Similar methods to the one used here have been attempted before, as described elsewhere in the text. They have however depended on the slope, found to a first approximation to be constant over the range considered (somewhat arbitrarily), of the current-voltage characteristic at constant electrode height, or of the applied voltage-height characteristic at constant current. Both of these approaches are shown to have led in the present work to absurd conclusions. Without further information,

the current-voltage characteristic tells nothing about conditions in the body of the flame, since a substantial part of any voltage drop takes place in the electrode sheath regions. It is easy to fall into the similar trap, with the voltage-distance characteristic, of assuming this describes the dependence in the main body of the hot gases, outside the sheath regions. On this assumption, one obtains a spurious electron density, from one to two orders of magnitude less than the true undisturbed positive ion density.

The basis of the method developed here is to locate by intersecting tangents the position in the current-voltage characteristic of a fairly well defined "elbow". It is postulated that, here, electrons and negative ions are just repelled from the electrostatic sheath that guards the cathode. By considering the velocity (predominantly convectional) at which positive ions leave the main body and enter the sheath, a determination is made of the positive ion concentration, since here there is no contribution to the current from negative species. The effects of diffusion, convection and electrically induced velocities are all considered in the analysis presented.

The results obtained compared well with ion or electron densities found by the other methods discussed. When combined with charge production rates derived from the saturation current versus height graphs, equally good results are obtained for the electron-positive ion recombination coefficient, as compared with the results found by other techniques. Further, an order of magnitude estimate was made for ionic recombination coefficient between potassium and hydroxyl ions. This again is in quite good agreement with another estimate by Hayhurst and Sugden [28]

of the same parameter, with a negative halogen ion in their case replacing the hydroxyl ion here.

It is not claimed that a rigorous theoretical treatment is given for obtaining the undisturbed ion density in the hot gases. Such a treatment would involve the analysis of the voltage and field distribution in the sheath regions. Even then there would still be no guarantee that one could locate more exactly that current at which negative charges are repelled from the cathode.

Despite the lack of such a rigorous theoretical base, the conclusion to be drawn from the results obtained is that the method developed is a valid one. Further analysis may possibly show that there are systematic errors, but they are no more likely to occur here than in other well-established, standard techniques.

Comparison of the measured positive ion density with those values expected from equilibrium considerations show that there are fewer free alkali atoms than in the equilibrium case. This is explained on the assumption that, in these lean hydrocarbon-air flames, the predominant mechanism for the production of alkali hydroxides is

$$A + OH + M \rightleftarrows AOH + M \qquad (5.27)$$

rather than the two body reaction favoured in fuel-rich hydrogen flames, viz.

$$A + H_2O \rightleftarrows AOH + H \qquad (5.26)$$

The latter reaction may however begin to compete in importance when flame radicals are present in numbers substantially greater than their equilibrium concentrations.

This is shown to give a partial explanation of the results observed, the three body reaction being feasible on the grounds

of standard kinetic considerations.

There is no evidence in the present work to support the reaction

$$A + O_2 + M \rightleftarrows AO_2 + M.$$

Due to the depletion of free atomic alkali by (5.27), a bar was encountered in trying to extend the temperature range of the experiments downwards. This was less noticeable at reduced pressure because of the relatively lesser effect of three body reactions. One could attempt to overcome this difficulty by burning a richer flame, but then complications arising from the competition between (5.26) and (5.27) would arise, and in order to get out of this somewhat awkward regime, flames so rich as to produce soot might have to be burnt.

It is therefore suggested that future work on this topic which attempts to extend the range downward might try, for example, a hydrazine decomposition flame or even a fuel-rich ammonia-air or -oxygen flame. In addition, to establish finally whether alkali superoxides are formed, and, if so, what are their equilibrium constants, something like a carbon monoxide-air or -oxygen flame would be necessary; alternatively an ozone decomposition flame might be used.

In all these, strict safety precautions would have to be observed. The problem in using the techniques developed in the present work would be that in the reaction zone there is little ionization, which plays a crucial role in raising the ion density of seeding material to equilibrium level, or possibly above, by a charge transfer mechanism. Trace amounts of a hydrocarbon might have to be added to ensure the attainment of Saha equilibrium. Other three body reactions may still however not be

balanced in the case of a hydrazine decomposition flame, since its burning velocity is much higher than that of the fuel, ethylene, used here, so measurements would have to be taken much nearer in time to the reaction zone.

It is suggested that future work along similar lines to the present also use techniques for measuring stable and radical species concentrations, otherwise conclusions drawn will be inferred from indirect circumstantial evidence rather than being based on direct observations.

The results found do have implications for another paper published recently, discussed more fully elsewhere in the thesis. In summary, Lawton's [117] results, coming from a flame of similar composition to those used here, are explicable on the basis of a super-equilibrium concentration of hydroxyl radicals, for which the electron affinity is high (1.78 eV). The hypothesis of negative water vapour ions has no validity.

Calculations (Appendix A) of the positive ion diffusion and mobility coefficients to be expected agree well with the recently experimentally determined one for H_3O^+ of Bradley and Ibrahim [27], whose value is however only about a quarter of that measured by Lawton [117]; a fairly large error here would not affect the results greatly, but it would become noticeable if the order of magnitude were that suggested by Kelly and Padley [61].

Last, two minor results come out of the thesis. The first is that if Thomson's [32], or Natanson's [36], expression is used for the recombination coefficient, even though it is not very well grounded theoretically,, a reasonable result is obtained for the fractional electron energy loss on collision with a water vapour molecule. The value of the recombination coefficient for

electrons with alkali ions is found to lie between the lower, semi-quantal limit and the upper, classical limit (assuming a continuum of energy states) as predicted by Bates, Malaviya and Young [42]. The sodium ion value is, in fact, just on the upper limit.

The second relates to the literature survey carried out on electron mobility (and summarised in Appendix B) over an energy range 0 to 1 eV for various gases, and the analytical expressions derived. For some of these, there is no point in making any change from Frost's [172] recommendation; his suggested expressions for water vapour and carbon dioxide do need some revision however. New expressions are suggested based on a least sqaures fit to the new data of the last decade. Based on these recommendations, values are obtained for the field distribution in the hot gas region and for the electron-neutral collision frequency (see Appendix B). This latter is in good agreement with the few experimentally observed values.

Certainly not everything put forward in Chapters 5, 6 and 7 has been established on a fully rigorous and satisfactory basis, but this is, more often than is usually admitted, the case with scientific work. However, the degree to which self consistency is achieved on the basis of the hypothesis advanced would seem to establish the present technique as a valid one, perhaps more so, than some others that have been used.

APPENDIX A THE POSITIVE ION MOBILITY

The question of finding a value for the mobility and diffusion coefficients of the alkali metal ions is a relatively straightforward one. We begin by quoting the Clausius-Mossotti-Lorentz-Lorenz law (C-M-L-L) for molar polarizability, Π , (C-M)[178,179] or molar refraction, R, (L-L)[180,181], in units of m^3

$$\Pi = R = \frac{N_{AV}\alpha^*}{3\varepsilon_o} = \frac{M}{\rho}\frac{\kappa^* - 1}{\kappa^* + 2} = \frac{M}{\rho}\frac{n^{*2} - 1}{n^{*2} + 2} \qquad (A.1)$$

where N_{AV} is Avogadro's number, ε_o the permittivity of free space, κ^* the complex permittivity (dielectric constant), n^* the complex refractive index, α^* the molecular polarizability, and M/ρ the volume occupied by a kilogram-molecular weight of the molecule considered. For the case of a non-polar gas at not too high a pressure, such that $n^*-1 \ll 1$, the C-M-L-L equation is seen to reduce to the simple, empirically observed Gladstone and Dale's [182] law,

$$\frac{n - 1}{\rho} = \text{const.} \qquad (A.2)$$

For polar gases, this simplified form does not hold since the molar polarizability is then of the form

$$\Pi = A + \frac{B}{T} \qquad (A.3)$$

where $A = \frac{N_{AV}(\alpha_e + \alpha_a)}{3\varepsilon_o}$, the subscripts e and a referring to components of the molecular polarizability arising from the electronic cloud and atomic spacing respectively, and

$B = \frac{N_{AV}}{3\varepsilon_o} \cdot \frac{|d|^2}{3k}$ where d is the permanent dipole moment and k Boltzmann's constant.

For water vapour, the only possessor of a permanent dipole moment present in appreciable quantities in the flame gases studied, OH and CO being ignored, a value for the refractive index of

$n = 1.000261$ is quoted in the "Handbook of Chemistry and Physics" [183] at S.T.P.

At the frequencies typical of white light, we may assume that the dipole of the molecule is unable to respond; this refractive index is then the equivalent of an "optical" polarizability, concerning only α_e and α_a. Hence

$$\frac{n^{*2} - 1}{3\varepsilon} \frac{M}{\rho} = \frac{N_{AV}(\alpha_e + \alpha_a)}{3\varepsilon_o} = A,$$

which is the equivalent of putting $T = \infty$ in A.3.

This leads to

$$A = \Pi_{opt.} = 3.90 \cdot 10^{-6} \qquad (A.4)$$

which corresponds to the intercept on the graph of von Hippel [184] for Π at $T = \infty$, thereby confirming our reasoning. B is easily calculable, since the dipole moment of water vapour is well known to be 1.85 Debye.

The full expression for the molar polarizability of water vapour is then

$$\Pi = \frac{\kappa^*_{H_2O} - 1}{\kappa^*_{H_2O} + 2} \frac{M}{\rho} = 3.90 \cdot 10^{-6} + \frac{2.122 \cdot 10^{-2}}{T}, \qquad (A.5)$$

or, since $\kappa^*_{H_2O} - 1 \ll 1$,

$$\frac{(\kappa^*_{H_2O} - 1)M}{3\rho} = 3.90 \cdot 10^{-6} + \frac{2.122 \cdot 10^{-2}}{T} \qquad (A.6)$$

For the non-polar gases involved, again taking values from the "Handbook of Chemistry and Physics", we obtain for Gladstone and Dale's law

$$\frac{n - 1}{\rho} = 0.227$$

Now, turning to Loeb [35(e)] we may express ionic mobility in terms of κ. The theory, due to Langevin [185] recomputed by Hasse [186] using the later considerations of Chapman and Enskog, assumes solid elastic impacts in consequence of repulsive forces and also inverse fifth-power attraction due to interactions with real or induced dipoles, the force law for this being

$$f = \frac{(\kappa - 1)e^2}{2\pi N r^5}$$

From this the ionic mobility is determined to be

$$\mu_+ = 0.462 \frac{3}{16Y} \frac{\rho_o}{\rho} \left[\frac{M + m}{mM_o(\kappa_o - 1)}\right]^{\frac{1}{2}} \text{cm}^2\ \text{V}^{-1}\ \text{s}^{-1} \qquad \text{(A.7a)}$$

$$= \frac{3}{16Y} \left[\frac{M + m}{m\rho(\kappa - 1)}\right]^{\frac{1}{2}} \text{cm}^2\ \text{statV}^{-1}\ \text{s}^{-1} \qquad \text{(A.7b)}$$

where here M_o is the molecular weight of an average gas molecule, M its mass and m the mass of the ion; ρ_o and κ_o are the density and dielectric constant at NTP (un-subscripted they refer to values at temperature T). 3/16Y is Langevin's quantity, plotted in Loeb (op. cit.), p.64, as a function of $1/\lambda$ where λ is a variable which allows for the effects of integration over all classes of orbits involved in the solid elastic impacts:

$$\frac{1}{\lambda} = \frac{\left[8\pi p_o \sigma^4\right]^{\frac{1}{2}}}{(\kappa_o - 1)e^2} \quad \text{(e.s.u. units used)} \qquad \text{(A.8)}$$

where σ is the effective distance between molecular centres for a collision between an ion and flame gas molecule. From Goldschmidt [187] it may be seen that suitable values for σ are 2.9 Å for K^+ and 2.55 Å for Na^+, both in collisions with nitrogen; the oxygen and carbon dioxide figures are not very different so it may be assumed that the water vapour figure is again similar, so calculations may

be made on this basis.

From what has gone before,

$$(\kappa_0 - 1) = (n_o^2 - 1)$$

and κ and n may be weighted according to the partial pressure of the species present. The value, at NTP, is

$$n_o^2 - 1 = 2.34 \cdot 10^{-3}$$

This leads to, at 1860 K, i.e. in the middle of our temperature range,

$$\bar{n} - 1 = 6.6 \cdot 10^{-5}$$

or $$\bar{\kappa} - 1 = 1.32 \cdot 10^{-4}$$

Values for $1/\lambda$ of 0.185 for K^+ and 0.14 for Na^+ result, so 3/16Y becomes 0.565 for K^+ and 0.55 for Na^+ - see either Fig. 1.27 or Table 1.4 of Loeb (op. cit.).

On substitution into (A.7) using a temperature of 1860 K, it is seen that

$$\mu_{Na^+} = 17.4 \text{ cm}^2 \text{ V}^{-1} \text{ s}^{-1}$$

and $$\mu_{K^+} = 15.3 \text{ cm}^2 \text{ V}^{-1} \text{ s}^{-1}$$

Since Einstein's ratio, recently shown by Sandler and Mason [188] to be exact in kinetic theory approximations higher than the first, at low field values, is

$$\frac{\mu_+}{D} = \frac{e}{kT},$$

then, again at 1860 K,

$$D_{K^+} = 2.45 \text{ cm}^2 \text{ s}^{-1}$$

and $$D_{Na^+} = 2.79 \text{ cm}^2 \text{ s}^{-1}$$

Dalgarno, McDowell and Williams [189] have put forward an alternative expression, derived like the above from the Langevin-

Hasse model and corresponding force laws. This is

$$\mu_+ = 35.9 \left(\frac{M + m}{mM\alpha^*}\right)^{\frac{1}{2}} \text{ cm}^2 \text{ V}^{-1} \text{ s}^{-1} \qquad \text{(A.9)}$$

As in the alternative expression, this, strictly speaking, is limited to the case of gases of small dipole moment. In (A.9), α^* is expressed in units of the cube of the Bohr radius, a_o, viz. $5.29 \cdot 10^{-9}$ cm. For the sake of completeness this molecular polarizability is, for O_2 10.9 a_o^3, for N_2 11.8 a_o^3 and for CO_2 18.0 a_o^3, all independent of temperature. For H_2O, the value at 273 K is 220 a_o^3, falling, at a typical flame temperature of this thesis, to 41.0 a_o^3. This latter value was used, though it may lead to error, as said.

We have after calculating the molecular polarizabilities, the following positive ion mobilities for the flame compositions used here:

At 2000 K, $\mu_{Na^+} = 19.6 \text{ cm}^2 \text{ V}^{-1} \text{ s}^{-1}$

At 1860 K, $\mu_{Na^+} = 17.5 \text{ cm}^2 \text{ V}^{-1} \text{ s}^{-1}$

At 1810 K, $\mu_{K^+} = 15.5 \text{ cm}^2 \text{ V}^{-1} \text{ s}^{-1}$

The last of these temperatures is midway between the highest and lowest temperatures encountered in flames B, C and D. The averaging expression used here, perhaps more correct than that using Loeb's equations, is

$$\mu_+^{-1} = \sum_i f_i (\mu_+)_i^{-1}$$

where f_i is the partial pressure of species i and $(\mu_+)_i$ the ion mobility in species i.

It is this process, and this particular form of the expression, that is used for calculations in the thesis (see Table 6.3).

Similar calculations have been carried out by Bradley and

Ibrahim (Bradley [190]) on the basis of a polarizability that is independent of temperature. Strictly speaking this is not true, but, as pointed out, the present approach may not fully compensate for the behaviour of water vapour since the expressions (A.7) and (A.9) may break down for molecules with large permanent dipoles. Bradley and Ibrahim suggest, at 2000 K,

$$\mu_{Na^+} = 23.07 \text{ cm}^2 \text{ V}^{-1} \text{ s}^{-1}$$

and $$\mu_{K^+} = 18.8 \text{ cm}^2 \text{ V}^{-1} \text{ s}^{-1}$$

The difference between the two sets of calculations is probably solely due to the differing role of water vapour in the two approaches.

The values obtained here compare with the experimentally determined ones of Lawton [117] who obtained $\mu_+ = 32.6 \text{ cm}^2 \text{ V}^{-1} \text{ s}^{-1}$ for, presumably, H_3O^+ in flame gases at 1870 ± 20°K, and Bradley and Ibrahim [27] who obtained $\mu_+ = 8.2 \text{ cm}^2 \text{ V}^{-1} \text{ s}^{-1}$ at 1730 K. This agreement between relatively simple theoretical expressions and experiment casts doubt on the values of μ_+ quoted by Kelly and Padley [61] from their empirical fit to what they assumed was a correct probe theory equation.

A further check on this is of course what is predicted at room temperature, for which experimental values are available for K^+ and N_2^+ in nitrogen. Due to a lack of consideration of charge exchange mechanisms, theoretical values for N_2^+ in N_2 are misleading. If a value of 2.9 Å is again taken for σ, then $\mu_+ = 2.84 \text{ cm}^2 \text{ V}^{-1} \text{ s}^{-1}$ at S.T.P., which is not too far distant from the value of 2.67 $\text{cm}^2 \text{ V}^{-1} \text{ s}^{-1}$ found by Mitchell and Ridler [62] who also however neglect charge exchange. These authors nevertheless do note that N_2^+ does seem to exhibit anomalous behaviour, explained much later by Moseley, Snuggs, Martin and McDaniel [191] who identify the presence

of N^+, N_2^+, N_3^+ and N_4^+ ions; μ_+ for N_2^+ in N_2 was found by them to be 1.87 $cm^2\ V^{-1}\ s^{-1}$. Agreement is quite good where there are no such complicating factors. The theoretical value for K^+ in N_2 is around 2.7 $cm^2\ V^{-1}\ s^{-1}$, with experimental values of 2.70 at 294 K (Mitchell and Ridler, op. cit.), and, of more recent years, 2.54 (Crompton and Elford [192]) and 2.55 $\pm$ 0.10 (Moseley, Gatland, Martin and McDaniel [193]). The theory is therefore seen to be adequate for non-polar molecules at room temperatures.

In the present work, the value of D_+ obtained at 1860 K was used as a base, and, rather than apply (A.7) and (A.8) with their attendant calculations of κ for each temperature, or calculate α^* for each temperature, it was assumed that $D \propto T^{1.5}$. Any error introduced thereby will be small. Values of D were then calculated at each temperature, and, by applying Einstein's relation, the corresponding values of μ_+ were obtained. Both μ_+ and D_+ are shown in Table 6.3.

APPENDIX B ELECTRON MOBILITY AND COLLISION FREQUENCY

In order to find expressions for electron mobility and the electron-neutral collision frequency, we follow the procedures of Margenan [194], who states that the accurate form of the distribution law for electrons of mean free path λ in an electric field of angular frequency ω, is, from Boltzmann's transport equation:

$$f_o = A \exp(-\varepsilon/kT) \left[1 + \frac{\varepsilon/kT}{\varepsilon_{1/kT} + \alpha}\right]^{\alpha}$$

where $\varepsilon = \frac{mv^2}{2}$, $\varepsilon_1 = \frac{m(\omega\lambda)^2}{2}$, $\alpha = \frac{M}{12m}\left(\frac{eE\lambda}{kT}\right)^2$ and A is the normalisation factor, $\left[\frac{m}{2\pi kT}\right]^{3/2}$.

In the case under consideration the applied electric field is DC, so $\varepsilon_1 = 0$, and $\alpha \ll 1$. Except for a minute fraction of the electrons $\varepsilon = 0(1)$, so, to a high degree of approximation,

$$f_o = \left[\frac{m}{2\pi kT}\right]^{3/2} \exp\left(-\frac{mv^2}{2kT}\right),$$

i.e. the distribution is the classical Maxwell-Boltzmann one. Any high energy tail to this distribution caused by the production, due to chemi-ionization, of electrons in the reaction zone, is destroyed in 10^{-8} secs in a flame burning at $5 \cdot 10^{-2}$ atmospheres (Bradley and Sheppard [26]) so here the time involved should be even less.

Because of the low mass and high mobility of electrons, the current density flowing through a plasma may be written as

$$I = ne\bar{v}_x = ne\mu_e E$$

$$= e \cdot \frac{eE}{m} \iiint v_x^2 f_1 \left(\cos\omega t + \frac{\omega\lambda}{v}\sin\omega t\right) v^2 dv \sin\theta \, d\theta \, d\phi$$

where $f_1 = \frac{-\lambda}{v^2 + (\omega\lambda)^2} \frac{df_o}{dv}$

$= \frac{mv\lambda f_o}{v^2\, kT}$ since $\omega = 0$. (This is equivalent to equation (27) of Margenau (op. cit.), except that there the factor 1/kT has inadvertently been dropped.) Since $\lambda = \frac{v}{\nu}$, the above expression becomes

$$\mu = \frac{e}{m} \frac{4}{3} \pi \frac{m}{kT} \int_o^\infty \left(\frac{m}{2\pi kT} \right)^{3/2} \frac{n}{\nu} \exp\left(\frac{-mv^2}{2kT} \right) v^4 \, dv$$

(Strictly speaking the upper integration limit should be c, the velocity of light.)

The substitution $x = \frac{mv^2}{2kT}$ is now made, giving

$$\mu = \frac{4}{3\sqrt{\pi}} \frac{e}{m} \int_o^\infty \frac{x^{3/2} e^{-x}}{\nu} \, dx \qquad \text{(B.1)}$$

There are two ways of dealing with this equation, both of which rely on expressing ν^{-1} as a power series

$$\nu^{-1} = \sum_i a_i u^i,$$

$u = \frac{mv^2}{2e} = \frac{xkT}{e}$ being the electron energy divided by electronic charge. Margenau expresses this in the form $\lambda = \sum_j b_j v^{-j}$, whereas the above in the form $\sum_i a_i u^i$ is the approach of Frost [172]; without great difficulty the two may be shown to be equivalent.

Equation (B.1) then becomes

$$\mu = \frac{4}{3\sqrt{\pi}} \frac{e}{m} \int_o^\infty \sum_i a_i \, x^{3/2 + i} \, e^{-x} \, dx,$$

which in terms of gamma functions is

$$\mu = \frac{e}{m} \sum_i \frac{\Gamma(5/2 + i)}{\Gamma(5/2)} a_i \left(\frac{kT}{e} \right)^i \qquad \text{(B.2)}$$

which, with the added proviso that $i > (-5/2)$, is Frost's (op. cit.) equation (10).

This form of the expression is useful only in the case of a rapidly converging series. As soon as we deal with a mixture of gases this is not necessarily true, and, in the present case, where there are two main contributors to the electron collision frequency, N_2 and H_2O, the series expansion diverges.

The much more useful approach here is that of a numerical integration of (B.1), using an analytic approximation for ν^{-1}, as, indeed has to be done by whatever method is convenient.

Frost (op. cit.) does, in his Table 1, list approximations which he expected to be accurate to $\pm$ 30% for many common gases. Since that paper, however, some of the data have become outmoded in the light of more recent work; especially is this the case for H_2O, and, to a lesser extent, CO_2, with only minor adjustments being necessary for one or two other gases.

Table B.1 lists values of $\frac{10^8 \nu}{N}$, where N is the neutral density, taken from Frost (op. cit.) in column 2 and with more recent approximations in column 3. These values are valid for the bulk of electrons found in flames, but at very low energies ($\varepsilon \lesssim .01$ eV) or above 1 eV other approximations may have to be used.

The original papers on which Frost's values of ν are based may be found by consulting Frost's paper. Since they are minor constituents and of unknown cross-section for electron collision, the NO, Na, OH and KOH contributions have been ignored.

The collision cross-section, Q_d, for electrons with water vapour was found by Pack, Voshall and Phelps [197] in the energy range 0.01-0.08 eV by an analysis of electron transit times in

TABLE B.1 ANALYTICAL COLLISION FREQUENCY EXPRESSIONS FOR VARIOUS SPECIES

Gas	$\frac{10^8\nu}{N}$ (from Frost)	More recent values of $\frac{10^8\nu}{N}$	Based on data from ref. nos:
H_2O	$10u^{-\frac{1}{2}}$	$19u^{-\frac{1}{2}}$	197, 198
CO_2	$1.7u^{-\frac{1}{2}} + 2.1u^{\frac{1}{2}}$	$10.72 - 23.88u^{3/2} + 15.65u^3$	196
O_2	$2.75u^{\frac{1}{2}}$	$4.28u^{\frac{3}{4}} - 0.054$	196
N_2	12u	10u + 0.17	173, 195
K	160	160	172
Na[a]	160	160	172
OH	$8.1u^{-\frac{1}{2}}$	$8.1u^{-\frac{1}{2}}$	172
O	$5.5u^{\frac{1}{2}}$	$5.5u^{\frac{1}{2}}$	172
CO	9.1u	10.6u + 0.65	196
H	$42u^{\frac{1}{2}} - 14u$	$42u^{\frac{1}{2}} - 14u$	172
H_2	$4.5u^{\frac{1}{2}} + 6.2u$	$4.5u^{\frac{1}{2}} + 6.2u$	172

a Na is assumed to have the same value of ν as K and Cs, but this, with our seeding levels, is negligible anyway.

a double shutter drift tube. If the log of the cross-section is plotted against the log of electron velocity, a straight line ensues which fits quite well on to the data observed at energies of just over 1 eV by Bruche [198], when it is realised that Bruche's work is over forty years old and open to inaccuracy. Indeed, even fairly recent work (Altshuler [199]) on water vapour now appears to have an error of a factor of two in it. The assumption made in the intermediate range, where no accurate data are available, is that the curve is just the extrapolation of the straight line referred to. Figure B.1 shows the assumed dependence of log $\frac{10^8 \nu}{N}$, i.e. log vQ_d, on electron energy, with a dashed line between 2 and 4 eV corresponding to Bruche's findings.

Q_d for electron-CO_2 collisions was measured by Hake and Phelps [196], and has an energy dependence that does not lend itself easily to an analytical approximation. It was eventually decided that a parabolic dependence was the best simple representation:

$$\frac{10^8 \nu}{N} = a_0 + a_1 z + a_2 z^2$$

where $z = u^{3/2}$. Values of a_0, a_1 and a_2 are given in Table B.1, and a comparison of this with experimental values is shown in Figure B.1. The two depart at electron energies of more than 1 eV, but since the electron distribution function then tails off to zero, this is not important. It does, however, limit the range of this approximation perhaps more than most of the others.

Vales used for O_2 are taken from Hake and Phelps' (op. cit.) analysis of swarm data, and are shown in Figure B.2. Those for CO are again taken from the same authors, and the expression for ν varies but little from that based on the old data published in

Healey and Reed [200].

There is general consensus among a number of workers - Engelhardt, Phelps and Risk [195], Pack and Phelps [173], and Crompton and Sutton [201] - for electrons in collision with nitrogen, and the expression finally decided on as the best approximation was

$$\frac{10^8\nu}{N} = 10u + 0.17$$

As advised by Frost (op. cit.), the total collision frequency is the sum of the partial pressure of each gas (see Table B.3) multiplied by the relevant expression for ν. The effect of all this is to reduce the value of μ_e and increase the value of ν, as compared with Frost's recommendations, mainly due to the new value of Q_d found for H_2O.

Table B.2 lists the composited values of ν for each flame, where, it is remembered, $x = \frac{mv^2}{2kT}$.

TABLE B.2 COLLISION FREQUENCY EXPRESSIONS USED FOR FLAMES ANALYSED

Flame	$\frac{10^8\nu}{N}$
A	$1.17 + 4.70x^{-\frac{1}{2}} + 0.011x^{\frac{3}{4}} + 1.36x - 0.163x^{3/2} + 0.008x^3$
B	$1.04 + 4.20x^{-\frac{1}{2}} + 0.059x^{\frac{3}{4}} + 1.27x - 0.135x^{3/2} + 0.006x^3$
C	$1.06 + 4.40x^{-\frac{1}{2}} + 0.040x^{\frac{3}{4}} + 1.22x - 0.127x^{3/2} + 0.005x^3$
D	$1.05 + 4.44x^{-\frac{1}{2}} + 0.051x^{\frac{3}{4}} + 1.16x - 0.119x^{3/2} + 0.005x^3$

The most convenient way of dealing with this was to take out a factor $x^{-\frac{1}{2}}$ and use the expression

$$\mu = \frac{4e}{3\sqrt{\pi}\,m} \frac{10^8}{N} \int_0^\infty \frac{x^2\, e^{-x}\, dx}{(x^{\frac{1}{2}}\,\nu)}$$

This was integrated numerically by Simpson's rule on a Hewlett-Packard 9100A desk-top calculator, using 100 strips from x = 0 to x = 20. Beyond this upper limit, there was negligible addition to the integrand. The electron mobility comes out to be ca. 6000 $cm^2\ V^{-1}\ s^{-1}$, and is shown for each flame in Table 7.2.

A value, $\bar{\nu}$, for each flame may be obtained by averaging over the Maxwell-Boltzmann distribution:

$$\frac{10^8\,\bar{\nu}}{N} = \frac{\int_0^\infty \frac{mv^2}{2kT} \exp\left(\frac{-mv^2}{2kT}\right) \nu(v)\,dv}{\int_0^\infty \frac{mv^2}{2kT} \exp\left(\frac{-mv^2}{2kT}\right) dv}$$

$$\text{or} \quad \frac{10^8\,\bar{\nu}}{N} = \frac{\int_0^\infty x^{\frac{1}{2}}\, e^{-x}\, \nu(x)\, dx}{\int_0^\infty x^{\frac{1}{2}}\, e^{-x}\, dx}$$

This statistically averaged electron-neutral collision frequency is to be found in Table B.3.

Frost (op. cit.) quotes the results of other authors' measurements of ν. Belcher and Sugden [46] obtain the somewhat low value of $8.8 \cdot 10^{10}\ s^{-1}$ while Hofmann, Kohn and Schneider [202] are stated by Frost to have observed a value of $2 \cdot 10^{11}$ at 2500 K and 2750 K, rising to $2.7 \cdot 10^{11}$ at 2100 K. The calculations here are in excellent agreement with this latter value, and, indeed, with an extrapolation of these results.

TABLE B.3 ELECTRON-FLAME GAS MOLECULE COLLISION FREQUENCIES

Flame	Useful temperature range (K)	ν. sec^{-1} x 10^{-11}
A	1977-2023	3.0
B	1848-1947	2.9
C	1765-1855	3.1
D	1686-1793	3.2

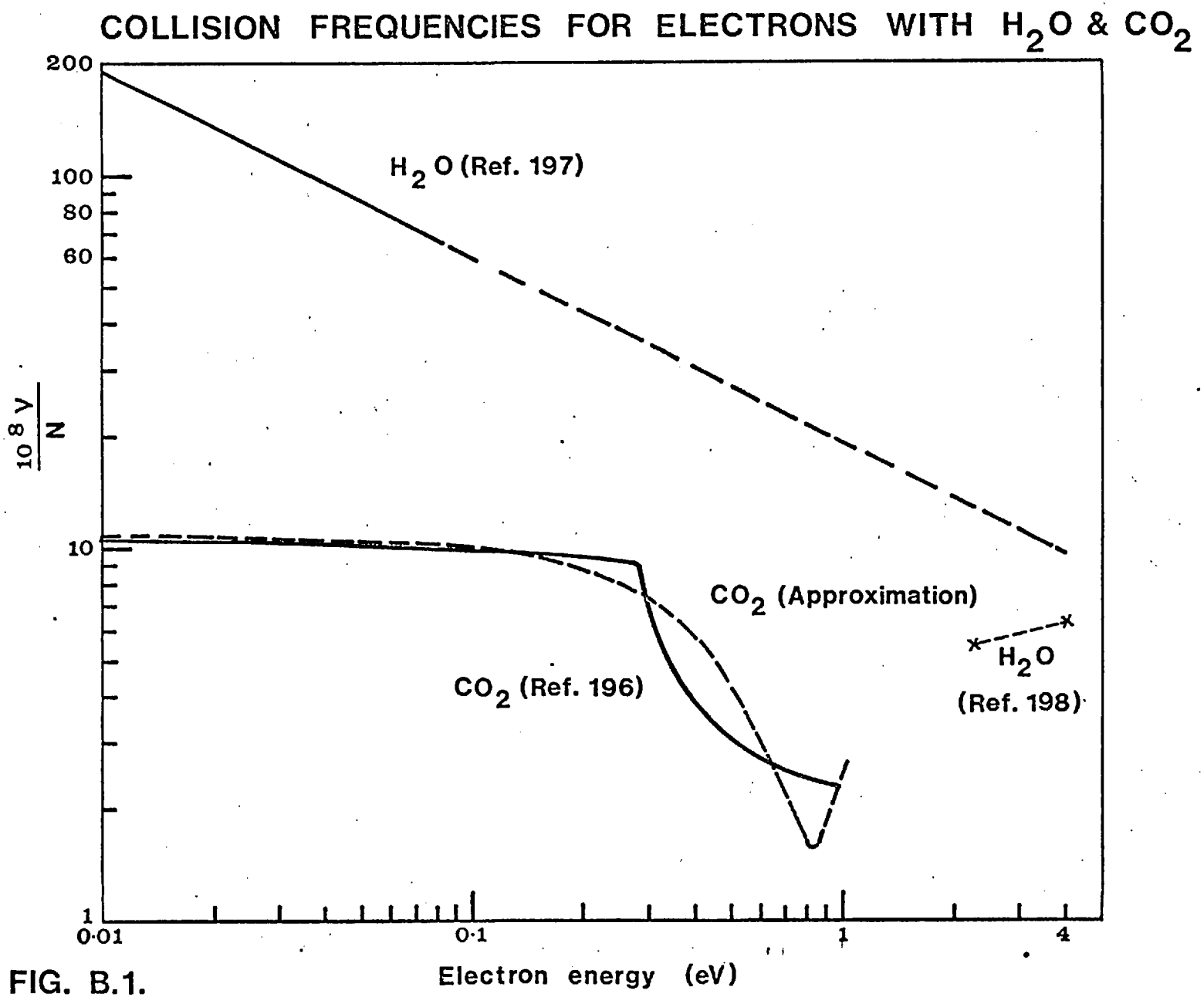
COLLISION FREQUENCIES FOR ELECTRONS WITH H_2O & CO_2
200
100
80
60
10
1
$10^8 \frac{\nu}{N}$
H_2O (Ref. 197)
CO_2 (Approximation)
H_2O
(Ref. 198)
CO_2 (Ref. 196)
0·01
0·1
1
4
Electron energy (eV)

FIG. B.1.

COLLISION FREQUENCIES FOR ELECTRONS WITH O_2.

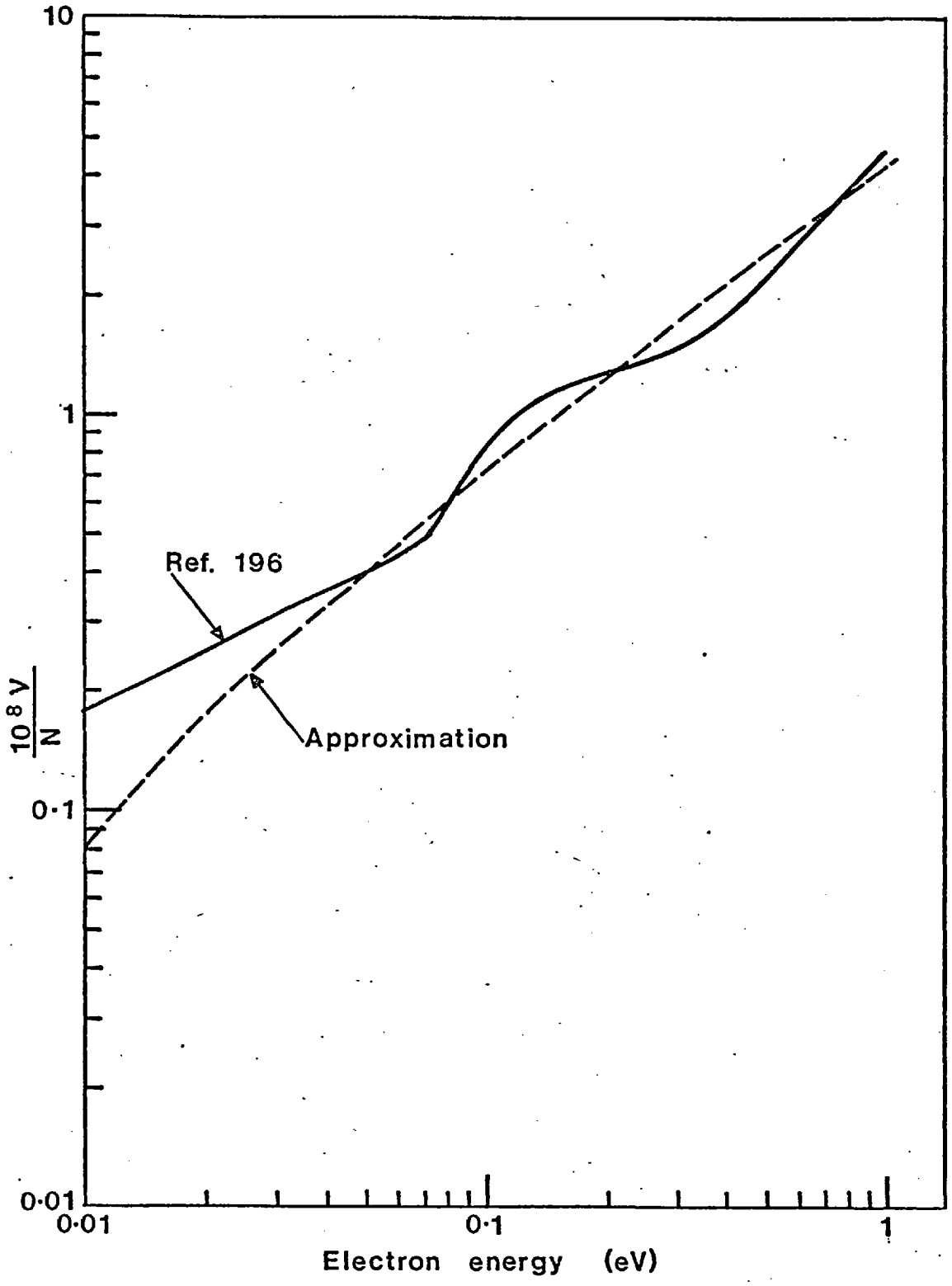

FIG. B.2.

APPENDIX C LIST OF SYMBOLS

Subscripts "+", "-" and "e", especially when used with j, μ, D and n, refer to positive ions, negative ions and electrons respectively; the latter can also refer to equilibrium conditions. The subscript "o" refers to conditions at STP.

a Radius of annular insulator in Clements and Smy's probe theory; as subscript, viz. β_a, means apparent value of β.

a_i i^{th} coefficient of series expansion.

a_o Radius of attraction in recombination theories of Thomson and Natanson; Bohr radius.

A Pre-exponential factor in rate expression; flame area; constant in molar polarizability expression; normalisation factor; alkali atom - with subscript "$_T$", refers to total alkali concentration in all forms.

A^+ Positive alkali ion density.

b Temperature exponent in rate expression; constant in radial diffusion theory.

b_j j^{th} coefficient of series expansion.

B Constant in molar polarizability expression.

B_o Parameter describing spacing of rotational energy levels, having dimensions of energy.

c Velocity of light; as subscript with β, corrected value of β and species concentrations arising from this.

d Dipole moment.

D Dipole moment divided by ea_o; diffusion coefficient - subscript "a" refers to ambipolar diffusion; dissociation energy.

e Electronic charge; base of natural logs.

E Electric field (subscript p refers to conditions in plasma); activation energy.

f Fractional energy loss for electron in collision with a neutral; attractive force.

f_i Partial pressure of i^{th} species.

f_o Distribution function.

f_1 Constant of order unity, relating Langevin and Harper recombination coefficients.

g Statistical weight.

h Planck's constant.

I Current in a circuit; probe current; integral in Preist's ionization theory; moment of inertia.

j Current density; subscript "n" refers to conditions at the "elbow" of the current-voltage curves, and "s" to saturation conditions.

J Current density; rotational quantum number.

k Boltzmann constant; rate coefficient (subscript "i" refers to ionization rate constant).

K Equilibrium constant.

l Length co-ordinate.

m Mass (subscript indicates species).

M Mass (of molecule or ion); third body in a collision; molecular weight.

n Charged or neutral species density (subscript indicates species); refractive index.

n_c Number of carbon atoms per second fed into flame.

n^* Complex refractive index.

N Number of ion pairs per second produced in reaction zone; number density (sometimes enclosed in brackets).

N_{AV} Avogadro's number.

$\underline{N}$ Total number of bound states in atom.

p Pressure; as subscript, refers to conditions in plasma.

q Ion production rate (ions cm^{-3} s^{-1}).

Q Quadrupole moment divided by ea_o^2; cross section - Q_d is the diffusion cross-section.

r Interionic distance in Natanson theory; radial distance from axis of gas flow; interatomic distance in a molecule; polar co-ordinate.

r_o Average radial displacement from origin at time t in diffusion theory.

r_p Probe radius,

R Molar refraction.

Ry Rydberg.

S_u Burning velocity.

t Time.

T Temperature (Kelvin). Subscripts i, f, m refer to initial, final and mean temperatures especially in van Tiggelen's flame thickness theory.

u Gas convection velocity; ratio of electron energy to electronic charge.

u Plasma convection velocity in Clements and Smy's probe theory.

v Velocity; ionic velocity is subscripted appropriately.

v_d Diffusion velocity.

V Voltage.

V_p Probe voltage.

V_T Total voltage across electrodes.

x Distance co-ordinate; $\frac{mv^2}{2kT}$ for electron.

X Molecule (species unspecified).

$\frac{3}{16Y}$ Langevin's quantity in positive ion mobility expression.

z $u^{3/2}$ where u is ratio of electron energy to electronic charge.

α Recombination coefficient in cm^3 $molecule^{-1}$ s^{-1}; constant in Margenau's electron mobility theory; subscripts 1 and 2 refer to electrons and negative ions as negative species in a three body recombination; subscripts H, L, P, N refer to recombination coefficient on basis of Harper, Langevin Pitaevskii and Natanson theories respectively.

α^* Complex molecular polarizability; subscripts e and a refer to contributions from electron cloud and atomic spacing.

β Constant of order unity in Natanson theory, n_e/n_+.

γ Exponential decay constant.

Γ Gamma function.

Δ Distance of electron energy level below ionization potential (i.e. electron, binding energy).

ϵ Electron kinetic energy.

ϵ_o Permittivity of free space.

η n_e/n_-; efficiency factor for a three body reaction - see p. 95.

Θ Ratio of alkali hydroxide to atomic alkali concentration

θ Polar co-ordinate

κ Permittivity; if asterisked complex permittivity.

λ Electron or ion mean free path; variable in expression for ion mobility.

λ_D Debye length.

μ Mobility (subscript refers to species); reduced mass.

ν Electron-neutral collision frequency.

Π Product (over i terms); molar polarizability.

ρ Density.

σ Conductivity; effective distance between molecular centres.

σ_i Ionization cross-section.

$\sum_i$ Sum (over i terms).

ϕ Polar co-ordinate.

ω Wave number; angular frequency of field.

$\bar{}$ Bar over parameter indicates average value.

$[\,]$ Indicates concentration in cm^{-3}; the subscript s refers to non-equilibrium steady state conditions.

REFERENCES

N.B. An unspecified, numbered "Symposium" refers to one of the biennial International Symposia on Combustion.

1. Bulewicz E.M. and Padley P.J., Trans. Farad. Soc., 67, 2337, 1971.
2. Bulewicz E.M. and Padley P.J., Proc. Roy. Soc. A323, 377, 1971.
3. Bulewicz E.M., Cotton D.H., Jenkins D.R. and Padley P.J., Chem. Phys. Letters 9, 467, 1971.
4. Boksenberg A., Kirkham B., Towlson W.A., Venis T.E., Bates B., Courts G.R. and Carson P.P.D., Nature Physical Science, 240, 127, 1972.
5. Green J.A. and Sugden T.M., 9th Symposium, p.607, Academic Press, New York and London, 1963.
6. Calcote H.F., 20th AGARD Propulsion and Energetics Panel, Pisa, 1963.
7. Peeters J., Vinckier Ch. and van Tiggelen A., Oxidation and Combustion Reviews 4, 93, 1969.
8. Peeters J. and van Tiggelen A., 12th Symposium, p.437, The Combustion Institute, Pittsburgh, 1969.
9. Miller W.J., 14th Symposium, p.307, The Combustion Institute, 1973.
10. Starkman E.S., 12th Symposium, p.593, The Combustion Institute, Pittsburgh, 1969.
11. Musgrove P.J., Physics Bulletin 23, 591, 1972.
12. Musgrove P.J., Electrical Review 189, 406, 1971.
13. Gourdine M.C., Proc. Int. Symp. on Electrohydrodynamics, p.164, Cambridge: MIT Press, 1969.
14. Bulewicz E.M., Padley P.J. and Smith R.E., Proc. Roy. Soc. A315, 219, 1970.

15. Fontijn A., Miller W.J. and Hogan J.M., 10th Symposium, p.545, The Combustion Institute, 1965.

16. Bulewicz E.M. and Padley P.J., 9th Symposium, p.638, The Combustion Institute, 1963.

17. Browne W.G., Porter R.P., Verlin J.D. and Clark A.H., 12th Symposium, p.1035, The Combustion Institute, 1969.

18. Jones F.L., Becker P.M. and Heinsohn R.J., Combust. Flame 19, 351, 1972.

19. Matthews C.S. and Warneck P., J. Chem. Phys. 51, 854, 1969.

20. Calcote H.F., Kurzius S.C. and Miller W.J., 10th Symposium, p.605, The Combustion Institute, 1965.

21. Kurzius S.C. and Boudart M., Combust. Flame 12, 477, 1968.

22. Miller W.J., Oxidation Combust. Rev. 3, 97, 1968.

23. Calcote H.F. and Jensen D.E., Ion Molecule Reactions in the Gas Phase, Advances in Chemistry Series No. 58 (R.F. Gould, Ed.), p.291, American Chemical Soc., 1969.

24. Boothman D., Lawton J., Melinek S.J. and Weinberg F.J., 12th Symposium, p.969, The Combustion Institute, 1969.

25. von Engel A. and Cozens J.R., Nature 202, 480, 1964.

26. Bradley D. and Sheppard C.G.W., Combust. Flame 15, 323, 1970.

27. Bradley D. and Ibrahim Said M.A. To be published in J. Phys. D: Appl. Phys. 1974.

28. Hayhurst A.N. and Sugden T.M., 20th I.U.P.A.C. Congress, Moscow, 1965.

29. Page F.M. and Sugden T.M., Trans. Farad. Soc. 53, 1092, 1957.

30. Padley P.J. and Sugden T.M., 8th Symposium, p.164, Williams and Wilkins, 1962.

31. van Tiggelen A. and de Jaegere S., Experimental Study of Chemi-ionization, University of Louvain. (Sponsored partly

by Aerospace Research Laboratories: Grant AF-EOAR-65-82).

32. Thomson J.J., Phil. Mag. 47, 337, 1924.

33. Langevin P., Ann. Chim. Phys. 28, 433, 1903.

34. Harper W.R., Proc. Camb. Phil. Soc. 28, 219, 1932.

35. Loeb L.B., Basic Processes of Gaseous Electronics, Univ. of California Press, Berkeley and Los Angeles, 1961.
a: pp.511 et seq; b: pp.635 et seq; d: p.208; c: pp.528-9; e: pp.64 et seq.

36. Natanson G.L., Soviet Phys. - Technical Physics 3, 1263, 1959.

37. Pitaevskii L.P., Soviet Phys. JETP 15, 919, 1962.

38. Dalidchik F.I. and Sayasov Yu.S., Soviet Phys. JETP. 22, 212, 1966.

39. Dalidchik F.I. and Sayasov Yu.S., Soviet Phys. JETP. 25, 1059, 1967.

40. Sayasov Yu.S., 8th International Conference on Phenomena in Ionized Gases, p.9. Springer-Verlag, Vienna, 1967.

41. Bates D.R. and Khare S.P., Proc. Phys. Soc. 85, 231, 1965.

42. Bates D.R., Malaviya V. and Young N.A., Proc. Roy. Soc. A320, 437, 1971.

43. Sugden T.M. and Thrush B.A., Nature 168, 703, 1951.

44. Sugden T.M. and Wheeler R.C., Disc. Farad. Soc. 19, 76, 1955.

45. Jensen D.E. and Padley P.J., Trans. Farad. Soc., 62, 2132, 1966.

46. Belcher H. and Sugden T.M., Proc. Roy. Soc. A201, 480, 1950.

47. Shohet J. and Moskowitz C., J. Appl. Phys. 34, 1622, 1965.

48. Bulewicz E.M., J. Chem. Phys. 36, 385, 1962.

49. Keen B.E. and Fletcher W.H.W., J. Phys. D. Appl. Phys. 4, 1695, 1971.

50. Langmuir I. and Mott-Smith H.M., Gen. Elec. Rev. 26, 731, 1923; 27, 449, 583, 616, 726, 810, 1927.

51. Bohm D., Burhop E.H.S. and Massey H.S.W., The Characteristics of Electrical Discharges in Magnetic Fields (Ed. Guthrie A. and Wakerling R.K.). McGraw-Hill, 1949.

52. Calcote H.F., 8th Symposium, p.184. Williams and Wilkins, Baltimore, 1962.

53. Porter, R.P., Clark, A.H., Kaskan, W.E. and Browne, W.E., 11th Symp., p.907. The Combustion Institute, London, 1967.

54. Calcote, H.F., 9th Symp., p.622. Acadamic Press, New York and London, 1963.

55. Lam, S.H., AIAAJ 2, 256, 1964.

56. Su, C.H. and Lam, S.H., Phys. Fluids, 6, 1479, 1963.

57. Bradley, D. and Matthews, K.J., Phys. Fluids, 10, 1336, 1967.

58. Bradley, D. and Matthews, K.J., 11th Symp., p.359. The Combustion Institute, Pittsburgh, 1967.

59. Soundy, R.G. and Williams, H., Proc. 26th AGARD Meeting, Pisa, 1965.

60. Kelly, R. and Padley, P.J., Trans. Farad. Soc. 67, 740, 1971.

61. Kelly, R. and Padley, P.J., Trans. Farad. Soc. 67, 1384, 1971.

62. Mitchell, J.H. and Ridler, K.E.W., Proc. Roy. Soc. A146, 911, 1934.

63. Clements, R.M. and Smy, P.R., J. Phys. D. Appl. Phys. 4, 1687, 1971.

64. Maise, G. and Sabadell, A.J., AIAAJ 8, 895, 1970.

65. Brown, S.C., Bekefi, G. and Whitney, R.E., J. Opt. Soc. Am., 53, 448, 1963.

66. Hubner, G., Jones, A.R. and Bose, K.C., Infrared Physics 13, 123, 1973.

67. Hubner, G. and Jones, A.R., J. Phys. D. Appl. Phys. 6, 774, 1973.

68. Borgers, A.J., 10th Symposium, p.627. The Combustion Institute, 1965.

69. Wilson, H.A., Rev. Mod. Phys., p.156, 1931.

70. Smithells, A., Dawson, H.M. and Wilson, H.A., Phils. Trans. Roy. Soc. A193, 89, 1900.

71. Wilson, H.A., Phys. Rev. 3, 375, 1914.

72. Bennett, J.A.J., Phil. Mag. Series 7, Vol. 3, 127, 1927.

73. King, I.R., Rept. TP-174A, Texaco Experiment Incorporated, Richmond, Va., 1961.

74. Poncelet, J., Berendsen, R. and van Tiggelen, A., 7th Symp., p.256, Butterworth's, 1959.

75. Kydd, P.H., Dept. No. 63-RL-3304C. General Electrical Research Laboratory, Schenectady, 1963.

76. Fristrom, R.M. and Westenberg, A.A., Flame Structure, p.222, McGraw Hill, 1965.

77. Feugier, A., Rev. Gen. Therm. 9, 1045, 1970.

78. Wortberg, G., 10th Symp., p.651, The Combustion Institute, Pittsburgh, 1965.

79. Porter, R.P., Combustion and Flame 14, 275, 1970.

80. Lapp, M. and Rich, J.A., Rept. No. 62-RL-3178G, General Electric Research Laboratory, Schenectady, 1962.

81. Harris, L.P., Rept. No. 63-RL-3278G. General Electric Research Laboratory, Schenectady, 1963.

82. Harris. L.P., Rept. No. 63-RL-3334G, General Electric Research Laboratory, Schenectady, 1963.

83. Hayhurst, A.N. and Telford, N.R., J.C.S. Faraday 1 68, 237, 1972.

84. Jensen, D.E. and Padley. P.J., Trans. Farad. Soc., 62, 2140, 1966.

85. Kelly, R. and Padley, P.J., Proc. Roy. Soc. A327, 345, 1972.

86. Hollander, Tj., Thesis, Univ. of Utrecht, 1964.

87. Hollander Tj., Kalff, P.J. and Alkemade, C.T.J., J. Chem. Phys. 39, 2558, 1963.

88. Botha, J.P. and Spalding, D.B., Proc. Roy. Soc. A225, 71, 1954.

89. Lawton, J., Ph.D. Thesis, Univ. of London, 1963.

90. Lawton, J. and Weinberg, F.J., Proc. Rpy. Soc., A277, 468, 1964.

91. Payne, K.G. and Weinberg, F.J., Proc. Roy. Soc. A250, 316, 1959.

92. Bolton, H.C. and McWilliam, I.G., Proc. Roy. Soc. A321, 361, 1971.

93. Melinek, S.J., Ph.D. Thesis, Univ. of London, 1969. a: p.126; b: p.170; c: p.241.

94. Arrington, C.A., Brennan, W., Glass, G.P., Michael, J.V. and Niki, H., J. Chem. Phys. 43, 1489, 1965.

95. Nesterko, N.A. and Rossikhin, V.S., Combustion, Explosions and Shock Waves, 4, 76, 1968.

96. Glushko, L.N., Tverdokhlebov, V.I. and Chirkin, N.N., Proceedings 9th International Conference on Phenomena in Ionised Gases, p.50. Editura Academei Republicii Socialiste Romania, Bucharest, 1969.

97. Tverdokhlebov, V.I. and Chirkin, N.N., Proc. Acad. Sci. U.S.S.R. 179, 248, 1968 (English translation and pagination).

98. Van Tiggelen, A. and Vaerman, J., Bull. Soc. Chim. Belg. 62, 653, 1953.

99. Taran, E.N. and Tverdokhlebov, V.I., Teplofizika Vysokikh Temperatura 6, 381, 1968 (English translation and pagination).

100. Knewstubb, P.F. and Sugden, T.M., Trans. Farad. Soc. 54, 372, 1958.

101. Exner, F., Ann. Phys. Lpz 155, 231, 1875.

102. Kurlbaum, F., Phys. Z. 3, 187, 1902.

103. Fery, C., Compt. Rend. Acad. Sci. 137, 909, 1907.

104. Gaydon, A.G. and Wolfhard, H.G., "Flames, their Structure, Radiation and Temperature", 2nd. edition, Chapman and Hall, London, 1960. a: pp. 235-9; b: p. 238; c: p. 221; d: p. 3o4.

105. Norrish, R.G.W. and Smith, W.MacF., Proc. Roy. Soc. A176, 295, 1941.

106. Boers, A.L., Alkemade, C.T.J. and Smit, J.A., Physica 22, 358, 1956.

107. Jenkins, D.R., Proc. Roy. Soc. A293, 493, 1966.

108. Gautier, A., Bull. Soc. Chim. Paris. 21, 391, 1899.

109. Godard, H.P. and Seyer, W.F., Trans. Roy. Soc. Canada 30, 85, 1936.

110. Johnson, G.M. and Smith, M.Y., Spectrochemica Acta. 27B, 269, 1972.

111. Von Engel, A., "Ionized Gases", pp.90-91, O.U.P., 1965.

112. Van Tiggelen, A., Mem. Acad. Roy. Belg. 27, 1, 1952.

113. Fristrom, R.M., Avery, W.F. and Grunfelder, C., 7th Symp., p.304, Butterworth, London, 1959.

114. Bell, J.C., Bradley, D. and Jesch, L.F., 13th Symp., p.345, The Combustion Institute, Pittsburgh, 1971.

115. Glushko, L.N. and Tverdokhlebov, V.I., Proc. Acad. Sci. USSR 179, 283, 1968 (English translation and pagination).

116. Kaskan, W.E., 6th Symp., p.134. Reinhold, New York, 1957.

117. Lawton, J., Combustion and Flame, 17, 7, 1971.

118. Fox, J.S. and Kihara, D.H., Combustion Science and Technology. 5, 17, 1972.

119. Thomson, J.J. and Thomson, G.P., "The Conduction of Electricity through Gases", Vol. I, 3rd edition, C.D.P., 1928. a: pp.139 et seq; b: p.31.

120. Toba, K. and Sayano, S., J. Plasma Phys. 1, 407, 1967.

121. Jaffe, G., Le Radium. 10, 126, 1913.

122. Einstein, A., Ann. Physik. 17, 549, 1905.

123. Weinberg, F.J., Combust. Flame 10, 267, 1966.

124. Kaskan, W.E., Combust. Flame 2, 226, 1958.

125. Kaskan, W.E., Combust. Flame 2, 286, 1958.

126. Baxendale, D.N., Livesey, J.B., Roberts, A.L., Smith, D.B. and Williams, A., Combust. Sci. Tech. 2, 287, 1971.

127. Sugden, T.M., Trans. Farad.Soc. 52, 1465, 1956.

128. Padley, P.J., Page, F.M. and Sugden, T.M., Trans. Farad. Soc. 57, 1552, 1961.

129. Bulewicz, E.M., James, C.G. and Sugden, T.M., Proc. Roy. Soc. A235, 89, 1956.

130. Freck, D.V., Brit. J. Appl. Phys. 15, 301, 1964.

131. Brogan, T.R. in "Gas Discharges and the Electricity Supply Industry", J.S. Forest (Ed.), Butterworth's, London, 1962.

132. Hand, C.W. and Kistiakowsky, G.B., J. Chem. Phys. 37, 1239, 1962,

133. Matsuda, S. and Gutman, D., Rev. Sci. Inst. 42, 858, 1971.

134. Saha, M.N., Phil. Mag. 40, 472, 1920.

135. Rossini, F.D. et al., "Selected values of physical and thermodynamic properties of hydrocarbons and related compounds". Carnegie Press, Pittsburgh, 1953.

136. Marteney, P.J., Combust. Sci. Tech. 1, 461, 1970.

137. Fenimore, C.P., 13th Symp., p.373, The Combustion Institute, Pittsburgh, 1971.

138. Cotton, D.H. and Jenkins, D.R., Trans. Farad. Soc. 65, 1537, 1969.

139. Acquista, N., Abramowitz, S. and Lide, D.R., J. Chem. Phys. 49, 780, 1968.

140. Acquista, N. and Abramowitz, S., J. Chem. Phys. 51, 2911, 1969.

141. Kuczkowski, R.L., Lide, D.R. and Krisher, L.C., J. Chem. Phys. 44, 3131, 1966.

142. Lide, D.R. and Kuczkowski, R.L., J. Chem. Phys. 46, 4768, 1968.

143. Smith, H. and Sugden, T.M., Proc. Roy. Soc. A219, 204, 1953.

144. Chamberlain, J.W. and Roesler, F.L., Astrophys. J. 121, 541, 1955.

145. Gordy, J., J. Chem. Phys. 14, 305, 1946.

146. Smith, S.J. and Branscomb, L.M., Phys. Rev. 99, 1657, 1955.

147. Branscomb, L.M., Advances in Electronics and Electron Physics, 9, 43, 1957.

148. Page, F.M., Disc. Farad. Soc. 19, 87, 1955.

149. Feugier, A. and Queraud, A., Symposium on Energy from MHD (Warsaw 1968) IAEA, Vienna 1968, p.2129.

150. Haber, F. and Sachsse, H., Z. Phys. Chem. (Bodenstein Festband), 831, 1931.

151. Bawn, C.E.H. and Evans, A.G., Trans. Farad. Soc. 33, 1580, 1937.

152. Kaskan, W.E., 10th Symp., p.41, The Combustion Institute, 1965.

153. McEwan, M.J. and Phillips, L.F., Trans. Farad. Soc. 62, 1717, 1966.

154. Carabetta, R. and Kaskan, W.E., J. Phys. Chem. 72, 2483, 1968.

155. Bernard, J., Labois, E. and Ricateau, P., Symposium on Energy from MHD (Warsaw, 1968). IAEA, Vienna, 1968, p.207.

156. Kelly, R. and Padley, P.J., Trans. Farad. Soc. 65, 355, 1969.

157. Jensen, D.E. and Padley, P.J., 11th Symp., p.351, The Combustion Institute, Pittsburgh, 1967.

158. King, I.R., J. Chem. Phys. 36, 553, 1962.

159. Ashton, A.F. and Hayhurst, A.N., Combust. and Flame, 21, 69, 1973.

160. Cuderman, J.F., Phys. Rev. 5, 1687, 1972.

161. Kelly, A.J., J. Chem. Phys. 45, 1723, 1966.

162. Harwell and Jahn, R.G., Phys. Fluids, 7, 214, 1964.

163. Matsuzawa, M., J. Chem. Phys. 55, 2685, 1971.

164. Fowler, G.N. and Preist, T.W., J. Chem. Phys. 56, 1601, 1972.

165. Preist, T.W., J. Chem. Soc. Faraday 1. 68, 661, 1972.

166. Chew, G.E. and Low, F.E., Phys. Rev. 113, 1640, 1959.

167. Ecker, G. and Weizel, W., Ann. Phys. Lpz. 17, 126, 1956.

168. Preist, T.W., J. Phys. B. 4, 1129, 1971.

169. Inglis, D.R. and Teller, E., Astrophys. J. 90, 439, 1939.

170. Takayanagi, K., J. Phys. Soc. Japan 21, 507, 1966.

171. Gerjuoy, E. and Stein, S., Phys. Rev. 97, 1671, 1955.

172. Frost, L.S., J. Appl. Phys. 32, 2029, 1962.

173. Pack, J.L. and Phelps, A.V., Phys. Rev. 121, 798, 1961.

174. Platzman, R. and Franck, J., J. Res. Coun. Israel (L. Farkas Memorial Volume), 1952.

175. Gray, P. and Waddington, T.C., Proc. Roy. Soc. A235, 481, 1956.

176. Knewstubb, P.F. and Sugden, T.M., Nature 196, 1311, 1962.

177. Cottrell, T.L. and Walker, I.C., Chem. Soc. Quarterly Reviews, p.153, 1966.

178. Mossotti, O.F., Mem. Soc. Ital. Sc. (Modena) 14, 49, 1850.

179. Clausius, R., "Die Mechanische Warmetheorie", Vol. II, p.94, Vieweg-Verlag, Brunswick, 1879.

180. Lorentz, H.A., Ann. Phys. 9, 641, 1880.

181. Lorenz, L., Ann. Phys. II, 70, 1880.

182. Gladstone, J.H. and Dale, J., Phil. Trans. 153, 317, 1863.

183. "Handbook of Chemistry and Physics", (52nd edition), p. E-204, Chemical Rubber Company, Cleveland, 1971.

184. Von Hippel, A., "Handbook of Physics", (Ed. E.U. Condon and H. Odishaw) p.4-112. McGraw Hill, New York, 1958.

185. Langevin, P., Ann. Chim. Phys. 5, 245, 1905.

186. Hasse, H.R., Phil. Mag. 1, 139, 1926.

187. Goldschmidt, V.M., Trans. Farad. Soc. 25, 253, 1929.

188. Sandler, S.I. and Mason, E.A., J. Chem. Phys. 48, 2873, 1968.

189. Dalgarno, A., McDowell, M.R.C. and Williams, A., Phil. Trans. A250, 411, 1958.

190. Bradley, D., Private Communication.

191. Moseley, J.T., Snuggs, R.M., Martin, D.W. and McDaniel, E.W., Phys. Rev. 178, 240, 1969.

192. Crompton, R.W. and Elford, M.T., Proc. Phys. Soc. 74, 497, 1959.

193. Moseley, J.T., Gatland, I.R., Martin, D.W. and McDaniel, E.W. Phys. Rev. 178, 234, 1969.

194. Margenau, H., Phys. Rev. 69, 508, 1946.

195. Engelhardt, A.G., Phelps, A.V. and Risk, C.G., Phys. Rev. 135, A1566, 1964.

196. Hake, R.D. and Phelps, A.V., Phys. Rev. 158, 70, 1967.

197. Pack, J.L., Voshall, R.E. and Phelps, A.V., Phys. Rev. 127, 2084, 1962.

198. Bruche, E., Annlu. Phys. 1, 93, 1929.

199. Altshuler, S., Phys. Rev. 107, 114, 1957.

200. Healey, R.H. and Reed, J.W., "The Behaviour of Slow Electrons in Gases", Amalgamated Wireless, Sydney, 1941.

201. Crompton, R.W. and Sutton, D.J., Proc. Roy. Soc. A215, 467, 1952.

202. Hofmann, F.W., Kohn, H. and Schneider, J, Duke Univ. Microwave Lab. Rept. No. 28, Nov. 1959-Feb. 1960.